Role of the RNA-binding Protein NONO in Regulating Circadian Gene Expression and Metabolism

---

Dissertation

zur

Erlangung der naturwissenschaftlichen Doktorwürde (Dr. sc. nat.)

vorgelegt der

Mathematisch-naturwissenschaftlichen Fakultät

der

Universität Zürich

von

Giorgia Benegiamo

aus Italien

Promotionskommission

Prof. Dr. Steven A. Brown (Vorsitz und Leitung der Dissertation)

Prof. Dr. Michael Arand

Prof. Dr. Christian Wolfrum

Prof. Dr. Satchidananda Panda

Zürich, 2017

Table of Contents

Summary 1

Zusammenfassung 3

1. GENERAL INTRODUCTION 7

BASIC PRINCIPLES OF MAMMALIAN CIRCADIAN BIOLOGY 9

CIRCADIAN REGULATION OF GENE EXPRESSION 12

The circadian cistrome 12
Circadian regulation, RNAPII occupancy and chromatin states 12
Genome-wide circadian RNA expression analysis 14
Evidences for the relevance of post-transcriptional mechanisms on circadian gene expression 15
Circadian regulation of splicing 17
Circadian regulation of transcription termination 19
Circadian regulation of polyadenylation 20
Circadian regulation of mRNA stability 21
Circadian regulation of translation and ribosome biogenesis 22

THE RNA-BINDING PROTEIN NONO (P54NRB) 24

The DBHS family 24
NONO functions at multiple levels to regulate gene expression 25
NONO can act as a transcriptional co-activator and co-repressor 25
The role of NONO in post-transcriptional processing, RNA stability and export 26
Paraspeckle formation and nuclear RNA retention 27
The role of NONO in the circadian clock and cell cycle 28

BASIC PRINCIPLES REGULATING METABOLIC HOMEOSTASIS 28

The liver plays a central role in metabolic homeostasis 29
Liver metabolism during the fasted state 29
Liver metabolism during the fed state 30

INTERPLAY BETWEEN THE CIRCADIAN CLOCK AND METABOLISM 32

The molecular players mediating the entrainment of the circadian clock by energetic status 32
Disruption of the clock leads to metabolic disorders in mouse models and humans 33
Systemic cues and the circadian clock 35

2. AIMS OF THE THESIS 39

3. RESULTS 43

THE RNA BINDING PROTEIN NONO COORDINATES HEPATIC ADAPTATION TO FEEDING 45

Abstract 46
Introduction 47
Results 49

Feeding increases the number of NONO-containing speckle-like structures in nuclei of liver cells 49
NONO interacts with RNA processing factors 49
The number of transcripts bound by NONO increases upon feeding 50
NONO regulates the rhythmicity of its target RNAs post-transcriptionally 51
NONO regulates glucose-induced gene expression post-transcriptionally and is required for normal glucose homeostasis 53
Nono^{gt} mice store less fat and exhibit increased fat catabolism 55
Discussion 57
Figures and Tables 61
Supplementary Figures 70
Materials and Methods 77
Key resources table 77
Mouse models 79
Liver immunostaining 79
Speckle-like structures and fluorescence quantification 80
Immunoprecipitation from liver nuclear lysates 80
Mass spectrometry analysis 81
Native RNA-immunoprecipitation (RIP) 82
RNA extraction 83
High-throughput RNA sequencing (RNA-seq) 83
RNA-seq and RIP-seq data analysis 84
Statistical analysis of rhythmic gene expression 84
Gene ontology and pathway over-representation analysis (ORA) 85
Gene Expression Analysis by RT-qPCR 85
Western Blotting 85
GTT and ITT 86
Blood measurements 86
Liver glycogen quantification 86
Adeno-associated Viruses (AAV) Strains, Propagation and Injection 86
Oil-Red-O staining 87
Liver triglycerides quantification 87
Body composition 88
Indirect calorimetry 88
Histology 88
Metabolomics analysis 88
Quantification and statistical analysis 88
Data and software availability 89
Authors contribution 89
Acknowledgements 89
4. GENERAL DISCUSSION AND OUTLOOK 91
5. ACKNOWLEDGEMENTS 101
6. LIST OF ABBREVIATIONS 103
7. REFERENCES 109
9. CURRICULUM VITAE 129
10. APPENDIX 133

Summary

Circadian rhythms represent a fundamental property of living organisms. Even when they are held in temporal isolation, most organisms from bacteria to humans exhibit behavioral and physiological rhythms with a period of approximately 24 h. These rhythms are driven by internal biological clocks.

In mammals, the molecular clock mechanism is driven by transcriptional-translational feedback loops of activator and repressor proteins. The transcriptional activators Circadian Locomotor Output Cycles Kaput (CLOCK) and Brain and Muscle ARNT-Like Protein 1 (BMAL1) heterodimerize and activate the transcription of the repressors *Periods* (*Per1, Per2 and Per3*) and *Cryptochromes* (*Cry1 and Cry2*) that in turn repress the activity of the CLOCK:BMAL1 complex. These cycles of activation and repression take about 24 h to complete and they generate oscillations in several *clock-controlled genes* (*CCGs*) with periods of ~24 h. It has been estimated that in any mammalian tissue, about 5-20% of the expressed genes exhibit circadian oscillations in their messenger RNA (mRNA) levels. Rhythms in mRNA abundance are the result of the interplay between the autonomous cellular clock and external time cues (i.e. the light/dark cycle and the fasting/feeding cycle). It has been demonstrated that the fasting/feeding cycle is the dominant *Zeitgeber* (“time giver”) that drives rhythms of mRNA abundance in peripheral tissues. It has been estimated that most cycling mRNAs do not have a corresponding rhythm in their nascent RNA, this suggested that post-transcriptional mechanism play an important role in generating mRNA and protein oscillation. However, little is known about the molecular mechanisms involved in generating mRNA rhythms at post-transcriptional level.

The nuclear RNA binding protein Non-POU Domain Containing Octamer Binding (NONO) is a multifunctional protein that has been involved in many different steps of the mRNA life cycle from transcription, to processing, RNA stability and export. Furthermore, NONO is one of the main components of a subset of nuclear speckles called paraspeckles, whose function in the cell remains unclear. Importantly, NONO was found to interact with PER proteins and affect circadian

rhythmicity in flies and mammals, however the specific mechanisms of its function in circadian RNA expression are unknown.

In my thesis I have investigated the role of NONO in mammalian circadian gene expression and physiology. We found that feeding induces an increase in the number of NONO-containing, speckle-like structures in the nuclei of liver cells. In order to investigate NONO function in the fasting-feeding transition, we performed immunoprecipitation of NONO complexes in the liver nucleus and characterized bound RNAs and proteins. We found that NONO interacts with several RNA processing factors and that it primarily binds promoter-proximal introns of transcripts. This led us to hypothesize that NONO might be involved in the processing of its target RNAs. Furthermore, we found that the number of NONO-bound RNAs increases upon feeding and that about 40% of NONO target genes display circadian rhythmicity in their mRNA expression. We then showed that NONO regulates the rhythmicity and phase of these genes post-transcriptionally.

To further explore the role of NONO in liver physiology we characterized the function of its bound RNAs. We found that a large fraction of circadian NONO-bound RNAs encodes proteins implicated in glucose uptake and macronutrient metabolism. The absence of NONO-mediated regulation of target RNAs profoundly impacts metabolic health. Indeed, NONO-deficient mice exhibit impaired glucose tolerance, which can be rescued by re-expression of NONO specifically in the liver. NONO-deficient mice also show reduced capacity to store glycogen and lipids in the liver. We also found that NONO-deficient mice burn more fat during the fasting (resting) phase and maintain a lean phenotype throughout their life. We therefore propose that NONO coordinates pre-mRNA processing of metabolic genes with the fasting/feeding cycle, thus allowing efficient energy utilization and storage. Disruption of the temporal coordination between metabolic demand and gene expression leads to the development of metabolic diseases, like obesity and diabetes. Our findings help to better understand how metabolic homeostasis is maintained in mammals, and identify novel therapeutic targets for treating diabetes and other associated metabolic dysfunctions.

Zusammenfassung

Zirkadiane Rhythmen sind eine fundamentale Eigenschaft lebender Organismen, wie Menschen aber auch Cyanobakterien. Unter Isolation von zeitlichen Einflüssen zeigen diese immer noch rhythmische Verhaltensweisen und Zellvorgänge mit einer Zeitspanne von ca. 24 h. Diese Rhythmen werden von unseren inneren biologischen Uhr bestimmt.

Bei Säugetieren wird dieser molekulare Taktmechanismus durch transkriptionelle und translatorische Rückkopplungsschleifen angetrieben. Die Transkriptionsaktivator-Proteine, CLOCK und BMAL1, bilden heterogene Komplexe und aktivieren die Transkriptionsrepressoren PERIOD (PER1, PER2, PER3) und CRYPTOCHROME (CRY1, CRY2), welche wiederum die Aktivität des CLOCK:BMAL1-Komplexes unterdrücken. Diese Aktivations-Repressions-Zyklen dauern ungefähr 24 Stunden und erzeugen Oszillationen mit der gleichen Periodenlänge in weiteren Uhr-gesteuerten Genen (CCGs). Mehrere Studien haben gezeigt, dass etwa 5-20% der exprimierten Gene in Säugetiergeweben zirkadiane Oszillationen in ihrer mRNA-Konzentration aufweisen. Diese rhythmischen Unterschiede in der mRNA Konzentration ist das Resultat des Zusammenspiels zwischen der unabhängigen zellulären Uhr und von externen Zeiteinflüssen. Zu diesen gehören beispielsweise der Licht/Dunkel Zyklus durch die Sonne aber auch der Zeitpunkt der Ernährung. Es ist bekannt, dass der Fasten/Fütterungszyklus der dominierende Zeitgeber für rhythmische RNA-Expression im peripheren Gewebe ist. Es wird angenommen, dass die meisten zyklischen mRNAs in ihrem naszierenden Zustand keinen Rhythmus aufweisen. Die deutet darauf hin, dass post-transkriptionelle Mechanismen eine Rolle bei der Erzeugung von Oszillationen in der mRNA- oder Protein-Konzentration spielen. Allerdings ist bis heute wenig über die grundlegenden molekularen Vorgänge bekannt, welche bei den rhythmischen post-transkriptionellen Modifikationen beteiligt sind.

Das multifunktionale, nukleäre, RNA-bindende Non-POU Domäne enthaltende Oktamer bindende Protein (NONO) ist in vielen verschiedenen Schritten des mRNA-Lebenszyklus wie Transkription, Verarbeitung, Stabilität und Export beteiligt. Darüber hinaus ist NONO einer der Hauptkomponente einer Sorte

zellkerninterner Aggregate, welche Paraspeckles genannt werden. Deren exakte Funktion in der Zelle ist bisher aber unklar. Eine wichtige Aufgabe von NONO ist jedoch seine Interaktion mit PER-Proteinen, wodurch es durch bisher unbekannte Mechanismen die zirkadiane Rhythmizität bei Fliegen und Säugetieren beeinflusst.

Das Ziel dieser Arbeit ist die Charakterisation der Rolle von NONO in der zirkadianen Genexpression und der Physiologie von Säugetieren. Wir haben herausgefunden, dass Ernährung eine Zunahme der Anzahl NONO-haltiger, aggregatartiger Strukturen im Zellkern der Leberzellen hervorruft. Um die NONO-Funktion im Ernährungs-Zyklus zu studieren, führten wir Immunopräzipitation von NONO-Komplexen im Leber Zellkern durch und charakterisierten gebundene RNAs und Proteine. Wir haben herausgefunden, dass NONO mit mehreren RNA-Verarbeitungsfaktoren interagiert und dass es primär proximale Promotor Introns von Transkripten bindet. Dieses Resultat führte uns zu der Hypothese, dass NONO an der Verarbeitung seiner assoziierten RNAs beteiligt sein könnte. Darüber hinaus haben wir festgestellt, dass die Anzahl der NONO-gebundenen RNAs bei der Fütterung zunimmt und dass etwa 40% der NONO-assoziirten Gene eine zirkadiane Rhythmizität in ihrer mRNA-Expression aufweisen. Wir haben ebenfalls gezeigt, dass NONO die Rhythmizität und Phase dieser Gene post-transkriptionell reguliert.

Um die Rolle von NONO in Leberzellvorgängen weiter zu erforschen, analysierten wir die Funktion der gebundenen RNAs. Ein grosser Teil der zirkadianen NONO-gebundenen RNAs kodiert Proteine, welche wichtig für die Glukoseaufnahme und den Makronährstoffmetabolismus sind. Abwesenheit NONO-vermittelter Regulation assoziirter RNAs wirkt sich stark auf die metabolische Gesundheit aus. Tatsächlich zeigen NONO-defiziente Mäuse eine beeinträchtigte Glukosetoleranz. Diese kann jedoch durch spezifische Expression des Proteins in der Leber NONO-defizienter Mäuse normalisiert werden. NONO-defiziente Mäuse zeigen auch eine reduzierte Kapazität, Glykogen und Lipide in der Leber zu speichern und verbrennen mehr Fett während der Fasten-/Ruhe-Phase, was zu einem mageren Phänotyp während ihres ganzen Lebens führt.

Unser Fazit ist deshalb, dass NONO die prä-mRNA-Verarbeitung metabolischer Gene mit dem Fasten-/Fütterungszyklus koordiniert und so eine effiziente Energienutzung und -speicherung ermöglicht. Störung zeitlicher Koordination zwischen metabolischer Nachfrage und Genexpression kann zur

Entwicklung von Stoffwechselerkrankungen wie Fettleibigkeit und Diabetes führen. Unsere Ergebnisse helfen deshalb, besser zu verstehen, wie metabolische Homöostase bei Säugetieren funktioniert, und zur Identifikation neuer therapeutischer Massnahmen zur Behandlung von Diabetes und anderer damit verbundenen metabolischen Dysfunktionen.

1. GENERAL INTRODUCTION

BASIC PRINCIPLES OF MAMMALIAN CIRCADIAN BIOLOGY (adapted from Benegiamo et al., 2016)

Circadian rhythms represent a fundamental property of living organisms. Most organisms, from bacteria to humans exhibit behavioral and physiological rhythms when kept in temporal isolation. These rhythms are driven by biological clocks and have a period of approximately 24 h (Bell-Pedersen et al., 2005; Dunlap, 1999; Panda et al., 2002a). Internal clocks have two main features: (1) they are temperature-compensated (i.e. they do not have shorter or longer period with low or high temperatures); (2) they can be entrained by external stimuli such as light, temperature or feeding schedules. In this way, the internal time becomes predictive of the external (solar) one (Takahashi et al., 2008). Thus, circadian clocks confers an adaptive advantage to the organism by anticipating the day-night cycle and by temporally segregating mutually antagonistic processes (Reddy and O'Neill, 2010). Indeed, it has been demonstrated in prokaryotes, plants and mammals, that circadian clocks confer competitive advantage (Dodd et al., 2005; Libert et al., 2012; Woelfle et al., 2004), whereas disruption of circadian timing in humans, as seen in rotational shift workers, causes significant long-term health costs (Barger et al., 2009).

In mammals, the molecular clock mechanism is driven by transcriptional-translational feedback loops of activator and repressor proteins. The transcriptional activators CLOCK and BMAL1 heterodimerize and activate the transcription of the repressors *Periods* (*Per1, Per2 and Per3*) and *Cryptochromes* (*Cry1 and Cry2*). PERs and CRYs heterodimerize, translocate to the nucleus, and repress the activity of the CLOCK:BMAL1 complex (Lee et al., 2001). Subsequently, the PER-CRY repressor complex is degraded, and CLOCK:BMAL1 can now activate a new cycle of transcription. In an interconnected loop, the nuclear hormone receptors REVERBs and RORs act as repressors and activators respectively, to drive rhythmic transcription of clock components (Preitner et al., 2002; Sato et al., 2004) (**Figure 1**). These cycles of activation and repression take about 24 h to complete and they generate oscillations in several *clock-controlled genes* (*CCGs*) with periods of ~24 h. It has been estimated that in any mammalian tissue, about 5-20% of the expressed

genes exhibit circadian oscillations in their mRNA levels (Zhang et al., 2014). The molecular oscillator is cell autonomous and is present in every cell of multicellular organisms. The communication between individual cells of the same tissue generates organ-specific clocks. This crosstalk ensures that different cells of the same organ are synchronized to the same phase. The oscillation of a large network of cells is more robust than the oscillation of one single cell (Hogenesch and Herzog, 2011). The whole system is synchronized and aligned with the environment through signals emanating form the hypothalamic Suprachiasmatic Nucleus (SCN), a region in the brain consisting of ~20,000 neurons referred to as the master circadian clock (Mohawk et al., 2012). The SCN receives direct light input from the retina. The external light/dark cycle is the most important external stimulus that synchronizes the circadian clock (Dibner et al., 2010). After reaching the SCN, light stimulates the activation of signaling cascades that result in both neuronal and humoral output. These signals are transmitted to the peripheral tissue clocks. The light acts as a resetting signal for the SCN, which then synchronizes the peripheral tissue clocks accordingly (**Figure 2**).

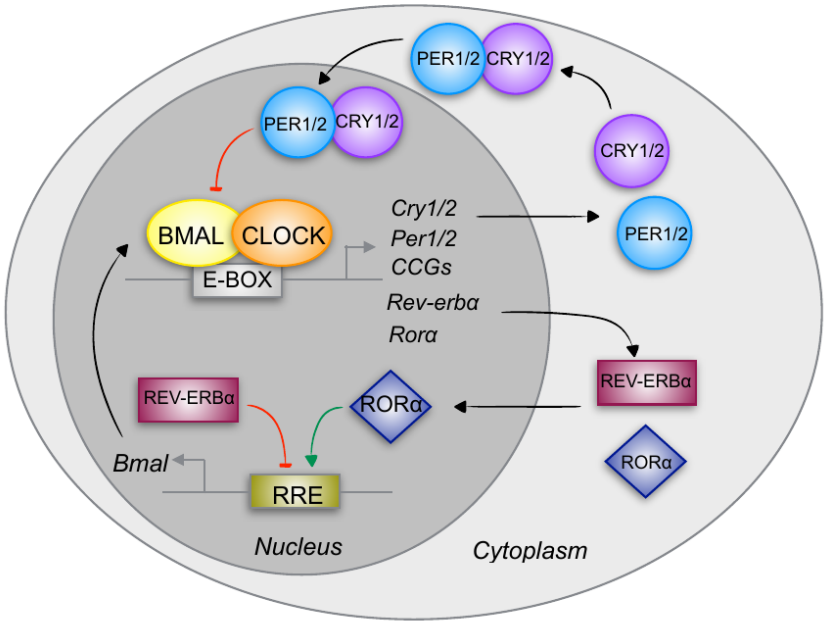

Figure 1. The mammalian circadian clock consists of negative and positive transcriptional transcriptional feedback loops. At the core of the positive feedback, the BMAL1/CLOCK heterodimer drives oscillating expression of clock-controlled genes (CCGs) with E-box containing promoters including Periods (Per1/2) and Cryptochromes (Cry1/2). The negative is feedback is driven by PER:CRY heterodimers that translocate back into the nucleus and repress their own transcription. Another layer of regulation is achieved through a second group of CCGs - RORα and REV-ERBα - that regulate BMAL1 transcription. The clock regulation on physiological processes, such as metabolism, is achieved through many genes with E-box containing promoters (CCGs).

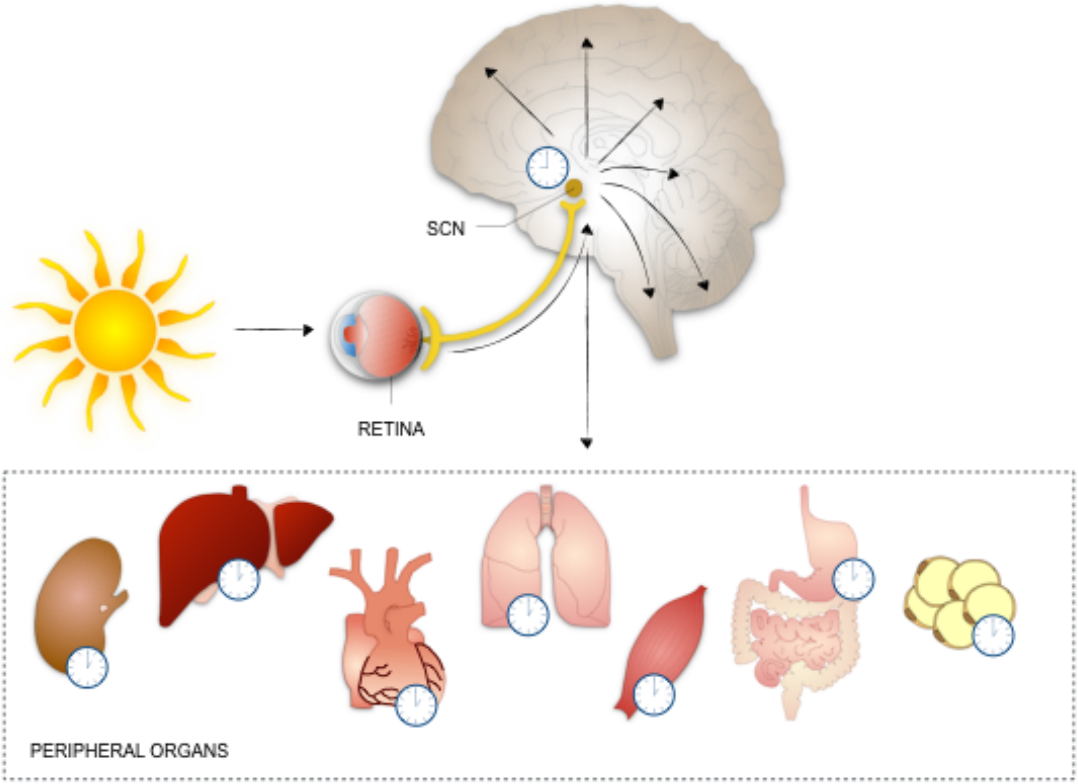

Figure 2. Hierarchical organisation of the circadian clock. The master pacemaker of the body is located in the suprachiasmatic nucleus (SCN) which receives direct light input through the eye. Neuronal and humoral signals from the SCN then synchronise clocks in other parts of the brain and in the peripheral organs to one another another and to the environment. Therefore, peripheral clocks show about 4 h phase delay with respect to the SCN. Adapted from Kondratova and Kondratov, Nat Rev Neurosci, 2012.

Most of our knowledge about genome-wide regulation of circadian gene expression in peripheral organs comes from experiments in mouse liver. In these experiments adult mice are fed a normal diet ad libitum and are entrained to a 12 h light: 12 h dark (LD) cycle. If the mice are held under LD cycle conditions during sample collection, the sampling times are defined as *zeitgeber* time (ZT) (from the German 'time giver'), where the time of lights-on is considered ZT0. If the mice are transferred to constant darkness prior to sample collection, the timing is represented as circadian time (CT), where CT0 corresponds to the subjective time of lights-on (equivalent to ZT0). The data collected from different times of at least one full day are fitted to a wave function, so that the probability values related to robustness of oscillation and the peak time of oscillation (phase) can be derived. Detected oscillation in molecules or their activities in the associated phases can be used to explain potential sequence of regulatory events. Due to changes in experimental conditions and sampling frequency, the circadian rhythm parameters might differ

among different studies.

CIRCADIAN REGULATION OF GENE EXPRESSION

The circadian cistrome (adapted from Benegiamo et al., 2016)

Although previous studies investigated the transcriptional regulation of CLOCK:BMAL1 on specific target genes, the identity of the circadian cistrome (i.e. the *in vivo* genome-wide location of core clock transcription factor binding-sites) has only recently been identified. Using chromatin immunoprecipitation followed by sequencing (ChIP-seq), several research groups have identified genome-wide DNA-binding sites for BMAL1, CLOCK, PER1, PER2, CRY1 and CRY2 in the mouse liver (Koike et al., 2012; Menet et al., 2012; Rey et al., 2011; Yoshitane et al., 2014). CLOCK and BMAL1 bind to more then 4600 and 5900 sites, respectively, corresponding to ~3000 unique genes in the liver (Koike et al., 2012). On a genome-wide level, CLOCK and BMAL1 occupancy peaks during the middle of the day (ZT3-5), however, although CLOCK:BMAL1 target genes are significantly enriched for rhythmic transcribed genes, there is a large discrepancy between the phases of rhythmic BMAL1 DNA binding and the phases of rhythmic transcription. The peaks of transcription of CLOCK:BMAL1 target genes appear much more broadly distributed. This wide, disconnect between the peak phases of CLOCK:BMAL1 DNA binding and the phases of rhythmic transcription of the target genes suggests that other factors and/or mechanisms may collaborate with CLOCK:BMAL1 binding and are critical to determine oscillation phases. In contrast to the activators, the repressors PER1, PER2 and CRY2 bind genome-wide at night between CT12 and CT20, peaking between CT15 and CT17. CRY1 has a distinct bimodal pattern, with a major peak at CT0. The repressors CRY1 and CRY2 bind to significantly more sites in the genome than PER1 and PER2, with many thousands of these sites being independent of CLOCK-BMAL1 and containing DNA-binding motifs for nuclear receptors (Koike et al., 2012; Takahashi, 2017)

Circadian regulation, RNAPII occupancy and chromatin states (adapted from Benegiamo et al., 2016)

In order to characterize global rhythms in transcription, RNA polymerase II (RNAPII)

occupancy has been measured during the circadian cycle in the mouse liver (Koike et al., 2012; Le Martelot et al., 2012). The large subunit of RNAPII contains a carboxy-terminal domain (CTD) that is post-translationally modified at different stages of transcription. When RNAPII gets recruited to the pre-initiation complex is hypophosphorylated (recognized by the 8WG16 antibody), whereas the first step in the initiation of RNAPII involves phosphorylation on Ser5 of the CTD (Chapman et al., 2007; Jones et al., 2004). Both RNAPII-8WG16 and RNAPII-Ser5 occupancy are highly circadian in the mouse liver, indicating that both recruitment and initiation of RNAPII are under circadian control (Koike et al., 2012). Rhythmic loading of RNAPII to promoters, rather than a rhythmic transition from a paused state to a productive elongation, seem to be responsible for the majority of rhythmic transcription in the mouse liver (Le Martelot et al., 2012).

Histone modifications associated with RNAPII transcription during the circadian cycle have also been investigated in recent studies (Koike et al., 2012; Le Martelot et al., 2012; Vollmers et al., 2012). Histone modifications define, alone or in a combinatorial manner, major chromatin domains at promoters (H3K4me3, H3K27ac, and H3K9ac), gene bodies (H3K36me3 and H3K79me2) and enhancers (H3K27ac and H3K4me1). Histone H3K4me3, H3K9ac, H3K27ac and H3K4me1 show robust circadian rhythms at transcription start sites (TSSs). Also the elongation marks, H3K36me3 and H3K79me2, display circadian modulation. Rhythmic histone modifications are observed both at promoter proximal sites and at distal intergenic enhancer sites. The genome-wide analysis of the rhythmicity and phase of these histone marks revealed that several genes exhibit circadian rhythms in histone modifications. However, the total number of histone modification sites does not seem to vary on a circadian basis. The recruitment (and initiation) of RNAPII seems to drive the variation in the amplitude on histone marks. Thus, circadian transcriptional regulation appears to be involved in the initial stages of RNAPII recruitment and initiation and the histone modification associated with these events to set the stage for gene expression on a global scale (Koike et al., 2012; Le Martelot et al., 2012; Vollmers et al., 2012).

Genome-wide circadian RNA expression analysis (adapted from Benegiamo et al., 2016)

To examine the functional consequences of the circadian cistrome, rhythmic RNAPII occupancy and rhythmic histone modifications, RNA sequencing (RNA-seq) has been used to profile cycling mRNA expression in the mouse liver (Koike et al., 2012; Le Martelot et al., 2012; Menet et al., 2012; Vollmers et al., 2012). As mentioned above thousands of genes (~5-20% of expressed genes) were found to cycle at the steady-state mRNA level in the liver as well as in many other tissues (Hughes et al., 2009; Zhang et al., 2014) and more then half of all genes have been found to cycle at the mRNA level in at least one tissue (Zhang et al., 2014).

A wide range of cycling RNA species has been found using RNA-seq. In addition to cycling protein-coding transcripts, oscillating long non-coding RNAs, microRNAs and antisense RNA transcripts have been found in the mouse liver. Furthermore, in addition to circadian transcription at promoters, circadian transcriptional activity at enhancer regions was recently demonstrated in the mouse liver (Fang et al., 2014) using global run-on sequencing (GRO-seq) (Core et al., 2008). Transcriptional activity at enhancers produces enhancer associated non-coding RNAs called enhancer RNAs (eRNAs; Kim and Shiekhattar, 2015). Thousands of circadian eRNAs have been found to oscillate in diverse phases and each phase group is enriched in binding motives for different classes of clock transcription factors. For example, E-box motifs are enriched between ZT6 and ZT9, corresponding to the peak of CLOCK-BMAL1 occupancy, whereas RORE and REV-DR2 motifs are enriched between ZT8 and ZT24, corresponding with the trough of REV-ERB repression. Circadian eRNAs transcription correlates and can predict rhythmic transcription of nearby genes. Circadian transcription factors like CLOCK/BMAL1 and REV-ERB α bind multiples sites in the genome; however, many of these genes are bound but don't seem to be regulated, due perhaps to inactive binding or long distance looping at different genes. Transcriptional activity at enhancers could be used as a marker to assess where a transcription factor is actually functional (Fang et al., 2014).

The contribution of transcriptional mechanisms in generating steady-state mRNA rhythms has been examined in the mouse liver either by using the intron

RNA-seq signal as a proxy for premature RNA (pre-mRNA) and the exon RNA-seq signal as a proxy for mature mRNA (Koike et al., 2012), or by using nascent-seq and mRNA-seq as a proxy for transcriptional activity and mature mRNA levels, respectively (Menet et al., 2012). In the mouse liver, cycling pre-mRNA levels (using the intron RNA signal) are coordinately expressed in time with a peak at CT15. Thus, there is a peak of globally coordinated circadian transcription that occurs at the beginning of the night during the active portion of the mouse circadian rhythm, which is not seen at the mRNA level (which has a bimodal pattern). The intron RNA peak also correlated with the peak of RNAPII-8WG16 occupancy at CT14 (Koike et al., 2012). These studies identified two divergent sets of cycling genes: cycling nascent transcripts and cycling mRNA levels. Only ~30% of cycling mRNAs also had a corresponding cycling nascent transcript, indicating that other RNA processes are likely to be contributing to steady-state circadian mRNA expression. At least three different classes of cycling transcripts have been observed: (1) cycling transcription and cycling steady-state mRNA; (2) cycling transcription and no cycling mRNA; (3) no detectable cycling transcription but cycling mRNA levels. To the first class belong the core circadian genes and their high-amplitude direct targets. The second class is typically composed of highly expressed genes in the liver that have mRNAs with long half-lives, such as albumin. The third class includes transcripts that may become rhythmic via circadian oscillation in post-transcriptional mechanisms such as mRNA turnover, splicing, polyadenylation, microRNA regulation and others (Takahashi, 2017). Taken together, steady-state mRNA rhythms are only one of a multitude of layers of circadian regulation in gene expression. Virtually every regulatory stage in gene expression that has been examined in detail – including transcription, splicing, termination, polyadenylation, nuclear export, microRNA regulation, translation and RNA degradation – has revealed additional layers of circadian control (Kojima and Green, 2015; Lim and Allada, 2013).

Evidences for the relevance of post-transcriptional mechanisms on circadian gene expression (adapted from Benegiamo et al., 2016)

Although circadian regulation of mRNA expression at the transcriptional level is important for circadian rhythms in gene expression, a growing body of evidence suggests that transcriptional mechanisms are not sufficient to sustain all rhythmic

mRNA expression. The transcription rate varies significantly in cells from different tissues (Schmidt and Schibler, 1995), yet the free-running endogenous circadian oscillator shows remarkable stability in period length among tissue types. Thus, the oscillator possesses a mechanism that allows compensating for differences in transcription rates. Furthermore, partial inhibition of transcription by α-amanitin treatment in mouse fibroblasts reduces RNAPII dependent transcription rate by up to threefold, but doesn't stop the cell-autonomous oscillator. The circadian oscillator, as measured by translated protein, continues to oscillate, albeit with dampened amplitude and slightly shorter periodicity (Dibner et al., 2009). This suggests that post-transcriptional mechanisms potentially involving mRNA-binding proteins can support translational rhythm even when transcriptional oscillation is blunted or inhibited.

Studies in human red blood cells, which have no DNA or nucleus (and therefore cannot perform transcription), showed that, at least in some cases, transcription is not required for circadian oscillation, and that non-transcriptional events seem to be sufficient to sustain peroxiredoxin rhythms. Indeed, it was demonstrated that red blood cells (RBCs) exhibit robust rhythms in peroxiredoxin redox cycles. This finding is consistent with the presence of a circadian clock within these cells despite the lack of nucleus and thus the inability to make new RNA. In normal nucleated cells, there is probably an intricate interplay between transcription-dependent processes and non-transcriptional oscillation, as there seems to be reciprocal regulation between these systems (O'Neill and Reddy, 2011).

A first study analyzing the liver circadian proteome using two dimensional difference gel electrophoresis (2D-DIGE) found up to 20% of soluble proteins in mouse liver being subject to circadian control and only 50% of them had a corresponding cycling mRNA, revealing for the first time the extent of post-transcriptional control mechanisms as circadian control points for protein oscillations. More recently, SILAC technology has been applied to study the circadian liver proteome (Mann, 2006). In two different studies about 3000 and 5000 different proteins were identified and 6-10% of them were determined to be rhythmic in the mouse liver. Among these proteins however only 50-80% had rhythmically expressed corresponding mRNAs, further indicating that rhythmicity in mRNA and rhythmicity in protein do not necessarily correlate (Mauvoisin et al., 2014; Robles et

al., 2014). Furthermore, for rhythmic proteins with corresponding rhythmic transcripts, there was a significant difference in the phase distribution between cycling transcripts and corresponding proteins. This divergence in the distribution of transcript and protein phase indicates that the cycles of protein abundance in the mouse liver do not always reflect mRNA changes and are instead likely influenced by post-transcriptional mechanisms. The delay between the peak phase of expression of each rhythmic transcript and its oscillating protein is about 2-6 h for almost 50% of the cycling mRNA and proteins. However, around 40% of oscillating proteins peaked more then 6 h later than their corresponding transcripts. This time delay between peaks of mRNA and protein revealed that post-transcriptional mechanisms likely define the circadian phases of the proteome. Importantly, rhythmic proteins associated to specific pathways had similar phases of oscillation regardless of whether and in which phase their transcripts were cycling. This implies that circadian post-transcriptional regulation coordinates individual metabolic pathways in the liver (Robles et al., 2014). Taken together, recent transcriptome and proteome studies revealed that post-transcriptional regulatory mechanisms are an important feature of the circadian clock and contribute to both steady state mRNA and protein oscillations.

Circadian regulation of splicing (adapted from Benegiamo et al., 2016)

Alternative splicing is a regulated process during gene expression that results in a single gene coding for multiple proteins. In this process, particular exons of a gene may be included within, or excluded from, the final, processed mRNA. Alternative splicing is of particular importance amongst the post-transcriptional processes that regulate gene expression, as it allows the human genome to direct the synthesis of many more proteins than would be expected from its 20,000 protein-coding genes. Alternative splicing is widespread in mammalian genes, affecting approximately 95% and 80% of multi-exon genes in humans and mice, respectively (Mollet et al., 2010; Wang et al., 2008). Moreover, alternative splicing is highly regulated by the activity, abundance and binding position of various splicing factors and heterogeneous nuclear ribonucleoproteins, and by the kinetics of transcription elongation and chromatin modifications (Luco et al., 2011; Nilsen and Graveley, 2010; Witten and Ule, 2011). Evidence for the existence of circadian oscillation in mammalian

alternative splicing came recently from a study that found several exons to be alternatively spliced in a circadian manner in the mouse liver (McGlincy et al., 2012). In a microarray based approach, 55 exon-probesets from 47 genes where identified to have significant circadian variation, corresponding to 0.4% of the genes detectable in the array. The 47 genes were enriched in pathways representing the circadian clock itself, drug detoxification, caffeine and retinol metabolism and the peroxisome proliferator-activated receptor (PPAR) signaling pathway. The circadian regulation of alternative splicing was shown to be tissue dependent, in terms of both phase and amplitude. For some of the exons identified the temporal relationship between alternative splicing and transcript level expression was preserved across tissues, suggesting that these two processes may be coupled. Alternative splicing of the identified exons was demonstrated to be under the control of the local liver clock (McGlincy et al., 2012). However, the proportion of alternative splicing events regulated by the circadian clock seems to be modest compared to other clock-controlled processes (e.g. circadian regulation of mRNA abundance, affecting 5-20% of expressed genes).

The same microarray study also reported circadian mRNA expression of 62 RNA-binding proteins, which might be involved in the regulation of circadian RNA-processing events. These 62 proteins include some known regulators of alternative splicing (*Srsf3*, *Srsf5*, *Tra2b* and *Khdrbs1* (*Sam68*)), one component of the U2 snRNP (*Sf3b1*), two RNA helicases (*Ddx46* and *Dhx9*), three hnRNP proteins (*Hnrnpdl*, *Cirbp* (hnRNP-A18) and *Pcbp2* (hnRNP E2)), and six other RNA-binding proteins that have less well characterized roles in RNA metabolism (*Gtl3*, *Rbms1*, *Thoc3*, *Pcbp4* and *Topors*). Some of these circadian splicing factors were found to be under the control of the liver clock, while others were rhythmic in response to systemic cues. Some of the known exon targets of these splicing factors where previously identified to be cycling exons. The discovery of robustly circadian splicing factors, and the fact that a number of their previously characterized target exons are circadian, provide candidates for further study into the molecular mechanisms regulating circadian exons and other post-transcriptional processes (McGlincy et al., 2012). The first functional connection between alternative splicing and the mammalian circadian clock was described for the mRNA encoding U2-auxiliary-factor 26 (U2AF26). U2AF26 undergoes rhythmic alternative splicing that contributes

to the regulation of *Per1* stability (Preußner et al., 2014). Specifically, U2AF26 undergoes circadian and light-induced alternative skipping of exons 6 and 7 (U2AF Δ E67) in mouse cerebellum and this splicing switch generates a shift in the mRNA reading frame. Skipping of U2AF26 exons 6 and 7 generates a domain with homology to Drosophila TIM and enables cytoplasmic, circadian expression of the U2AF26 Δ E67 isoform. U2AF26 Δ E67 interacts with PER1 and induces its proteasomal degradation; this limits the light induced increase of PER1 and it's proposed as buffering mechanism against sudden light changes (Preußner et al., 2014).

Circadian regulation of transcription termination (adapted from Benegiamo et al., 2016)

Transcriptional termination is a newly identified target for negative feedback regulation of the clock. In addition to its well known transcriptional repressor function, PER rhythmically associates with the RNA helicases DEAD-box polypeptide 5 (DDX5), DEAH-box protein 9 (DHX9) and Senataxin (SETX). DDX5 and DHX9 are components of the 3' transcriptional termination complex (Shi et al., 2009). This PER-containing termination complex specifically binds clock gene transcripts such as *Per1* and *Cry2* mRNAs in a circadian time-dependent manner. After cleavage of the nascent transcript, unwinding of the RNA-DNA duplex by SETX at the 3′ termination site permits the XRN2 nuclease to degrade the downstream 3′ RNA and thereby release the polymerase (Skourti-Stathaki et al., 2011). PER complex inhibits SETX activity, blocking subsequent processing by XRN2 and thus blocking transcription termination. Inhibition of termination reduces the rate of transcription, and as a consequence during the negative feedback, RNA polymerase II accumulates at the 5′ site as well as at the 3′ site of *Per* and *Cry* genes (Padmanabhan et al., 2012). Thus, the mammalian PER complex has at least two actions in circadian feedback: (1) it represses transcription by recruiting a SIN3 histone deacetylase complex to clock gene promoters (Duong et al., 2011), and (2) it inhibits termination by antagonizing the action of SETX at the 3′ termination site. Both processes contribute to circadian *Per* gene repression, but one or the other could predominate at different target genes (Padmanabhan et al., 2012).

Circadian regulation of polyadenylation (adapted from Benegiamo et al., 2016)

In eukaryotes, polyadenylation of RNA (i.e. the addition of a tail consisting of multiple adenosine monophosphates at the 3' end of an RNA) is part of the process that produces mature mRNA. Most eukaryotic mRNAs are polyadenylated and this process is required for nuclear export and stability of mature transcripts and for efficient translation (Sachs, 1990). The length of the poly(A) tail is important, as mRNAs with tails that are too short are, in general, subjected to enzymatic degradation (Guhaniyogi and Brewer, 2001) or stored in a translationally dormant state (D'Ambrogio et al., 2013). Although the addition of a poly(A) tail seems to occur by default, the subsequent control of its length is highly regulated both in the nucleus and in the cytoplasm, thereby contributing to the regulation of the stability, transport and translation of mature transcripts (Zhang et al., 2010).

One of the earliest examples of daily regulation of poly(A) tail lengths was reported for vasopressin, a key rhythmic neuropeptide in the SCN (Robinson et al., 1988). Later, the deadenylase nocturnin (*Noc*) was identified as a rhythmically expressed gene in the *Xenopus laevis* retina (Green and Besharse, 1996), as well as in several mouse tissues (Wang et al., 2001). A serum shock and the phorbol ester TPA can induce *Noc* transcript levels in quiescent NIH3T3 cultures while dexamethasone and forskolin, which are known to induce other clock genes in culture, have no effect. Hence, in addition to its robust circadian regulation, *Noc* expression can be regulated acutely and it can respond directly and specifically to physiological cues (Garbarino-Pico et al., 2007). In mice, disruption of the *Noc* gene confers resistance to diet induced obesity but does not affect free-running locomotor rhythms or clock gene expression, suggesting its role in circadian output pathways (Green et al., 2007).

The question of global clock control of polyadenylation state has been addressed most completely in the mouse liver (Kojima et al., 2012). About 2.3% of all expressed mRNA exhibit statistically significant rhythmicity in their poly(A) tail length. Most of these "poly(A) rhythmic" (PAR) mRNAs have their peak in poly(A) tail length during the night (ZT16-ZT20). Based on the pre-mRNA and steady-state mRNA profiles, the PAR mRNAs can be categorized into three classes: Class I PAR

mRNAs (49.2%) are rhythmic in their poly(A) tail length and pre-mRNA and steady-state mRNA levels, class II PAR mRNAs (32.3%) are rhythmic in their poly(A) tail length and pre-mRNA expression but not in steady-state mRNA levels, and class III PAR mRNAs (18.5%) are rhythmic in their poly(A) tail length rhythms but not in pre-RNA or steady-state mRNA levels. Most likely, for the class I/II PAR mRNAs, nuclear polyadenylation follows rhythmic transcription, since both classes exhibit rhythmic pre-mRNA levels. The defining characteristics of these two classes are the differences in the steady-state mRNA rhythmicity and mRNA stability (the lack of rhythmicity in the class II PARs mRNAs probably reflects the longer half-lives of these mRNAs). Class III mRNAs display robust rhythmicity in their poly(A) tail length, but are not rhythmically transcribed and have longer half-lives. Thus, this class employs some non-transcriptional mechanisms to control their rhythmic poly(A) tail lengths. The analysis of the peak phase distribution of class III PAR mRNAs revealed that for more then 80% of them the longest poly(A) tail occurred during the day. The mRNA level of several components of the cytoplasmic polyadenylation machinery in the liver were rhythmically expressed with phases similar to the majority of the class III PAR mRNAs. These components included the Cytoplasmic Polyadenylation Element Binding Protein 2 and 4 (Cpeb2, Cpeb4), the Polyadenylate Specific Ribonuclease (Parn), and Gld2. Thus, the poly(A) rhythms of the class III mRNAs are likely to be controlled by rhythmic cytoplasmic polyadenylation mechanisms. The rhythmic poly(A) tail lengths correlate with the circadian expression profiles of the corresponding protein, with the protein usually peaking ~4–8 h after the time of the longest poly(A) tail. In conclusion, it was demonstrated that poly(A) tail rhythms are capable of generating rhythmic protein levels even when in the absence of rhythm in the steady-state mRNA levels (Kojima et al., 2012).

Circadian regulation of mRNA stability (adapted from Benegiamo et al., 2016)

The control of mRNA half-life can potentially generate rhythms in mRNA abundance in the absence of rhythms in newly synthesized pre-mRNA. The post-transcriptional regulation of mRNA stability is mediated by cis elements in the mRNAs that interact with RNA-binding proteins and/or microRNAs. In most cases, these cis elements reside in the 3’ untranslated region (UTR). The 3’ UTR-dependent mRNA decay is

involved in the regulation of the circadian oscillation of *Per2* mRNA. The polypyrimidine tract binding protein (PTB), also known as heterogeneous nuclear ribonucleoprotein I (hnRNPI), binds to *Per2* 3' UTR and destabilizes its mRNA. Indeed, rhythmic abundance in *Per2* mRNA is in antiphase with that in cytoplasmic PTB protein levels and depletion of PTB results in *Per2* mRNA stabilization (Woo et al., 2009). The 3′ UTR is also important for the mRNA stability of *Cry1*. The 3' UTR of *Cry1* contains a destabilizing element that affects its mRNA stability. The RNA-binding protein hnRNPD was found to oscillate and bind to the middle region of *Cry1* 3' UTR with a rhythmic profile. The binding of hnRNPD to *Cry1* 3' UTR is responsible for the rapid decay of its mRNA during its declining phase and modulates *Cry1* circadian rhythm (Woo et al., 2010). The stability of mouse *Period3* (*Per3*) is also regulated in a circadian phase-dependent manner. In the case of (*Per3*), the control of its circadian mRNA stability requires the cooperative function of both the 5' and 3' UTRs. The RNA-binding protein hnRNPQ binds to both the 5' and 3' UTR in the *Per3* mRNA and destabilizes the mRNA. Indeed, downregulation of hnRNPQ reduces the translation efficiency but also increases *Per3* mRNA stability. The binding of hnRNPQ to *Per3* 5' UTR is phase dependent and maintains robust *Per3* oscillation (Kim et al., 2011).

Circadian regulation of translation and ribosome biogenesis (adapted from Benegiamo et al., 2016)

In addition to mRNA stability, cis-regulatory elements can influence the translation efficiency of the mRNA. Heterogeneous nuclear ribonucleoproteins (hnRNPs) have been shown to be involved in translation of clock and clock-related transcripts through their association with target UTRs in mammals. The RNA binding protein RBM4 (homologous of the Drosophila Lark) has been shown to activate the post-transcriptional expression of the mouse *Per1* mRNA. A strong circadian cycling of the RBM4 protein is observed in the suprachiasmatic nuclei with a phase similar to that of PER1, although the level of the *Rbm4* transcripts are not rhythmic. RBM4 protein binds directly to a cis-element in the 3' UTR of the *Per1* mRNA and causes increased PER1 protein levels, by activating *Per1* mRNA translation. Alterations of *Rbm4* expression in cycling cells causes significant changes in circadian period, with *Rbm4* knockdown by siRNA resulting in a shorter circadian period, and *Rbm4*

overexpression resulting in a lengthened period (Kojima et al., 2007). HnRNPQ binds and activates internal ribosome entry site (IRES)-dependent translation (hence, cap-independent) from 5' UTRs in *Per1* and the arylalkylamine N-acetyltransferase (AANAT) gene, which encodes an enzyme important for pineal melatonin rhythms (Kim et al., 2007; Lee et al., 2012). IRES-dependent translation of Rev-erbα is also enhanced by hnRNPQ and PTB (Kim et al., 2010).

Interestingly, among rhythmically expressed genes in the liver, there are a large number of genes encoding proteins involved in translation. These proteins include components of the translation pre-initiation complex (Hughes et al., 2009; Panda et al., 2002b). In the inactive state, the pre-initiation complex is composed of the mRNA cap-binding protein eukaryotic translation initiation factor 4E (EIF4E) bound to the hypophosphorylated form of EIF4E-binding protein (4E-BP) that acts as a repressor of translation. Upon stimulation, 4E-BP is phosphorylated and EIF4E is released. EIF4E can then interact with the eIF4G and with the rest of the EIF4F complex (EIF4A, EIF4B, and EIF4H) to initiate translation. Analyses of other factors involved in translation initiation by reverse transcription (RT)-PCR confirmed that the mRNAs of most of them are rhythmically expressed. While their protein abundance does not oscillate, these factors undergo rhythmic phosphorylation. The relative amount of polysomal RNA fraction (a RNA subfraction composed mainly of actively translated RNAs) follows a diurnal cycle, suggesting that rhythmic translation does occur in the mouse liver. Approximately 2% of the expressed genes are rhythmically translated but have no rhythm in mRNA abundance. While the total mRNA levels are constant, the polysome-bound mRNA levels oscillate with a period of 24h. Among genes regulated at the level of translation, 70% were found in polysomes in the same time interval. Most of the translationally regulated genes had phases starting at ZT8, before the start of the mouse feeding phase, and finishing at the end of the dark phase (Jouffe et al., 2013). More recently ribosome profiling coupled with RNA-seq (RPF-seq) was used to determine the position of translating ribosomes transcriptome wide and to establish a quantitative, high-resolution map of the mouse liver translatome around the clock. This strategy identified a set of 147 rhythmically translated, but otherwise non-oscillating, mRNAs with a dominant peak phase distribution around the day-to-night transition (ZT10-ZT16) (Janich et al., 2015). Interestingly, mRNAs coding for ribosomal proteins (RPs) are also associated with

polysomes only towards the end of the light phase (ZT8) and during the dark phase. Therefore, RPs oscillates with highest expression during the night. The synthesis of the 45S rRNA (a ribosome constituent precursor) is also circadian and it's synchronized with RP mRNA transcription. This indicated that all the elements involved in ribosome biogenesis are transcribed in concert and coordinated with the feeding period. Ribosomal protein synthesis in eukaryotes is a major metabolic activity that involves hundreds of individual reactions; this energy-consuming process has to be confined to a time when energy and nutrients are available in sufficient amounts, which, in the case of rodents, is during the night (Jouffe et al., 2013).

THE RNA-BINDING PROTEIN NONO (P54NRB)

The regulation of gene expression involves the dynamic interaction between proteins, DNA and RNA. To control and integrate numerous different components throughout gene regulation, cells need factors that can bridge nucleic acids and proteins. One such example of bridging protein is the 'multifunctional' RNA-binding protein Non-POU domain-containing octamer-binding (NONO, a.k.a. p54nrb) (Knott et al., 2016). NONO belongs to the Drosophila behavior human splicing (DBHS) family of RNA binding proteins. The DBHS family as well as the multiple known functions of NONO are discussed below.

The DBHS family

The DBHS proteins are defined by highly conserved tandem N-terminal RNA recognition motifs (RRMs), a NonA/paraspeckle domain (NOPS) that mediates protein-protein interactions and a C-terminal low complexity coiled-coil. These domains constitute the conserved core of ~300 amino acids defined as the 'DBHS domain' (Dong et al., 1993). Outside of this conserved domain, the members of the DBHS family are significantly different, both in their length and in their sequence complexity (**Figure 3**). The DBHS proteins are found exclusively within vertebrates and invertebrates. In mammals, there are three members of the family: NONO, splicing factor proline/glutamine rich (SFPQ a.k.a PSF) and paraspeckle protein component 1 (PSPC1 a.k.a. PSP1). In contrast, invertebrates have one or two

members: NonA and NonA-like in *Drosophila melanogaster*, and NONO-1 in *Caenorhabditis elegans*. DBHS proteins are predominantly nuclear as their C-terminus contains a nuclear localization signal. In certain conditions, these proteins can be found in subnuclear bodies named paraspeckles or localized to chromatin or DNA damage foci (Bond and Fox, 2009; Fox and Lamond, 2010; Shav-Tal and Zipori, 2002). All the three members of the DBHS family can form homo- and heterodimers with each other and structural and biological data suggest that they rarely function alone. Possessing both protein-protein and protein-nucleic acid binding sites, DBHS proteins can behave as a 'molecular scaffold'.

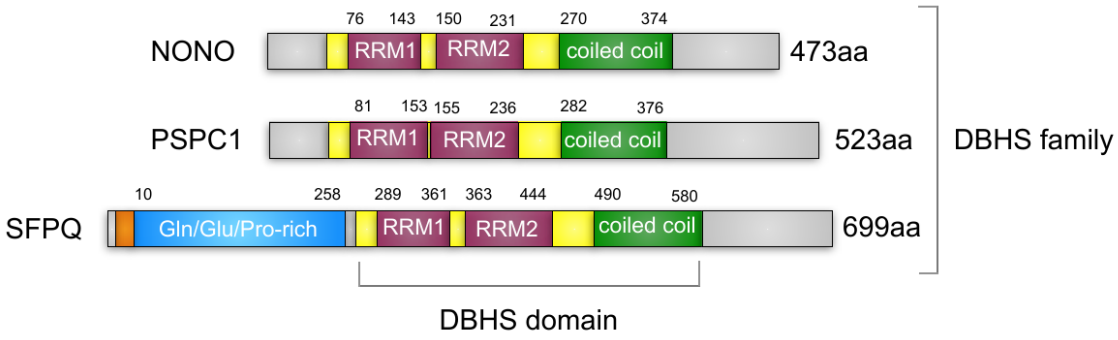

Figure 3. DBHS proteins domain architecture. Schematic representation of DBHS protein domain architecture with the structurally characterised RNA recognition motifs RRM1 and RRM2 (purple) and the coiled-coil domain (green). The region of homology among the three members of the DBHS family is defined as 'DBHS domain'. The corresponding amino acid boundaries are indicated above the schematic for NONO, PSPC1 and SFPQ (*Mus Musculus*). The total length in amino acid is indicated on the right of each protein.

NONO functions at multiple levels to regulate gene expression

NONO can act as a transcriptional co-activator and co-repressor

NONO, alone or in complex with other members of the DBHS family, has been involved in both transcriptional activation and repression. Transcriptional repression seem to be largely driven by and dependent on interaction with SFPQ and recruitment of epigenetic silencers such as Sin3A and HDAC (Dong et al., 2005, 2007, 2009). Instead, transcriptional activation seems to be driven mostly by NONO, and it involves both the binding and processing of the nascent RNA as well as the interaction with components of the transcriptional machinery. SFPQ/NONO heterodimer can act as transcriptional repressors by sequestering activators away

from target promoters (Dong et al., 2005). Contrary to transcriptional silencing, it appears that transcriptional activation is dependent on the presence of the nascent RNA, which may act as a scaffold (Knott et al., 2016). NONO can associate with many transcriptionally active genes (Yadav et al., 2014). In order to mediate transcriptional activation, NONO interacts with other transcriptional activators. For example, NONO interact with photoreceptor transcription factor, and enhances rhodopsin expression (Yadav et al., 2014). NONO was found to facilitate the association of RNAPII with cAMP-dependent promoters (Amelio et al., 2007). The recruitment of NONO into transcriptionally active contexts appear to be also dependent on the presence of the RNA, as for the activation of *Survivin* expression (Yamauchi et al., 2012). It is not clear if these functions of transcriptional activation can be attributed to NONO alone, or in complex with other DBHS members. Whether NONO acts as an activator or a repressor on a specific gene might be dependent on its binding partners, modification status, cell-type specific expression and localization (Knott et al., 2016).

The role of NONO in post-transcriptional processing, RNA stability and export

It has been suggested that NONO may couple transcription to post-transcriptional processing (Emili et al., 2002; Montes et al., 2012), namely through a persistent association with nascent RNA. NONO and SFPQ have been identified as spliceosome-associated proteins (Gozani et al., 1994; Hallier et al., 1996; Lutz et al., 1998) and associated with U5 snRNA early in the formation of the spliceosome (Peng et al., 2002). NONO interacts with the 5' splice site (Kameoka et al., 2004) and SFPQ was found in the spliceosome (Peng et al., 2006). However, DBHS proteins are not essential components of the spliceosome, but rather play a role in alternative and co-transcriptional splicing. The SFPQ/NONO heterodimer can also facilitate polyadenylation and pre-mRNA cleavage (Hall-Pogar et al., 2007; Kaneko et al., 2007; Liang and Lutz, 2006).

Beyond post-transcriptional processing, NONO is thought to contribute to maintaining transcript stability. For example, NONO and SFPQ are known to regulate the stability of non-coding RNA, such as the non-coding RNA Neat1 (Fox et al., 2002). Given its diffuse localization and broad nucleic acid specificity; it is likely that NONO may function in degenerately coating nascent transcripts for stabilization (Knott et al., 2016).

NONO can also remain associated with the processed messenger ribonucleoprotein particle (mRNP) once formed. In neuronal cells NONO and SFPQ are components of RNA transport granules in the neurites (Kanai et al., 2004). RNA transport in neurons is important for local translation at the synapses. SFPQ and NONO can stimulate the export of snRNA by facilitating the recruitment of the phosphorylated adaptor for RNA export (PHAX) (Izumi et al., 2014).

Paraspeckle formation and nuclear RNA retention

NONO is a main component of nuclear paraspeckles. Paraspeckles are subnuclear bodies located in the interchromatin space of the nucleus (Fox et al., 2002) and are defined by the colocalization of the DBHS proteins with the long non-coding RNA *Neat1*. NONO seem to be essential for paraspeckle formation and integrity, as paraspeckles disassemble upon siRNA knockdown of NONO (Sasaki et al., 2009). NONO directly bind *Neat1* and likely stabilizes the RNA, as loss of NONO was reported to reduce *Neat1* levels (Sasaki et al., 2009). Although the function of paraspeckles is not fully understood, the identity of the associated proteins provides some clues (Scadden, 2009). Specifically, the presence of NONO in paraspeckles suggests that they may be involved in retention of mRNAs that have undergone A-to-I editing by dsRNA-dependent adenosine deaminases (ADARs). Indeed, previous studies showed that a NONO-containing complex specifically interacts with mRNAs having structured or edited 3'-UTRs to prevent their nuclear export (Chen and Carmichael, 2009; Chen et al., 2008; Zhang and Carmichael, 2001). mRNAs subject to this type of regulation include those with inverted repeated *Alu (*IR*Alu)* elements within their 3'UTR. One example of RNA regulated in this way is the mouse nuclear transcript CTN-RNA, which is edited within its 3'UTR and localizes to paraspeckles. During stress, CTN-RNA is cleaved and released into the cytoplasm as *mCat2* mRNA (Prasanth et al., 2005). Although the precise molecular mechanism is still unclear, NONO may mediate nuclear retention by interacting simultaneously with both *Neat1* and the target mRNA within paraspeckles. While the precise physiological role of paraspeckle is unknown, and they seem to be not essential in mice (Nakagawa et al., 2011), a general consensus that paraspeckle fine-tune gene expression under stress conditions is emerging (Bond and Fox, 2009; Fox and Lamond, 2010; Nakagawa and Hirose, 2012; Sasaki and Hirose, 2009)

The role of NONO in the circadian clock and cell cycle

NONO is involved in coordinating cell cycle and circadian rhythm by regulating different nodes of the circadian network (Kowalska et al., 2013). NONO has been found in complex with PER proteins; the reduction of NONO expression by RNA interference attenuates circadian rhythms in mammalian cells, and fruit flies carrying a hypomorphic allele are arrhythmic (Brown et al., 2005). The binding of NONO to PER protein displays circadian rhythmicity and NONO has later been shown to interact with PER at Dbp and REV-ERB α promoters acting as a co-repressor (Kowalska et al., 2012). SFPQ has been also found in complex with PER (Duong et al., 2011). Both factors can recruit SIN3A-HDAC complex to the DNA to repress transcription (Dong et al., 2007; Duong et al., 2011). In mice, loss of NONO leads to increased cell proliferation and decreased senescence. This is likely because NONO binds to the p16-Ink4A cell cycle checkpoint gene promoter and potentiates its circadian activation in a PER protein dependent fashion (Kowalska et al., 2013). As a regulator of circadian gene expression NONO can act as both an activator and a repressor of transcription depending on the molecular and cellular context. It has later been demonstrated that all the three members of the DBHS family play a role in the mammalian circadian oscillator by binding directly to the promoter of *Rev-erb* α in a circadian and PER protein-dependent fashion. In cultured cells overexpression or silencing of any one of the DBHS family members affects clock period and amplitude. However, these roles are likely redundant since NONO-deficient mice show only a 20-min reduction in circadian behavioral period when in constant darkness (Kowalska et al., 2012).

BASIC PRINCIPLES REGULATING METABOLIC HOMEOSTASIS

Metabolism is a combination of two processes: anabolism and catabolism. Anabolic pathways require energy to generate macromolecules such as glycogen, lipids and nucleotides, whereas the catabolic pathway breaks molecules to produce energy. Catabolic and anabolic pathways are tightly interconnected with the fasting/feeding, rest/activity and sleep/wake circadian cycles, during which homeostasis is

maintained by reciprocal activation of glucose and lipid metabolism (Schwartsburd, 2017). Although free fatty acids are the main fuel for most organs, glucose is the obligate metabolic fuel for the brain under physiologic conditions and decreased plasma glucose levels (hypoglycemia) can lead to impaired brain function and death. On the other hand, even mildly elevated plasma glucose concentrations, which occur in patients with impaired glucose tolerance, dramatically increase risk for cardiovascular morbidity (Shrayyef and Gerich, 2010). Thus, the survival of multicellular organisms depends on the organisms' ability to maintain glucose homeostasis in times of low/high nutrient availability or low/high energy needs. This is achieved by the organisms' ability to support equilibrium between energy-producing catabolic processes and energy consuming anabolic pathways that makes possible to maintain metabolic homeostasis during fasting/feeding and sleep/wake cycles (Schwartsburd, 2017). Glucose homeostasis is regulated by nutrient sensing mechanisms and hormonal signaling. These mechanisms control the rate at which glucose is utilized and produced by each tissue (Sharabi et al., 2015). The main tissues that contribute to the maintenance of normal blood glucose levels are the liver, muscle, adipose tissue and brain. After a carbohydrate-rich meal, about 33% of the glucose is taken up by the liver, about 33% is taken up by muscle and fat tissue, and the rest of the glucose is taken up by brain, kidney and RBCs (Moore et al., 2012).

The liver plays a central role in metabolic homeostasis

As the major site in the body for carbohydrate and lipid biosynthesis, the liver has a central role in the regulation of systemic glucose and lipid fluxes during feeding and fasting.

Liver metabolism during the fasted state

Under fasting conditions, when nutrients become scarce, insulin levels decrease and glucagon is secreted by the pancreas to promote hepatic glucose production (HGP). HGP is achieved by two main mechanisms: glycogen breakdown (glycogenolysis) and *de novo* glucose synthesis (gluconeogenesis) from available precursors like pyruvate, lactate, glycerol and amino acids. Glucagon, via protein kinase A (PKA)-mediated phosphorylation, activates glycogen phosphorylase while inhibiting glycogen synthase (Sharabi et al., 2015). Nearly 80% of the endogenous glucose

production comes from the liver and the rest from the kidney (Gerich, 2010). Liver glycogen content is limited and is mostly depleted after an overnight fast. Therefore, while glycogenolysis is predominant during short-term fasting, gluconeogenesis becomes the main source of glucose after prolonged fasting. The adipose tissue contributes to liver gluconeogenesis by releasing free fatty acids (FFAs) and glycerol that are taken up by the liver. The inflow of FFAs from adipose tissue lipolysis sustains an increased flux through β-oxidation in the liver. The acetyl-CoA produced is fully oxidized to CO_2 by the Krebs cycle. This process generates an abundance of ATP and reducing equivalents that sustain the conversion of pyruvate, glycerol and other anaplerotic substrates into glucose via gluconeogenesis. Under conditions where acetyl-CoA generation from β-oxidation exceeds the oxidative capacity of the Krebs cycle, the acetyl-CoA overflow is diverted into ketone body synthesis (Jones, 2016).

Liver metabolism during the fed state

The liver plays a unique role in postprandial nutrient metabolism because it has first access to most ingested nutrients by virtue of their absorption into the hepatic portal vein. As a result the liver is exposed to higher nutrient levels than are other peripheral tissues (Moore et al., 2012). Under this condition, the liver receives a range of different nutrients via the portal vein, including simple sugars, amino acids and short chain fatty acids. Some, such as fructose, glycerol, butyrate and propionate, are efficiently extracted and rapidly incorporated into hepatic intermediary metabolism. Others, such as glucose and lactate, are only partially cleared from the circulation. The abundance of these substrates in portal vein blood, in conjunction with high level of insulin resulting from beta cells stimulation, promotes hepatic glycogen synthesis and de novo lipogenesis, while fatty acid oxidation and endogenous glucose production are suppressed (Jones, 2016).

Insulin and glucose regulate hepatic glycogen synthesis through mechanisms that alter the activity of three enzymes: glucokinase (GCK), glycogen synthase (GYS2) and glycogen phosphorylase. The transport of glucose into the hepatocytes occurs by facilitated diffusion through glucose transporter 2 (GLUT2), and, consequently, intrahepatic glucose concentrations parallel those in the plasma. GLUT2 has high capacity for glucose but low affinity, and thus functions as a “glucose sensor”. Unlike other glucose transporters present in other tissues, GLUT2

does not rely on insulin for facilitated diffusion. Once glucose has entered the hepatocyte, GCK – which catalyzes the phosphorylation of glucose to glucose-6-phosphate – functions as the gatekeeper for glucose metabolism in the hepatocytes (Petersen et al., 2017). In its phosphorylated form, glucose can no longer be exported to the circulation and it's retained in the hepatocytes. Unlike other hexokinases, GCK has low affinity for glucose (thus it's most active when glucose concentration is high) and it's not inhibited by its product. GCK strongly regulates hepatic glycogen deposition. Transgenic mice that have an extra copy of the *Gck* displayed more then threefold greater hepatic glycogen deposition then wild-type mice during hyperglycemic clamp studies. Similarly, the glucose intolerance of mice that have liver-specific deletions of the genes that encode AKT (*Akt1*$^{-/-}$/*Akt2*$^{-/-}$) is rescued by the liver-specific overexpression of *Gck* (Titchenell et al., 2016). Conversely, patients with maturity onset diabetes mellitus of the young type 2 (MODY2) – which is caused by loss of function mutations in GCK – have reduced hepatic glycogen synthesis in the post-prandial state. Although GCK has a high control coefficient for glycogen synthesis in the hepatocyte, GYS2 also shares control (Agius, 2008). This shared control of glycogen synthesis is probably partly attributable to the GCK-dependent production of glucose-6-phosphate, which is the key allosteric activator of GYS2. Furthermore, insulin stimulates hepatic glycogen synthesis. By activating Akt, insulin induces phosphorylation and inactivation of GSK-3 and a subsequent activation of GYS2 (Sharabi et al., 2015). Another important action of insulin is the inhibition of adipose tissue lipolysis. Insulin-mediated suppression of lipolysis indirectly suppresses hepatic gluconeogenesis through two main mechanisms: first, it decreases the delivery of FFA to the liver, which results in an acute reduction in hepatic mitochondrial acetyl-CoA levels and a consequent decrease in pyruvate carboxylase activity; second, it decreases the turnover of glycerol, which decreases hepatic gluconeogenesis from this substrate (Petersen et al., 2017).

INTERPLAY BETWEEN THE CIRCADIAN CLOCK AND METABOLISM

Although 5-20% of genes display 24 h oscillation in transcript abundance in each tissue, the identity of those cyclic genes differs significantly between tissues, suggesting organ-specific integration of central cues and local signals to induce cyclic fluctuations relevant to the organ (Zhang et al., 2014). In the liver, these transcripts encode key or rate-limiting enzymes important or glucose, lipid and bile acid metabolism as well as mitochondrial function (Panda, 2016), anticipating fasting and feeding phases and participating to the partitioning of exclusive metabolic pathways (Mayeuf-Louchart et al., 2017).

The molecular players mediating the entrainment of the circadian clock by energetic status

The identification of the molecular links that permit sensing of the metabolic status by the clock is an intense area of research. The alternation of feeding and fasting periods is paralleled by variations of the AMP/ATP and NAD^+/NADH ratios that reflect changes in energy state. Recent studies have demonstrated that clock proteins are directly regulated by energy sensors that modify their expression or stability (Mayeuf-Louchart et al., 2017). AMP kinase (AMPK) senses the AMP/ATP ratio and is activated by a low energy state. On the one hand, AMPK activity as well as nuclear localization is circadian in the mouse liver indicating that it is controlled by the molecular clock. On the other hand, AMPK directly phosphorylates CRY1 thus increasing its degradation, conveying rhythmic changes in energy status directly to clock components (Lamia et al., 2009). The clock is also sensitive to changes in the NAD^+/NADH ratio. NAD^+ levels increase upon fasting or after exercise, but decrease upon high fat diet. NAD^+ is a co-factor for many metabolic enzymes and for sirtuins (SIRT). SIRT display protein (including histone) deacetylation activity, thereby transducing changes in metabolic status to transcriptional/chromatin modifications (Mayeuf-Louchart et al., 2017). The CLOCK:BMAL heterodimer directly activates the transcription of the gene coding for the nicotinamide phosphoribosyltransferase (NAMPT) which is the rate limiting enzyme of the NAD^+ salvage pathway, resulting in

circadian oscillation of the intracellular NAD^+ level (Nakahata et al., 2009; Ramsey et al., 2009). NAD^+ is a co-factor for cytosolic and nuclear SIRT1 and 6, as well as mitochondrial SIRT3 whose activity is circadian. SIRT1 rhythmically deacetylases BMAL1 as well as PER2 promoting their degradation, and exerts feedback on CLOCK:BMAL1 transcriptional activity (Asher et al., 2008; Nakahata et al., 2008) while the nuclear SIRT6 controls circadian recruitment to chromatin to regulate specific hepatic transcriptional networks involved, for instance, in lipid metabolism (Masri et al., 2014). FAD is another co-factor catalyzing metabolic reactions and a sensor of the intracellular redox state. Riboflavin kinase, an enzyme of the FAD synthesis pathway, oscillates in the nucleus, resulting in rhythmic FAD levels. In turn, FAD controls CRY stability by competing with the ubiquitin ligase FBXL3 which labels CRY for degradation (Hirano et al., 2017). Sensing of the cellular metabolic state results in the fine adjustment of the clock by nutrient availability, and points to a potential mechanism by which alteration of the metabolic state, by high-fat content food or by food intake at irregular times, may deteriorate clock function (Mayeuf-Louchart et al., 2017). Vice versa, disruption of the clock leads to metabolic disorders. The reciprocal regulation of metabolism and the circadian clock and the deleterious effects of its dysregulation on metabolic health are summarized in the next two sections.

Disruption of the clock leads to metabolic disorders in mouse models and humans

Peripheral organs contain autonomous endogenous oscillators as was shown by culturing *ex vivo* liver, lung and muscle tissues (Yamazaki et al., 2000). Oscillations in peripheral tissues progressively dampened and were desynchronized in SCN lesioned animals, suggesting that the SCN synchronizes peripheral clocks (Yoo et al., 2004). Mice with whole-body loss of function of hypomorphic alleles of circadian genes often develop perturbations in glucose and lipid homeostasis, insulin resistance, and other hallmarks of metabolic disease (Zarrinpar et al., 2016). Early observations of severe metabolic dysregulation in $Clock^{mut}$ and $Bmal1^{-/-}$ mice (Rudic et al., 2004) led to a systematic investigation of metabolic homeostasis in almost every circadian mutant mouse model. Later studies demonstrated that local clocks are also necessary for circadian function and metabolic homeostasis (Atger et al.,

2017; Brown, 2016). For example, mice with a liver-specific deletion of *Bmal1* exhibited hypoglycemia restricted to the fasting phase, exaggerated glucose clearance, and loss of rhythmic expression of hepatic glucose regulatory genes. The liver clock is thus important for buffering circulating glucose in a time-of-day-dependent manner (Lamia et al., 2008). Loss of pancreatic clocks caused a delay in the phase of oscillation of islet genes involved in growth, glucose metabolism and insulin signaling. Both *Clock* and *Bmal1* mutants show glucose intolerance, defective insulin production, and defects in size and proliferation of pancreatic islets that worsen with age (Marcheva et al., 2010; Perelis et al., 2015; Sadacca et al., 2011). Adipocyte-specific deletion of *Bmal1* results in obesity in mice. Ablation of the adipocyte clock is also associated with a reduced number of polyunsaturated fatty acids in adipocyte triglycerides (Paschos et al., 2012). The relationship between clock function and metabolism is bidirectional. Environmental disruption of the circadian cycle can lead to metabolic disease (Arble et al., 2010). For example, a classic 'shift work' experiment, in which nocturnal rats are required to be active during daytime, leads to alteration of circadian gene rhythmicity, obesity, and other metabolic disturbances (Salgado-Delgado et al., 2008). When mice are housed in constant bright/dim light, they consume more food during the subjective light phase. These mice exhibit significantly increased body mass and reduced glucose tolerance compared with mice under standard light/dark cycles, despite similar caloric intakes and total motor activity (Fonken et al., 2010). Restricting feeding of mice to daytime leads to weight gain (Arble et al., 2009).

There is strong evidence that this phenomenon also exists in humans. Several clock gene polymorphisms have been associated with altered metabolic parameters. For example, polymorphisms in *Cry2* have been associated with elevated fasting glycaemia and reduced liver fat content in large cohorts (Dupuis et al., 2010; Machicao et al., 2016). Two known common *Clock* polymorphisms were associated with the development of the metabolic syndrome (Scott et al., 2008). Similarly, two *Bmal1* haplotypes were associated with type 2 diabetes and hypertension (Woon et al., 2007). Furthermore, polymorphisms in *Rev-erb* α and *Per2* were associated with obesity (Garaulet et al., 2010, 2014). Environmental disruption of the circadian cycle in humans has been studied at a population level in shift workers, as well as under laboratory settings. There is strong evidence that shift

workers are particularly predisposed to obesity and metabolic syndrome (Brum et al., 2015; Canuto et al., 2013; van Drongelen et al., 2011; Wang et al., 2014). This is perhaps due to uncoupling of clock systems and the hypothalamus-pituitary-adrenal (HPA) axis (Fujino et al., 2006; Nicolaides et al., 2014; Sookoian et al., 2007). Simulated night shit work laboratory studies on humans induced a reduction in daily energy expenditure of approximately 12-16% (McHill et al., 2014). Decreased levels of leptin and peptide YY, which signal satiety, were also observed. When individuals were subjected to circadian misalignment for 10 days they had elevated post-prandial glucose, elevated insulin, and increased mean arterial pressure (Scheer et al., 2009). In conclusion, there is mounting evidence in both animal models and humans that genetic and environmental disruption of circadian clock severely affects metabolic homeostasis leading to metabolic disease.

Systemic cues and the circadian clock

The SCN entrains peripheral clock rhythmicity through the modulation of hormone secretion, body temperature rhythms, and feeding/fasting rhythms (Balsalobre et al., 2000; Brown et al., 2002; Damiola et al., 2000; Vujovic et al., 2008). Fasting/feeding rhythms influence both temperature and humoral rhythms. Feeding behavior is highly rhythmic. Mice consume about 80% of their total daily food intake in the dark phase (Atger et al., 2017). SCN-lesioned rats eat similar amounts of food during the light and dark phase. Thus, a functional clock is required for proper feeding rhythms (Nagai et al., 1978). Genetic alterations of the molecular clock components disrupt rhythmic food consumption in multiple whole-body circadian mutant models (Lamia et al., 2008; Turek et al., 2005; Vollmers et al., 2009).

Daily feeding-fasting rhythms were shown to be the predominant *Zeitgeber* for peripheral oscillators. An inverted feeding regimen can rapidly invert peripheral clocks in liver, kidney, heart, and pancreas but has almost no effect on the central oscillator (Damiola et al., 2000; Stokkan et al., 2001). The phase shifting induced by food occurs in both light-dark conditions and in constant darkness. This indicates that synchronization of peripheral clocks under restricted feeding conditions is likely independent of the SCN. Furthermore, restricted feeding can in part restore rhythmicity of gene expression in liver of mutant mouse models with a disrupted clock (Vollmers et al., 2009). Phase shifting of peripheral clocks induced by food

occurs only progressively; 12 h inversions of liver oscillation take approximately 1 week (Damiola et al., 2000; Saini et al., 2013). However, in SCN-ablated mice entrainment of the peripheral clocks by inverted feeding occurred more rapidly. Thus, the SCN may play a role in counteracting peripheral clocks uncoupling imposed by an altered food regimen, this is likely mediated by the rhythmic secretion of glucocorticoids (Le Minh et al., 2001).

The SCN is connected to the adrenal gland and controls the daily release of glucocorticoids (Buijs et al., 1999). Glucocorticoids increase during the light phase and reach their peak at the transition between day and night. In nocturnal rodents this glucocorticoid peak anticipates the active/feeding phase (Ishida et al., 2005). Glucocorticoid response elements are present in the promoter of core clock genes like *Bmal1, Cry1, Per1*, and *Per2* (Reddy et al., 2007; So et al., 2009; Yamamoto et al., 2005), thus the two systems are tightly interconnected (Weger et al., 2016). Glucocorticoids are indeed capable of entraining peripheral clocks, as suggested by the ability of dexamethasone to synchronize oscillations in rat fibroblasts (Balsalobre et al., 2000).

Temperature oscillations were also proven to synchronize peripheral clocks (Brown et al., 2002; Buhr et al., 2010; Saini et al., 2012). Temperature rhythms can modulate circadian periods in fibroblasts (Dibner et al., 2009). Temperature can also affect rhythmic gene expression through the modulation of mRNA splicing efficiency, as it was demonstrated recently for the cold-inducible RNA-binding protein CIRBP (Gotic et al., 2016).

Restricting food access to only a few hours during the resting phase enhances rhythmicity of metabolic factors like glucose, FFAs, and glucocorticoids (Krieger, 1974). This short time window of food availability during the day alters behavioral rhythms and enhances locomotor activity that anticipates food availability (Stephan, 2002; Stephan et al., 1979). Food-anticipatory activity (FAA) persists even when the food is removed. Importantly, most of the mouse models with a disrupted circadian clock exhibit normal FAA (Pitts et al., 2003; Stephan, 2002; Storch and Weitz, 2009). Furthermore, entrainment to food can occur in SCN-lesioned mice. This indicated that the neuronal locations responsible for the FAA are at least in part distinct from those responsible for entrainment to light (Krieger et al., 1977; Stephan, 2002). Although the brain locations responsible for FAA still need to be identified,

some studies suggested that peripheral organs might participate in FAA through humoral signals. For example, oxyntomodulin secreted by the gut is involved in the entrainment of the clock through feeding stimuli (Landgraf et al., 2015). Furthermore, Ghrelin-secreting cells in the stomach represent another potential food-entrainable oscillators. The hormone ghrelin stimulates food intake, and Ghrelin receptor-deficient mice exhibit a reduction in FAA (Laermans et al., 2015; LeSauter et al., 2009). *Per2* has recently been shown to mediate the action of the liver upon FAA. Whole-body *Per2* mutant animals have impaired food anticipation and the liver-specific *Per2* mutation is sufficient to disrupt this circadian behavior (Chavan et al., 2016; Feillet et al., 2006). The adipocyte clock constitutes another example because it's involved in the rhythmic leptin secretion (Paschos et al., 2012). Leptin induces a reduction in appetite, and its signaling is attenuated in animals with disrupted clock (Kettner et al., 2015). Specific deletion of *Bmal1* in adipocytes results in disrupted of leptin levels in plasma, as well as altered feeding behavior. To conclude, the regulation of feeding behavior seem to integrate several layers of regulation that involve not only the central clock but also food-entrainable oscillators employing central and peripheral organs.

1. AIMS OF THE THESIS

Immediately after transcription initiation and throughout their life cycles, RNAs are bound by a large number of RNA-binding proteins (RBPs), some of which remain stably bound while others are subject to dynamic exchange. These complexes containing RNAs and their associated proteins constitute the ribonucleoprotein particles. The combination of factors binding to a particular RNA and their position along the transcript determines every step of RNA regulation throughout its lifetime. Very little is known about the role of RNA binding proteins in regulating circadian mRNA expression in mammals. The RNA binding protein NONO has been shown to interact with clock components and affect circadian rhythmicity in flies and mammals, however the specific mechanisms of its function in circadian RNA expression are unknown.

The liver is the most studied organ in the circadian field, and it has been demonstrated that the feeding/fasting cycle is the main Zeitgeber for the peripheral organs, including the liver. The first objective of my thesis project was to determine whether NONO expression and/or localization was changing in the liver nucleus following fasting or feeding. As a first step, liver staining, imaging and image analysis techniques had to be optimized in order to quantify changes in NONO localization and abundance. After successful implementation of these techniques we found that NONO abundance was unchanged following fasting and re-feeding (feeding after 12 h fasting), however the number of NONO-containing speckle-like structures increased in number in the liver nuclei 2 h after re-feeding.

Since we observed changes in NONO localization following re-feeding, the second objective was to determine NONO protein and RNA interactors in the liver nucleus upon fasting and re-feeding. NONO was immunoprecipitated from liver nuclei in native conditions and either bound proteins or bound RNAs were isolated. Among NONO interacting proteins we found that several HNRNPs, splicing factors and RNA-binding proteins. We also found that the number of RNAs bound by NONO increased upon re-feeding. Gene ontology annotation of NONO targets revealed carbohydrate and lipid metabolism as major clusters.

Given that NONO bound to several genes regulating metabolic processes and the number of bound targets increases upon re-feeding the third objective was to determine the profile of expression of NONO target genes in WT and NONO-deficient mice. We found that 36% of NONO target genes had 24 h rhythm in

expression that was abolished or delayed in NONO-deficient mice.

Finally, since nono has a profound effect on the rhythmicity of its target genes, and these genes are mainly involved in glucose and lipid homeostasis; the 4th aim of the project was to determine the metabolic consequences of NONO deficiency both in the liver and at the whole organism level. We found that NONO-deficient mice have impaired glucose tolerance, reduced capacity to store glycogen and lipids in the liver, and a lean phenotype. Our data demonstrates that NONO coordinates circadian mRNA expression of metabolic genes with the feeding/fasting cycle, thereby playing a critical role in energy homeostasis.

3. RESULTS

THE RNA BINDING PROTEIN NONO COORDINATES HEPATIC ADAPTATION TO FEEDING

Giorgia Benegiamo[1,2], Ludovic S. Mure[2], Galina Erikson[3], Hiep D. Le[2], Ermanno Moriggi[1], Steven A. Brown[1,4*] and Satchidananda Panda[2,4*]

[1]Chronobiology and Sleep Research Group, Institute of Pharmacology and Toxicology, Winterthurerstrasse 190, 8057 Zürich, Switzerland.

[2]Regulatory Biology Laboratory, Salk Institute for Biological Studies, La Jolla, CA, 92037, USA

[3]The Razavi Newman Integrative Genomics and Bioinformatics Core Facility, Salk Institute for Biological Studies, La Jolla, CA, 92037, USA

[4]These authors contributed equally to this manuscript.

[*]Correspondence: panda@salk.edu; steven.brown@pharma.uzh.ch

Abstract

The mechanisms by which feeding and fasting drive rhythmic gene expression for physiological adaptation to daily rhythm in nutrient availability are not well understood. Here we show that, upon feeding, the RNA binding protein NONO accumulates within speckle-like structures in liver cell nuclei. Combining RNA-immunoprecipitation and sequencing (RIP-seq), we found that an increased number of RNAs are bound by NONO after feeding. We further show that NONO binds and regulates the rhythmicity of genes involved in nutrient metabolism post-transcriptionally. Finally, we show that disrupted rhythmicity of NONO target genes has profound metabolic impact. Indeed, NONO-deficient mice exhibit impaired glucose tolerance and lower hepatic glycogen and lipids. Accordingly, these mice shift from glucose storage to fat oxidation, and therefore remain lean throughout adulthood. In conclusion, our study demonstrates that NONO post-transcriptionally coordinates circadian mRNA expression of metabolic genes with the feeding/fasting cycle, thereby playing a critical role in energy homeostasis.

Introduction

Diurnal rhythms in gene expression are crucial for metabolic homeostasis. Such rhythms synchronize the transcription of genes necessary for anabolic and catabolic metabolism with periods of feeding and fasting, respectively (Panda, 2016). These oscillations are driven in part acutely in response to feeding and fasting, in part by an endogenous circadian oscillator present in nearly all cells and tissues, and in part systemically (Brown, 2016). Indeed, genetic disruption of the molecular clock or an erratic eating pattern can each disrupt the temporal coordination between metabolic demand and gene expression, leading to metabolic disease (Baron and Reid, 2014; Bass and Takahashi, 2010; Zarrinpar et al., 2016). However, mechanisms by which the feeding/fasting cycle and gene expression are temporally coordinated have not been fully elucidated.

The liver plays an important role in metabolic homeostasis, as it is the primary site for the daily metabolism of macronutrients (e.g. carbohydrates, lipids and amino-acids). In turn, glycogen is predominantly stored there during feeding, and during fasting this glycogen is largely returned to glucose each day. Consistent with this rhythmic function, ~24h rhythms in both mRNA and protein levels are associated with a large fraction of the liver coding genome (Hughes et al., 2009; Reddy et al., 2006; Vollmers et al., 2012; Zhang et al., 2014). While a number of these genes have daily expression patterns driven primarily by transcriptional rhythms, cycling of most mature mRNAs is not driven by underlying rhythms in transcription (Koike et al., 2012; Menet et al., 2012), suggesting the importance of as yet unknown post-transcriptional mechanisms.

Importantly, comparing genes induced by fasting and feeding with genes that exhibit diurnal patterns of gene expression (in terms of mature mRNA levels) revealed a dramatic overlap. This indicates that the feeding/fasting cycle is a critical driver of daily rhythm in mRNA levels (Atger et al., 2015; Damiola et al., 2000; Sobel et al., 2017; Vollmers et al., 2009). Accordingly, when fasted mice are given food, a large number of liver transcripts are rapidly upregulated. Such increases in mRNA levels also likely involve both transcriptional and post-transcriptional mechanisms.

Circadian rhythms in cellular function are mostly driven by a circadian oscillator composed of a cell-autonomous transcriptional-translational feedback loop,

in which heterodimers of the activator proteins CLOCK and BMAL bind to E-box promoters and drive the expression of the repressors CRYs (*Cry1*, *Cry2*) and PERs (*Per1*, *Per2*, *Per3*). CRY and PER heterodimers then translocate back into the nucleus, and repress activities of the BMAL-CLOCK complex, thus establishing circadian rhythmicity in gene expression (Lowrey and Takahashi, 2011; Panda et al., 2002a).

Post-transcriptional regulatory mechanisms (such as splicing, localization, polyadenylation, stabilization and degradation) are driven by RNA binding proteins (RBPs) that often mediate complex activities involving interactions with other proteins and RNA species (Uren et al., 2012). The RBP non-POU domain-containing octamer binding (NONO) belongs to the Drosophila Behavior Human Splicing (DBHS) family that includes the paralogues SFPQ and PSPC1. These predominantly nuclear proteins have two RNA-recognition motives (RRMs) and are defined as 'multifunctional', as they regulate gene expression in numerous ways, affecting transcriptional activation and inhibition, as well as RNA splicing, stabilization, and export (Knott et al., 2016). NONO, SFPQ, and PSPC1, together with other pre-mRNA splicing factors, transcription factors, and heterogeneous nuclear ribonucleoproteins (hnRNPs), are also components of paraspeckles - subnuclear bodies assembled on the long non-coding RNA Neat1 (Fox and Lamond, 2010; Fox et al., 2002; Yamazaki and Hirose, 2015). Interestingly, NONO interacts with PER proteins and affects circadian rhythmicity in flies and in mammalian cell lines (Brown et al., 2005; Kowalska et al., 2012, 2013). A second, and likely not mutually exclusive, aspect of DBHS family proteins is their role in regulating RNA expression in response to stress stimuli (Prasanth et al., 2005).

Here we find that feeding increases the number of NONO-containing, speckle-like structures in nuclei of liver cells. NONO interacts with RNA processing factors in the liver and the number of NONO-bound RNAs increases upon feeding. NONO primarily binds promoter-proximal introns of transcripts. A large fraction of NONO-bound RNAs encodes proteins implicated in glucose uptake and macronutrient metabolism. Furthermore, we demonstrate that NONO post-transcriptionally regulates mRNA levels of these genes in response to a nutritional stimulus. The absence of NONO-mediated regulation of target RNAs profoundly impacts metabolic health. Indeed, NONO-deficient mice exhibit impaired glucose tolerance, reduced

capacity to store glycogen and lipids in the liver, and a lean phenotype. Together these results indicate that NONO coordinates the pre-mRNA processing of metabolic genes in response to nutritional stimuli. We therefore propose that post-transcriptional mechanisms directed by NONO represent an important regulatory node at the intersection between cycles of feeding/fasting and rhythmic gene expression.

Results

Feeding increases the number of NONO-containing speckle-like structures in nuclei of liver cells

To investigate whether NONO plays a role in driving feeding-dependent rhythms in mRNA levels, we first analyzed NONO protein levels in the mouse liver in response to fasting and feeding. Mice were fed a normal chow only during the dark phase of a 12 h light:12 h dark cycle (i.e., a 12:12 LD cycle) for one week. Livers were then harvested after 12 h of fasting, after 2 h of re-feeding (i.e., 2 h of feeding following the 12 h fast) or 60 minutes after an intraperitoneal glucose injection following light-phase fasting. In these conditions, NONO protein levels remained unchanged, as shown by immunoblotting and nuclear immunostaining (**Figure S1A, S1B** and **S1E**). Using super-resolution microscopy, however, we observed dramatic changes in NONO subnuclear localization (**Figure 1A** and **1D**). In general, NONO was diffusely distributed throughout liver-cell nuclei after fasting. After feeding, or an intraperitoneal administration of glucose, the number of NONO-containing subnuclear speckle-like structures increased (**Figure 1B, 1C, 1E,** and **1F**). This increase in the number of speckle-like structures was not due to an increase in nuclear volume (**Figure S1C, S1D, S1F, S1G**). Feeding-induced speckle-like structures localized to the interchromatin space of the nucleus, spatially separated from heterochromatin rich DAPI foci. The increased number of NONO-containing speckle-like structures in liver nuclei after feeding or an acute glucose challenge suggests that NONO may play a role in hepatic responses to nutritional stimuli.

NONO interacts with RNA processing factors

Most RBPs interact with each other and with other proteins in macromolecular complexes to regulate every step of the RNA life cycle, such as transcription,

splicing, transport, and translation (Gehring et al., 2017). To characterize NONO-containing macromolecular complexes in different nutritional conditions, we performed immunoprecipitation followed by mass spectrometry (IP-MS) of NONO from mouse liver nuclei collected at three different times of the day. Again, mice were fed only during the dark phase of a 12:12 LD cycle, and samples were collected after 10 h of fasting (ZT10), 2 h after re-feeding (ZT14), and towards the end of the feeding period (ZT22) (**Figure S2A** and **S2B**). We found that the most abundant interactions were common to all the three time points (**Figure S2C**). Among NONO interacting proteins were the two known paralogues and direct NONO interactors; SFPQ and PSPC1. We also found that several HNRNPs, some splicing factors, RNA-binding proteins and one of the main components of the DBC1–ZIRD complex (DBIRD) were NONO interactors (**Table 1**). Several of these interacting factors also localize to paraspeckles (Naganuma et al., 2012; Yamazaki and Hirose, 2015) and/or were previously identified as components of messenger ribonucleoprotein complexes (mRNPs), involved in mRNA metabolism and post-transcriptional gene regulation (Close et al., 2012; Mannen et al., 2016; Sánchez-Jiménez and Sánchez-Margalet, 2013; Weidensdorfer et al., 2009). Although NONO was previously shown to interact with the PER protein complex (Brown et al., 2005), no circadian clock proteins were identified in our IP-MS analysis, suggesting that the circadian sub-complex may not be a major component of the NONO complex in the liver. This detailed characterization of NONO complexes suggests that NONO interacts with ribonucleoprotein complexes in the liver and may play a role in mRNPs assembly, RNA metabolism and post-transcriptional gene regulation.

The number of transcripts bound by NONO increases upon feeding

To identify RNAs bound by NONO complexes in different nutritional conditions, we performed RNA immunoprecipitation followed by sequencing (RIP-seq) of NONO from mouse liver nuclei collected after 10 h of fasting (ZT10), 2 h after re-feeding (ZT14) and towards the end of the feeding period (ZT22) (for mice fed during the dark phase of a 12:12 LD cycle) (**Figure 2A** and **2B**). We identified a total of 1140 transcripts that bound NONO during at least one of the three time points. Importantly, NONO bound more transcripts at ZT14 (2h after re-feeding), compared with the two other time points; NONO bound 373 genes at ZT10, 833 at ZT14, and 452 at ZT22 (**Figure 2C**). At ZT14 the average size of NONO binding peaks (i.e., the

number of base pairs encompassed by each peak) also increased; average peak sizes were 2203 ± 1611 bp at ZT10, 3060 ± 1723 bp at ZT14 and 2202 ± 1141 bp at ZT22 (**Figure 2D** and **2E**). This difference was confirmed when we compared only the 134 transcripts that were common to the three time-points (**Figure S3A**), suggesting increased binding of NONO to its target RNAs at the beginning of the feeding phase. Among NONO targets at ZT10 was the non-coding RNA NEAT1, which serves as a scaffolding RNA for the formation of paraspeckles (Fox et al., 2002). About 80% of NONO binding sites were within introns, especially in the 5' proximal introns (**Figure 2F** and **2G**). Relative distance of the identified intron peaks from the TSS normalized to gene size showed similar results (**Figure S3B**). Moreover, NONO did not bind uniformly throughout each intron, but instead was enriched within specific regions of each bound intron (**Figure 2I** and **Figure S3C-E**). In silico analyses identified 6 putative binding-site motifs significantly enriched at introns (**Figure 2H**). (It should be noted that although the composition of these binding site motifs was consistent across time points, more stringent mapping techniques and mutation analyses would be needed to establish more precise consensus sequences). Together, these data suggest that: 1) NONO primarily binds to pre-mRNA, 2) the number of NONO-bound RNAs increases at the beginning of the feeding phase, and 3) NONO may regulate the processing of its target RNAs in response to nutritional stimuli.

NONO regulates the rhythmicity of its target RNAs post-transcriptionally

The liver's circadian transcriptome results from the combined actions of the circadian clock and feeding/fasting rhythms (Damiola et al., 2000; Vollmers et al., 2009). Since: 1) the number of NONO-containing speckle-like structures increased in response to feeding, 2) NONO interacted with RNA processing factors, and 3) NONO bound to introns of a large number of protein coding genes; we hypothesized that NONO may contribute to the daily rhythm of hepatic gene expression. To address whether NONO contributes to rhythmic gene expression in response to feeding/fasting, circadian liver transcriptomes were assessed in *nono*^{gt} mice (i.e. mice lacking *Nono* mRNA and protein expression; Kowalska et al., 2012) and wildtype (WT) littermates. *Nono*^{gt} mice exhibit a slight change in circadian period length when placed in constant darkness, but under a 12:12 LD cycle their daily activity:rest cycle is indistinguishable from WT littermates (Kowalska et al., 2012).

Mice were habituated to have food available only at lights off (ZT12-24) for one week. During the second week, mice were collected every 2 h throughout the 24h day (**Figure 3A**). Both total and nuclear RNAs from a pool of two biological replicates were sequenced at two-hour resolution (**Figure 3B**). (For statistical reasons to determine accurate circadian phase, we favored a higher density of time points over a lower one with conventional identically-timed replicates (Li et al., 2015)). In these conditions NONO mRNA and protein levels showed constant amount across the 24 h (**Figure S4A** and **S4B**).

In the total-RNA fraction the majority of reads (71%) mapped to exons, whereas in the nuclear-RNA fraction, 76% of reads mapped to introns, suggesting that the nuclear RNA is enriched in pre-mRNAs and newly transcribed RNAs (**Figure 3C**). Thus, for further analysis we considered the exon FPKM (Fragments Per Kilobase per Million mapped reads) from the total-RNA fraction (tExon) as an estimation of mature mRNA levels, and the intron FPKM from the nuclear-RNA fraction (nIntron) as an approximation of pre-mRNA levels and transcriptional activity (Gaidatzis et al., 2015).

In the experimental conditions described above, 22% (3152 out of 14527) of the genes expressed in the liver of WT mice showed a 24 h rhythm in mature mRNA levels (tExon dataset, **Figure 3D** left), with peak mRNA levels coinciding with the end of fasting or feeding time periods (**Figure S4E**), in agreement with other recent studies (Atger et al., 2015; Vollmers et al., 2012). However, only 32% of these cycling mRNAs were transcribed in a cyclical fashion (nIntron dataset). This suggests that post-transcriptional mechanisms likely account for the cycling of most mature mRNAs, as has been suggested by other recent reports (Koike et al., 2012; Menet et al., 2012). Comparing the NONO RIP targets that resulted to be expressed in the liver (n=943) with the cycling transcriptome revealed that 36% (338) of these NONO targets exhibited circadian rhythm in mature mRNA levels (**Figure 3D** right). Importantly, daily fluctuations in the mature mRNA levels for these genes were altered in *nono*^{gt} mice, such that mature mRNA levels for 107 genes were no longer rhythmic, and peak levels of mature mRNA for 231 genes were delayed by 2h on average (**Figure 3E** and **3G**). This delay is likely induced post-transcriptionally: for the subset of genes that were rhythmic both transcriptionally (nIntron dataset) and at the level of mature mRNA accumulation (tExon dataset), 58 genes in total, the delay

in peak expression between *nono*^{gt} and WT mice was only observed in the tExon dataset (**Figure 3F**, right), whereas timing within the nIntron dataset remained identical between the two genotypes (**Figure 3F**, left).

Even at the genome-wide level, for genes that cycled in both WT and *nono*^{gt} mice, irrespective of whether or not they were NONO targets, peak levels of mature mRNAs were also delayed by 1h on average, but peak levels of transcription were not (**Figure S4C-F**). The phase delay observed when exon sequences from the total RNA were compared with intron sequences from the nuclear RNA did not result from differences in RNA preparation, since we did not observe any delay when comparing the intron phases of expression from the nuclear and total RNA fractions (nIntron vs tIntron, **Figure S4F**). Together, these data suggest that: 1) for NONO direct targets, the loss of NONO severely impacts both rhythmicity and phase of their mature mRNA, but not transcription of the genes themselves, and 2) the loss of NONO also indirectly affects the phase of oscillation for mature mRNAs associated with other cycling genes in the liver.

Daily patterns of both mature mRNA levels (tExon) and transcription (nIntron) of known core circadian clock components did not show large alterations in their oscillation profile in *nono*^{gt} liver (**Figure S5H-J**). All core clock genes showed strong rhythmicity in transcription, which preceded rhythms in mature mRNA levels by 1-2 h in both genotypes. Thus, the effects we document are likely independent of oscillations in core clock components.

NONO regulates glucose-induced gene expression post-transcriptionally and is required for normal glucose homeostasis

We have shown that the number of NONO-bound RNAs increases upon feeding and that NONO regulates the oscillation of its target mRNAs post-transcriptionally. To test the physiological relevance of NONO function, we examined the predicted functions of its rhythmic target genes. NONO target genes were significantly enriched in gene ontology terms related to metabolism. KEGG functional annotation of the same genes revealed anabolic metabolism (specifically carbohydrate and amino-acid metabolism) as major functional clusters (**Figure 4A, 4B**).

Consistent with the mechanistic role we propose for NONO, under a 12-h fasting:12-h feeding cycle, peak levels of *Glucokinase (Gck)* and *Glucose transporter-2* (*Glut2)* mRNAs were delayed in *nono*^{gt} mice (**Figure S5A** and **S5E**).

Correspondingly, delays in these mRNA peaks affected GCK and GLUT2 protein levels in the liver, as levels of both proteins were reduced at the beginning of the feeding phase in *nono*^{gt} mice (**Figure 4C**).

To further test and confirm our hypothesis that NONO is important for pre-mRNA processing of these transcripts, we measured their expression before and after an acute intraperitoneal injection of glucose into WT and *nono*^{gt} mice (**Figure 4D**). Sixty minutes (T60) after glucose injection, the fold induction (compared to time 0 (T0)) for *Gck* and *Glut2* spliced mRNA was significantly lower in *nono*^{gt} mice compared to the WT littermates. In contrast, no differences in intron induction were seen between the two genotypes, demonstrating that NONO regulates these genes post-transcriptionally in response to glucose (**Figure 4E**).

Both Glut2 and Gck bind glucose with low affinity and act as glucose sensors for the hepatocytes during the fed state, when glucose levels rise in the blood (**Figure 5A**; Massa et al., 2011; Thorens and Mueckler, 2010). Thus, reduced levels of GLUT2 and GCK in *nono*^{gt} mice would be predicted to cause physiological changes in glucose utilization. This is exactly what we find: *nono*^{gt} mice showed increased post-prandial blood glucose levels when administered a glucose tolerance test (GTT) (**Figure 5B**), whereas their insulin sensitivity was unaffected (**Figure 5C**). In addition, *nono*^{gt} and *WT* mice exhibited similar fasting glucose and insulin levels (**Figure 5D** and **5E**). These data suggest that the impaired glucose tolerance in *nono*^{gt} mice reflects the role played by NONO in regulating glucose uptake in the hepatocytes. In the liver, glucose-6-phosphate is used in glycogen synthesis, glycolysis, and the pentose phosphate pathway, and is eventually stored as fat (**Figure 5A**). Accordingly, we measured lower levels of hepatic glycogen at the end of the feeding period in *nono*^{gt} mice compared to WT controls (**Figure 5F**).

Changes in glucose metabolism and glycogen storage could theoretically derive either from alterations in the liver (the site of this metabolism and storage) or in the pancreas (secreting the insulin and glucagon that regulate it). To test the extent to which loss of NONO from adult mouse liver cells contributes to glucose intolerance, we restored NONO expression in *nono*^{gt} mice using adeno-associated viruses (AAVs) that expressed NONO under the control of the liver-specific TBG promoter. We injected two different AAV2/8 viral vectors, one that expressed wildtype NONO, and one that expressed a mutant version of NONO with 4 point

mutations (2 in each of the RRM domains) (**Figure 6A** and **6B**). These mutations disrupt the ability of NONO to bind RNA (Kuwahara et al., 2006). Levels of AAV-derived NONO protein in liver cells were comparable to those observed in WT mice (**Figure 6C**). Glucose tolerance was tested in *nono*^{gt} mice before and 4 weeks after AAV injection (**Figure 6D**). Liver-specific re-expression of WT NONO significantly improved glucose tolerance (**Figure 6E**), whereas this was not the case for mice expressing the NONO RRM-mutant (**Figure 6F**). This demonstrated that NONO functions in the liver to influence whole-body glucose homeostasis, and that the ability of NONO to bind RNA is required for this function. Together these data suggest that NONO binds and post-transcriptionally regulates the expression of glucose-responsive genes in the liver, and that NONO is important for whole-body glucose homeostasis and glycogen storage in hepatocytes.

Nono*^{gt} *mice store less fat and exhibit increased fat catabolism

To further characterize the role of NONO in liver metabolism we analyzed the metabolomes of fasted and re-fed animals, both *nono*^{gt} and WT. Livers were collected toward the end of the fasting phase (ZT8, ZT10, and ZT12) and toward the beginning of the feeding phase (ZT14, ZT16, and ZT18). Principal component analysis of the 12 samples showed their separation along genotype and feeding condition. Consistent with our RNA analyses, we found more separation between WT and *nono*^{gt} mice when the two re-fed groups were compared (**Figure S6A**). We found 182 significantly affected bio-chemicals when comparing *WT* and *nono*^{gt} fed groups, whereas only 86 metabolites changed in comparisons between *WT* and *nono*^{gt} fasted groups (**Figure S6B**). In the fed state, *nono*^{gt} livers contained significantly lower levels of the glycolytic intermediates 3-phosphoglycerate, and phosphoenol pyruvate (PEP), as well as the pentose phosphate pathway intermediate 6-phosphogluconate (**Figure S6C-E**). In contrast, the mitochondrial TCA cycle intermediates were elevated (**Figure S6F-I**). In the transcriptome dataset, the cycling NONO target *ATP-citrate-lyase* (*Acly*) exhibited reduced level of expression and a phase delay (**Figure S5D**). ACLY uses citrate (an intermediate in the TCA cycle) and coenzyme A (CoA) to synthesize cytoplasmic Acetyl CoA. Accordingly, we found increased amounts of citrate, aconitate, succinate, and CoA in *nono*^{gt} livers during the fed state (**Figure S6F-I**). Cytoplasmic acetyl CoA is the building block for many molecules, including fatty acids. Another NONO target gene

that is important for lipid metabolism is mitochondrial *glycerol-3-phosphate acyltransferase* (*Gpam*). GPAM catalyzes the initial and committing step in glycerolipid biosynthesis and plays a pivotal role in the regulation of cellular triacylglycerol levels. *Gpam* is expressed at high level during the feeding phase, however *nono*^{gt} mice showed delayed and reduced levels of *Gpam* mature mRNA (**Figure S5B**). Accordingly, *nono*^{gt} livers had reduced levels of triglycerides, reduced overall liver lipid content, and increased levels of glycerol-3-phospate (**Figure 7A, 7B** and **S6J**). Increases in glycerol-3-phosphate in the fasted and fed states might be due to increased breakdown of triglycerides. Indeed, we also found high levels of triglyceride catabolism intermediates (diacylglycerols, monoacylglycerols and fatty acids) in the livers of *nono*^{gt} mice during the fed state (**Figure S6J**).

To assess the physiological consequence of NONO deficiency, we evaluated the metabolic phenotype of *nono*^{gt} mice. *Nono*^{gt} mice are born at Mendelian ratio and survive normally into adulthood. At 10 weeks of age, *nono*^{gt} mice weighed 10% less than WT littermates (**Figure S7A**). When fed a normal chow ad libitum, *nono*^{gt} mice and WT littermates consumed equivalent amounts of food, and exhibited comparable daily activity levels (**Figure 7D, 7E and S7B**). Over the next 32 weeks, *nono*^{gt} mice gained less weight, such that at 42 weeks they weighed 20% less than their WT littermates (**Figure 7C** and **S7A**). Body composition analysis revealed that *nono*^{gt} mice accumulated less fat mass, whereas their gains in lean mass were similar to those seen in WT mice (**Figure 7H** and **7I**). Both leptin and ghrelin levels were reduced in nonogt mice (**Figure S7C** and **S7D**). However, since food consumption in any case was unaltered, we turned to energy utilization as the more likely source of body weight differences.

To examine whole-body energy utilization, we assessed *nono*^{gt} and WT littermates using indirect calorimetry. During the fed state, the respiratory exchange ratio (RER) for both genotypes was equivalent and close to 1, indicating that carbohydrates were used as the predominant energy source. However, during the light period, when mice are usually at rest and have reduced food intake, the RER slowly dropped to ~0.8 in WT mice, whereas in *nono*^{gt} mice, the RER rapidly dropped to 0.7 (**Figure 7J**), indicating increased reliance on fatty acids as an energy source for *nono*^{gt} mice. The relatively quick decline in fasting RER in *nono*^{gt} mice may also indicate reduced energy storage during the feeding phase. *nono*^{gt} mice

also exhibited reduced abdominal fat deposits and smaller adipocytes (**Figure 7F, 7G** and **7K**).

When *nono*^{gt} mice were fed a normal chow (60% of the energy coming from carbohydrates), they weighed less and had less body fat. This reduced adiposity could have resulted from a primary defect in fat absorption and storage. To test this hypothesis, we subjected *nono*^{gt} and *wt* littermates to ad libitum feeding of a high fat diet (HFD; 60% of the energy coming from fat) for 12 weeks. The two genotypes consumed equivalent amounts of food (**Figure S7F**). After 12 weeks of a HFD, the *nono*^{gt} and *wt* mice had equivalent body weights and whole-body fat mass (**Figure S7E** and **S7G**). As anticipated, *nono*^{gt} mice fed a HFD were more glucose intolerant compared to their *wt* littermates (**Figure S7H**). This demonstrates that a HFD can compensate for the inefficient glucose uptake seen in *nono*^{gt} mice fed a normal chow. Together, these data indicate that *nono*^{gt} mice have three inter-related metabolic defects in the liver: 1) reduced glucose utilization in glycolytic and glycogen synthesis pathways, 2) impaired triglycerides synthesis, and 3) increased reliance on fatty acids as an energy source during fasting.

Discussion

Here we report a novel role for the nuclear RNA-binding protein NONO in metabolic homeostasis. Specifically, NONO binds to pre-mRNAs encoding several key regulators of liver glucose and fat metabolism. NONO enhances the processing of these pre-mRNAs, allowing for robust daily oscillation in mRNA levels. This facilitates subsequent translation of these metabolic regulators, which is necessary to store excess nutrients (as glycogen and triglycerides) during the postprandial period. Mice that lack of NONO exhibit disruptions in this temporal regulation, such that animals shift from storing glucose as glycogen and fat to fat oxidation. This results in reduced glucose tolerance, reduced levels of glycogen and triglycerides in the liver, and reduced levels of body fat and body weight (**Figure 8**).

Rhythms in gene transcription are the first step toward generating oscillations in mRNA levels, but recent studies have revealed that a wide range of factors contribute to this oscillations. Regulators of transcription elongation, as well as RNA processing, transport, translation, and degradation may affect steady-state mRNA levels at any given time (Benegiamo et al., 2016). It has been suggested that the dynamic regulation of transcription, mRNA processing, and mRNA degradation are all required to generate high-amplitude oscillation in mRNA levels (Rabani et al., 2014).

Here we show that the RNA-binding protein NONO plays an important role in

coordinating the circadian expression of genes involved in glucose and fat metabolism with the feeding/fasting cycle. Furthermore, NONO regulates these genes post-transcriptionally. We propose a mechanism in which NONO enhances the processing of target RNAs to allow robust in-phase oscillations (**Figure 8**). Further studies are required to understand precisely how NONO affects this process. Previous studies have shown that NONO and SFPQ interact with the carboxy-terminal domain of RNA-polymerase II, leading to the hypothesis that these factors couple transcription to post-transcriptional events (Emili et al., 2002). Our mass spectrometry data further support this idea, and we speculate that NONO may function as a molecular scaffold to assemble the mRNA processing machinery on target RNAs. For example, levels of *Gck* mature mRNA peak toward the end of the night, yet NONO binds to *Gck* pre-mRNA at all time points tested (ZT10, ZT14 and ZT22). Thus, we hypothesize that NONO primes its target pre-mRNAs for processing. In the absence of NONO, this recruitment is less efficient, leading to delays in the phase of oscillation or loss of rhythmicity.

In agreement with what has been demonstrated for NonA, the *Drosophila* homolog of NONO (McMahon et al., 2016), we found that NONO bound primarily to introns. Since our data further point to a role for NONO in post-transcriptional processing, it might therefore play a role in Intron-Mediated Enhancement (IME), an unknown mechanism by which introns may increase gene expression through recruitment of splicing and mRNA export machineries (Gallegos and Rose, 2015; Reed and Hurt, 2002). Consistent with this idea, our data show that NONO preferentially bound promoter-proximal introns, and promoter-proximal introns are more likely to contain signal sequences important for IME (Rose et al., 2008).

One major unanswered question is how metabolic signals result in the accumulation of NONO in speckle-like structures. This question also remains for all other subnuclear structures containing NONO. One possibility is that increased transcription itself may play a role: not only is transcription required for the formation of *Neat1*-containing paraspeckles (Mao et al., 2011), but also chromatin modifying complexes associated with transcriptional activation (Kawaguchi et al., 2015). Since feeding in the liver is associated with increase in cellular RNA content (Sinturel et al., 2017), the increase in speckle-like structures may be due simply to increases in transcription. Alternatively, specific phosphorylation events could play a role, as suggested in the case of MNK kinase (Buxadé et al., 2008) or during mitosis (Proteau et al., 2005).

NONO, SFPQ, and PSPC1 often function as heterodimers, and have been described as multifunctional proteins whose specific role in cellular processes may depend on the molecular and cellular context (Knott et al., 2016). Several other roles have been proposed

for these factors. As the principal components of nuclear paraspeckles, NONO has been postulated to play a role in nuclear RNA retention by binding to stem-loop structures in the 3' untranslated regions (UTRs) of messages (Prasanth et al., 2005). Such UTR regions can even heterologously confer circadian rhythmicity in transcript oscillations (Torres et al., 2016). Yet again, NONO and related factors have been implicated as transcriptional cofactors, binding to histone modifiers to regulate chromatin structure and circadian function (Brown et al., 2005; Duong et al., 2011). Recent research suggests that several different classes of NONO-containing nuclear speckle-like structures may exist (Li et al., 2017), and gel filtration analyses suggest that only a subset of NONO-containing speckle-like structures are circadian in nature (Brown et al., 2005). It is tempting to speculate that these different functions may exist in spatially distinct structures such as the feeding-induced speckle-like structures we describe here. Indeed, our mass spectrometric analyses did not detect clock proteins in these feeding-induced NONO complexes, nor were chromatin-modifying complexes abundant, suggesting that they are entities different from the circadian structures described previously. It is also unclear whether these structures contain the long noncoding RNA *Neat1* that defines bona-fide paraspeckles.

Further studies are required to assess whether the other two members of the DBHS family function with NONO to regulate metabolic homeostasis. Recent studies have shown that PSPC1 plays a role in adipose tissue development (Wang et al., 2017). It is therefore likely that DBHS proteins play complementary roles in different organs to regulate different aspects of metabolism. In this respect, NONO itself has been shown to: 1) regulate phosphodiesterase mRNA splicing and degradation in human adrenocortical cells to affect glucocorticoids production (Lu and Sewer, 2015), 2) positively regulate lipogenesis in breast cancer cells through SREBP1 (Zhu et al., 2015), and 3) act as an mTOR cofactor (Amelio et al., 2007). We predict that each member of the DBHS family will have unique and common targets in each tissue, and mediate both unique and redundant functions. Here we demonstrate that NONO functions in the liver to maintain whole-organism glucose homeostasis. However, we cannot exclude the possibility that NONO plays important roles in other organs (e.g. the pancreas and muscle) to regulate responses to nutritional stimuli.

Our data provide evidence that the RNA-binding protein NONO is important for coordinating hepatic gene expression with the feeding/fasting cycle, and for maintaining whole-organism metabolic homeostasis. Disruption of the temporal coordination between metabolic demand and gene expression leads to the development of metabolic diseases, like obesity and diabetes. The role of RNA-binding proteins in regulating gene expression under diverse environmental conditions is only now beginning to be elucidated. Our findings help to better understand how metabolic homeostasis is maintained in mammals, and

identify novel therapeutic targets for treating diabetes and other associated metabolic dysfunctions.

Figures and Tables

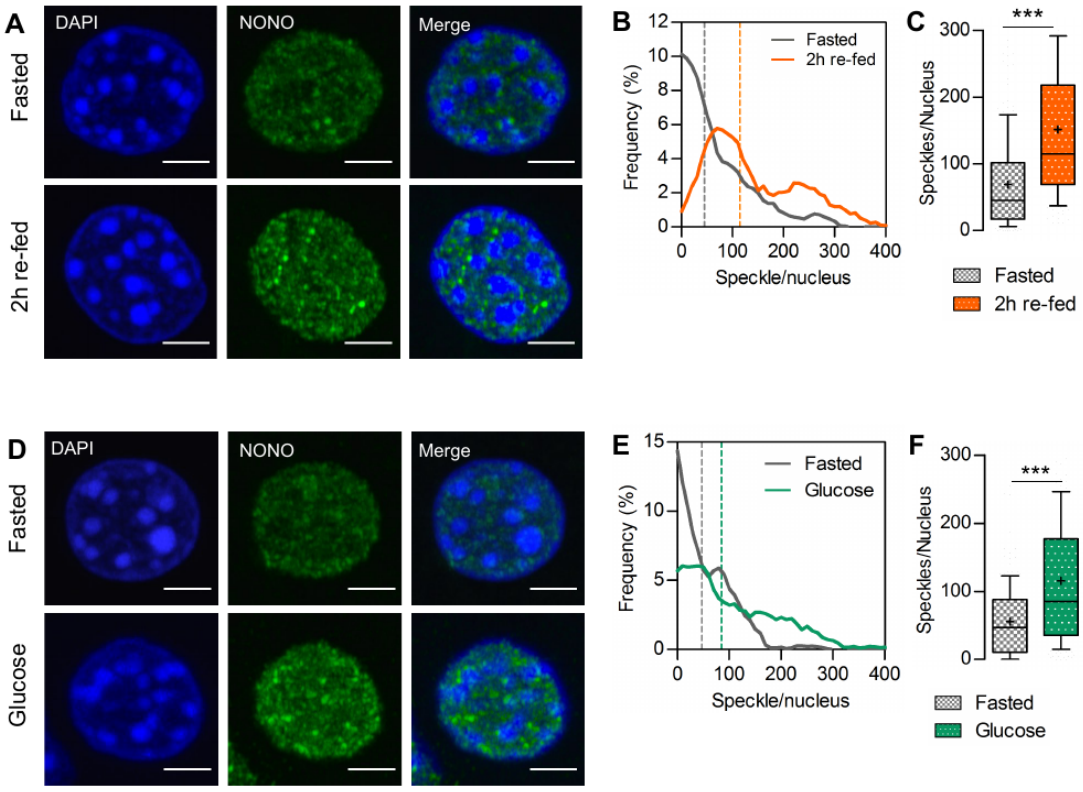

Figure 1. NONO-containing speckle-like structures increase in the nucleus of the hepatocyte upon feeding
(A) NONO immunostaining on liver cryosections in fasted mice or 2h after re-feeding. (B) Distribution of the number of speckles per nucleus in fasted mice or 2h after re-feeding. (C) Average number of speckles per nucleus. (D) NONO immunostaining on liver cryosections in fasted mice or 1h after glucose injection. (E) Distribution of the number of speckles per nucleus in fasted mice or 1h after glucose injection. (F) Average number of speckles per nucleus. (B), (C), (E), and (F), n>170 nuclei. In (C) and (F) results are represented as box and whiskers: 10-90 percentile range, '+' sign represents mean. Statistical analysis student t test, ***p<0.0001. Scale bar=3µm.

	Gene Name	emPAI (ZT14)
DBHS family	Nono*	7.03±0.15
	Sfpq*	4.75±0.11
	Pspc1*	3.91±0.23
RNA binding	Hnrnpa2b1*	5.52±1.10
	Hnrnpa3*	2.62±0.08
	Hnrnpc*	2.10±0.25
	Hnrnpk*	2.28±0.03
	Hnrnpa1*	1.70±0.09
	Hnrnpab	1.62±0.07
	Hnrnpu*	1.70±0.08
	Hnrnpl	1.45±0.21
	Hnrnpf*	1.33±0.13
	Hnrnpd*	1.18±0.03
	Hnrnph2*	1.16±0.07
	Elavl1*	1.62±0.17
	Khsrp	1.51±0.22
	Raly*	1.44±0.24
	Matr3*	1.15±0.01
Nuclear Lamina/Nuclear Pore complex	Lmna	2.49±0.09
	Nup50	2.14±0.14
	Lmnb1	1.98±0.19
	Nup35	1.47±0.03
	Lmnb2*	1.66±0.15
Splicing	Snrpa1	1.72±0.12
	Sf3a3*	1.51±0.22
	Snrpd1	1.19±0.15
Transcription Regulation	Snd1	1.74±0.11
	Tardbp*	2.03±0.20
	Dpy30	1.31±0.00
	Tceb1	2.10±0.06
	Yy1	1.09±0.08
	Ruvbl2	1.19±0.05
	Mta2	1.04±0.10
	Smarce1	0.96±0.21
DBIRD Complex	Ccar2 (DBC1)*	1.15±0.01

Table 1. Main classes of NONO interactors. (*) proteins that were previously identified in paraspeckles or interacting with NONO (Close et al., 2012; Fong et al., 2013; Naganuma et al., 2012; Salton et al., 2010; Tenzer et al., 2013; Zhang and Carmichael, 2001)

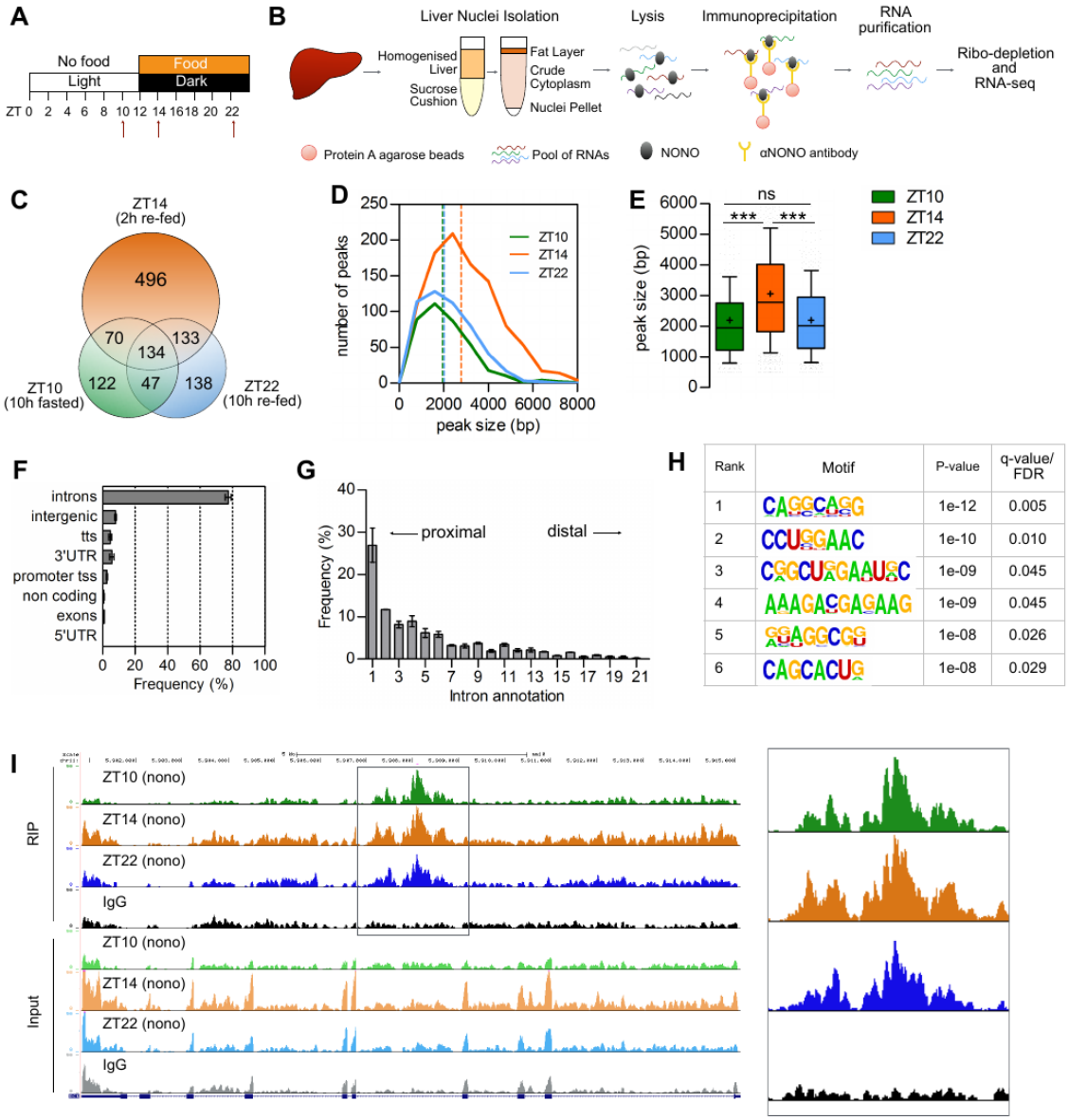

Figure 2. NONO preferentially binds introns and its binding activity increases 2h after re-feeding
(A) Experimental scheme indicating the time points at which liver were collected for the RIP-seq. Livers were collected at the end of the fasting phase (ZT10), 2h after the start of the feeding phase (ZT14) and at the end of the feeding phase (ZT22). (B) Outline of the experimental methods for the NONO RIP-seq in liver nuclei (see also methods). Liver was homogenized and ultracentrifuged on a sucrose cushion to isolate liver nuclei. Nuclear lysates were incubated with anti-NONO antibody-coated agarose beads and NONO-bound RNAs were extracted with Trizol reagent and sequenced. (C) Number of genes bound at each time point and overlap among time points. (D) Peak size distribution at each time point, number of peaks = 380(ZT10), 986 (ZT14), 497 (ZT22). (E) Average peak size for all the peaks identified at each time point. (F) Annotation of the NONO RIP peaks, n=3. (G) Intron position distribution of the RIP-seq peaks, n=3; (H) Significantly enriched RNA motives among the RIP-seq intron peaks; (I) UCSC genome browser view of the RIP-seq reads mapping to Gck gene, the right panel highlights the NONO RIP-seq peaks in Gck intron 4. Each time point is a pool of 2 independent RIP experiments. In (E) results are represented as box and whiskers: 10-90 percentile range, '+' sign represents mean value. In (F) and (G) results are represented as mean±SEM. Statistical analysis one-way ANOVA, ***p<0,0001

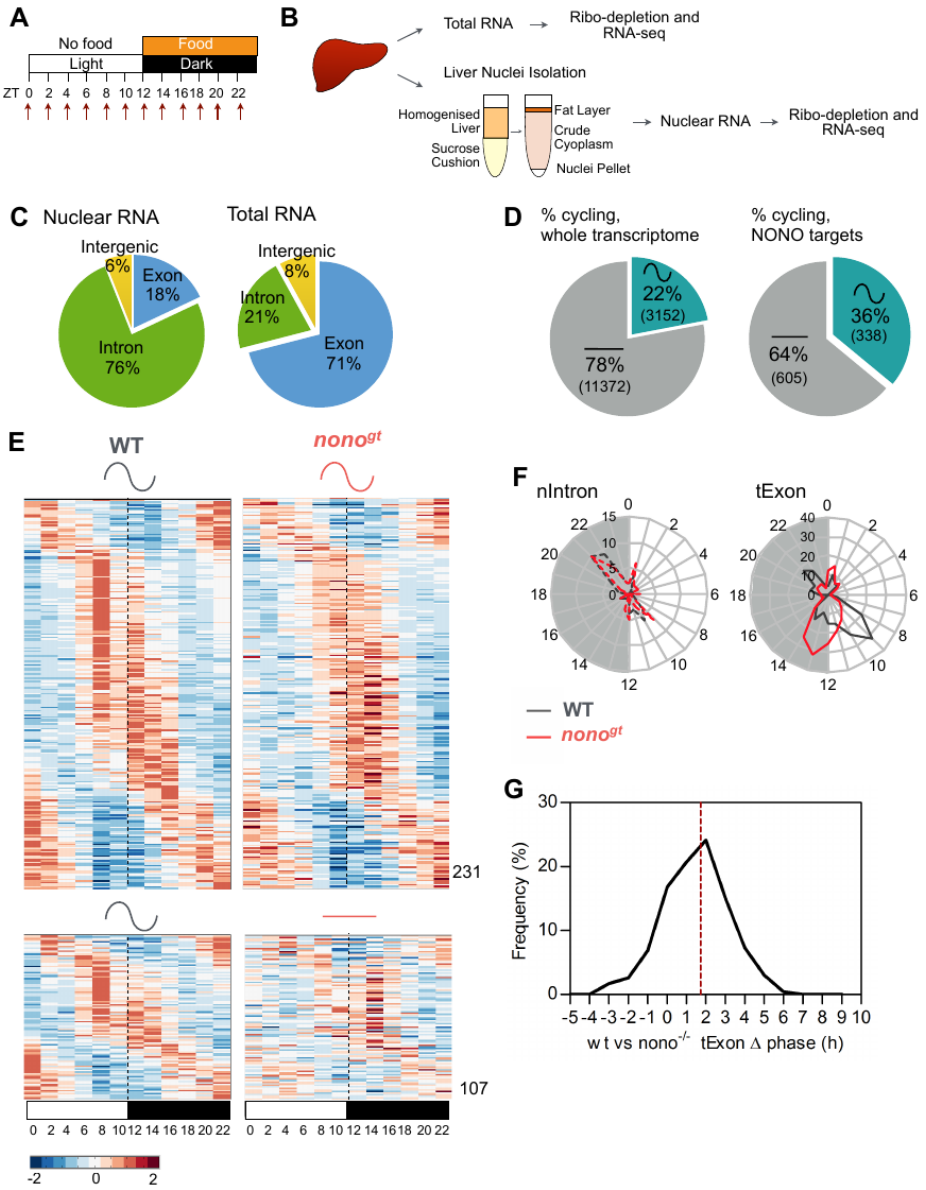

Figure 3. NONO regulates the rhythmicity of its target RNA post-transcriptionally
(A) Experimental scheme indicating the time points at which livers were collected for transcriptome analysis. Mice were habituated to nighttime feeding for one week. On day 7, livers were collected every 2h over an entire 24-h day. (B) Schematic of the experimental methods for the liver transcriptome. One portion of the liver was snap frozen to isolate total RNA, the rest of the tissue was homogenized to isolate liver nuclei and extract nuclear RNA. Both fractions were depleted of ribosomal RNA and sequenced (see also methods). (C) Distribution of high throughput sequencing signal within exon (blue), intron (green) and intergenic sequences (yellow) in the nuclear RNA-Seq (left panel) and in the total RNA-Seq (right panel) datasets. (D) Percentage of genes cycling at the mature mRNA level (tExon dataset) in the whole liver transcriptome (left panel) and among the NONO target genes (right panel) calculated by combining the RIP-seq and WT diurnal transcriptome datasets. (E) Normalized profile of expression of NONO-bound cycling genes (mature mRNA, tExon dataset) in WT and *nono*^{gt} mice at the indicated time points. High expression is displayed in orange, low expression in blue. (F) Peak phase distribution of the same genes as in (E) separated by bins of 1h: right panel mature mRNA peak phases (tExon, n=231), left panel corresponding pre-mRNA peak phases (nIntron, n=58). (G) Distribution of the mature mRNA (tExon) peak phase difference between WT and *nono*^{gt} mice. Dashed line indicates mean phase difference (1.7h).

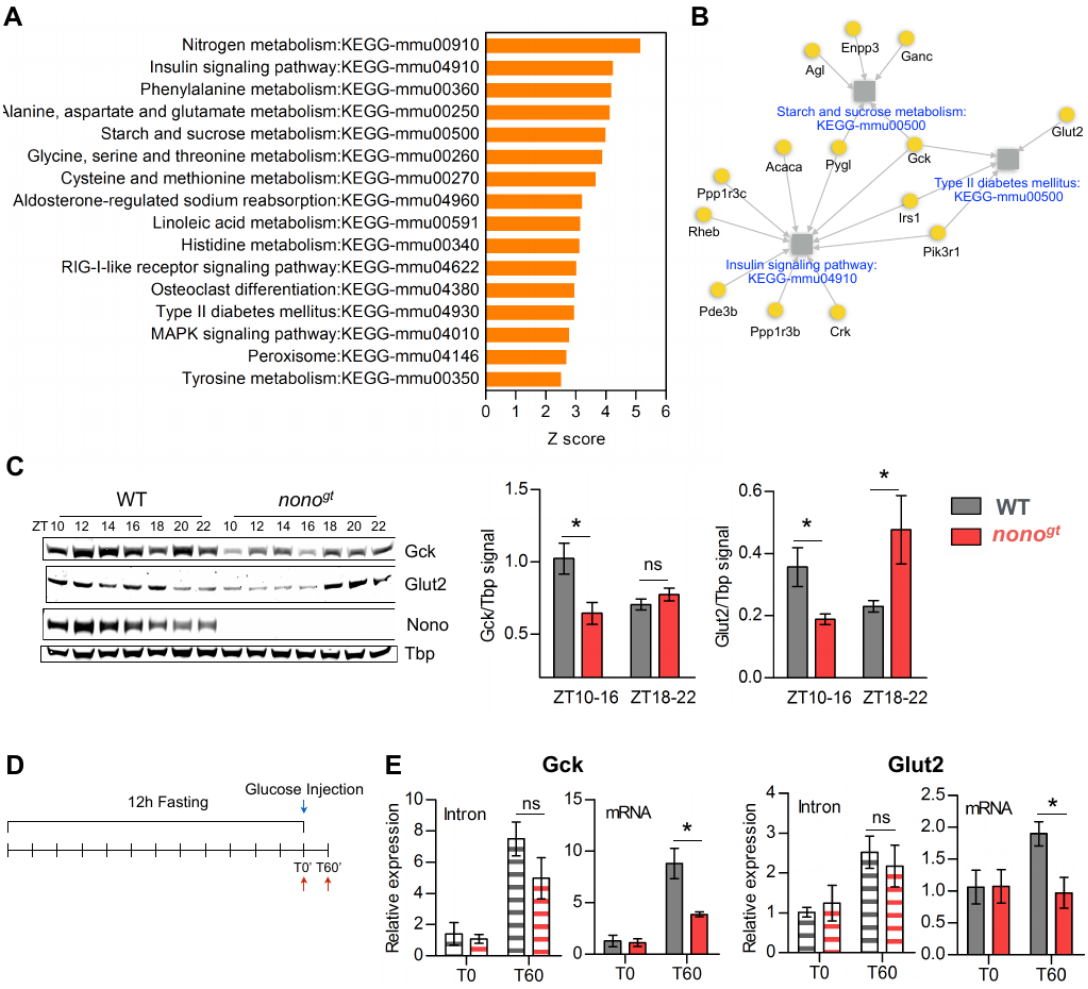

Figure 4. NONO regulates glucose induced gene expression post-transcriptionally
(A) Enriched KEGG pathways (Z-score >2.5) among the NONO-bound cycling genes. (B) Glucose metabolism related pathways enriched among the NONO-bound cycling genes. Grey squares represent pathways; pathways names are indicated in blue. NONO target genes are represented as yellow circles, for each NONO-target gene the gene name is indicated in black. Grey arrows connect each gene to the pathways it belongs to. (C) GCK and GLUT2 protein expression during the dark/feeding phase and protein quantification (right panels) at the beginning of the dark phase (ZT10-16) and at the end of the dark phase (ZT18-22). ZT10-16 n=4 per group, ZT18-22 n=3 per group. (D) Experimental scheme for (E), in order to acutely induce *Gck* and *Glut2* expression mice were fasted for 12 hours and injected intraperitoneally with glucose (2g/kg). WT and *nonogt* liver were collected either at T0 or 60 minutes after glucose injection (T60); (E) qPCR of *Gck* and *Glut2* intron or spliced mRNA levels at T0 and T60, n=3-4 per group per time point. Statistical analysis for (E), two-way ANOVA, Bonferroni posttest. Statistical analysis for (C), student t test. *p<0.05, **p<0.01. Results are represented as mean±SEM.

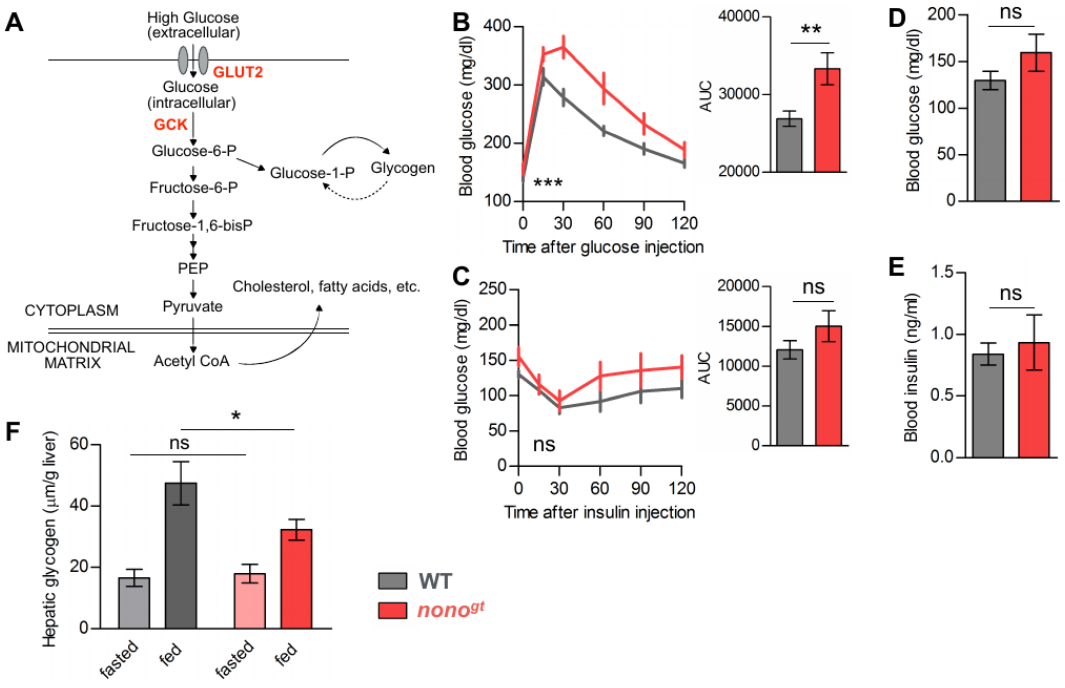

Figure 5. NONO expression in the liver is required for normal glucose homeostasis
(A) Illustration of the role of GCK and GLUT2 in glucose uptake in the hepatocyte. (B) Glucose tolerance test. Mice were fasted for 12h during the light phase and injected intraperitoneally with glucose (2g/kg). Right panel: area under the curve (AUC), n=10 per group. (C) Insulin tolerance test. Mice were fasted for 12h during the light phase and insulin was injected intraperitoneally (0.5U/kg). Right panel: AUC, WT n=9, *nono*^{gt} n=8. (D) Fasting glucose and (E) fasting insulin measured in the same group of mice after 12h of light-phase fasting, WT n=10, *nono*^{gt} n=8. (F) Hepatic glycogen content at the end of the fasting phase (fasted: ZT8-12) and at the end of the feeding phase (fed: ZT18-22), n=6 per group. Statistical test for (B) and (C) two-way ANOVA; statistical test for (D), (E), (F) and AUC histograms student t test. *p<0.05, **p<0.01, ***p<0.001.

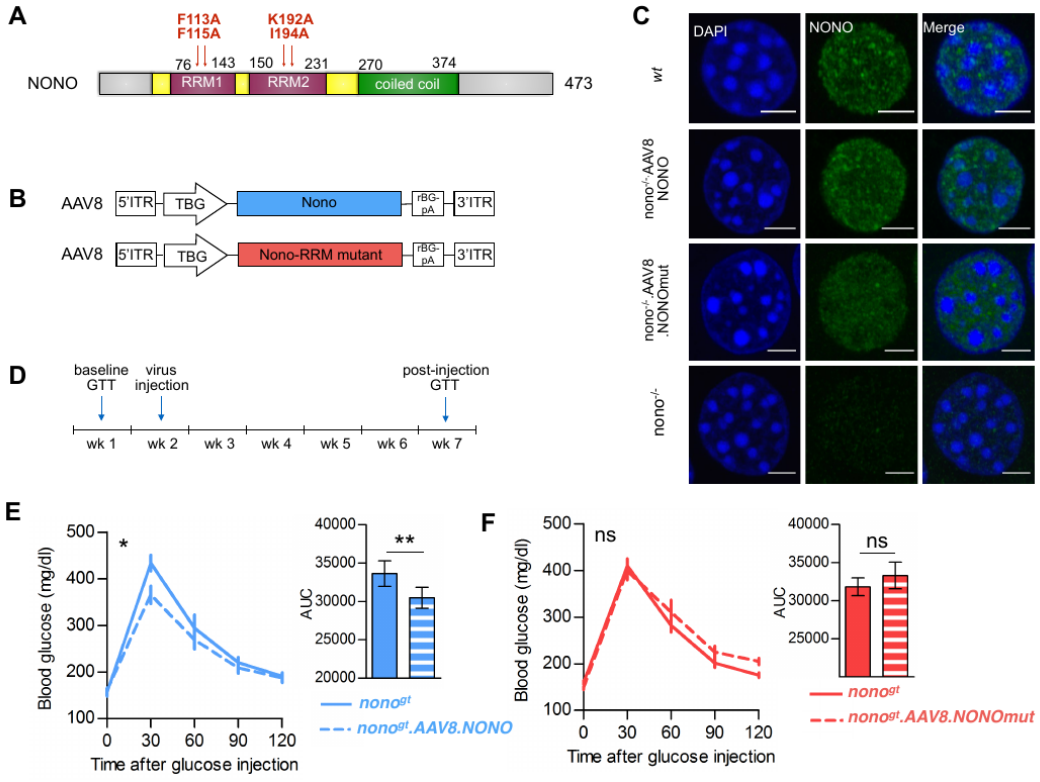

Figure 6. NONO expression in the liver is required for normal glucose homeostasis
(A) Scheme of NONO protein main domains, in red are indicated the mutations in the NONO protein sequence that disrupt the ability of NONO to bind RNA used for the experiment in (F). (B) Scheme of the AAV8 viral constructs used for the experiment in (E) and (F). (C) NONO immunostaining on liver cryosections of WT, *nono*^{gt} mice or *nono*^{gt} mice infected with either AAV8.NONO or AAV8.NONOmut, scale bar=3µM. (D) Experimental scheme for (E) and (F): on week 1 glucose tolerance was measured in *nono*^{gt} mice and on week 2 the same mice were injected with either AAV8.NONO (blue) or AAV8.NONOmut (red). After 30 days from the injection glucose tolerance was measured again in the same mice. (E) and (F) Glucose tolerance test in *nono*^{gt} mice before and 30 days after injection with AAV8.NONO (E) or AAV8.NONOmut (F), histograms on the right represent AUC, AAV8.NONO n=5, AAV8.NONOmut n=7. Statistical test for (E) and (F) two-way ANOVA; statistical test for AUC histograms student t test. *p<0.05, **p<0.01.

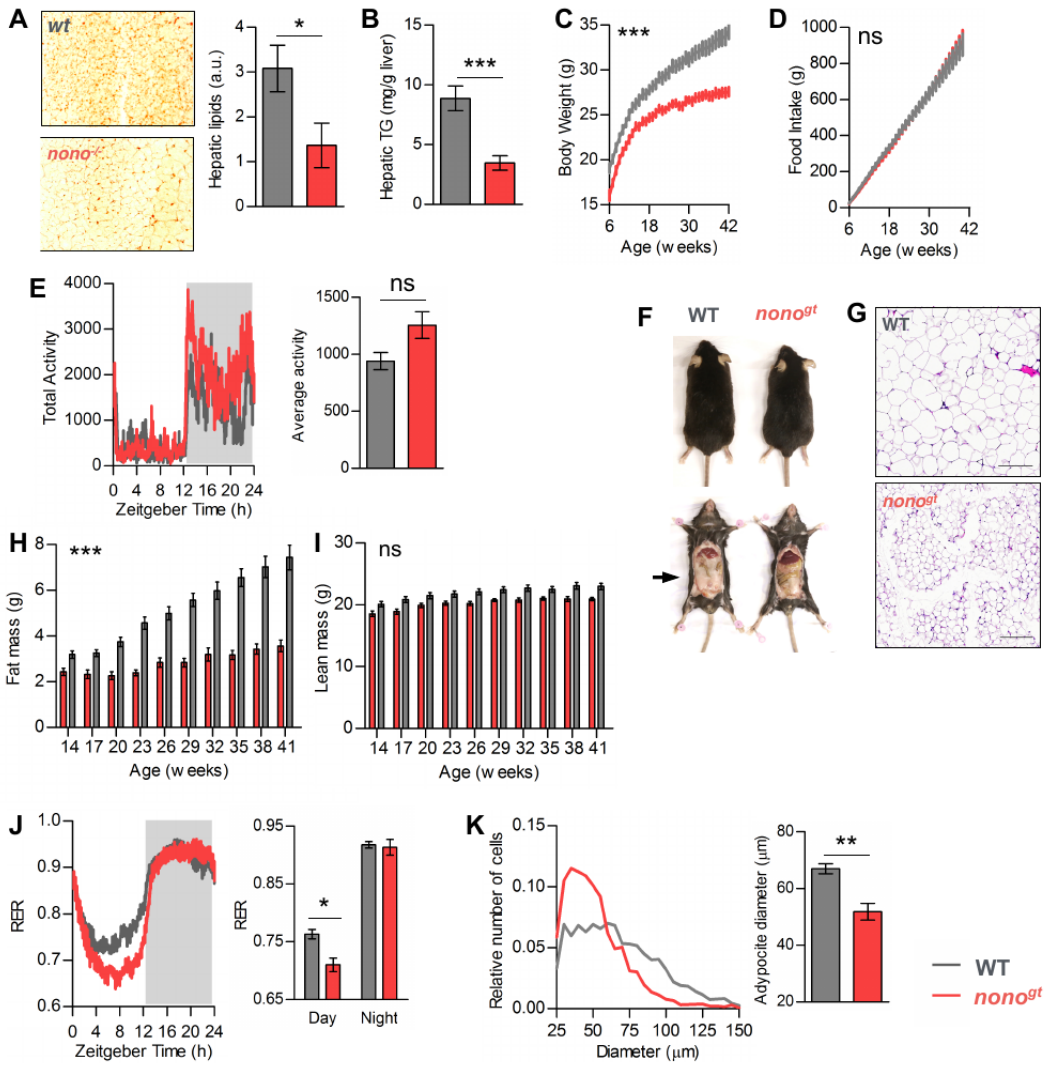

Figure 7. *Nonogt* mice have reduced body fat and body weight
(A) Representative image of hepatic lipid staining by Oil-Red-O (ORO) in WT and *nonogt* mice at 45 weeks of age and quantification of the ORO staining signal (right panel), n=3 per group. (B) Hepatic triglycerides content quantification, WT n=11, *nonogt* n=8. (C) Body weight of WT and *nonogt* mice form 6 to 42 weeks of age measured weekly, WT n=14, *nonogt* n=13. (D) Cumulative food consumption of the same mice as in (C), calculated from the cage average food consumption measured weekly, n=4 cages per group. (E) Cage activity (15 minutes bin) average of 4 consecutive days and 24h average cage activity (right panel), n=4 per group. (F) Representative images of WT and *nonogt* mice. (G) Representative H&E staining images of the epididymal fat pads at 42 weeks of age, scale bar=200µm. (H) and (I) Fat mass and lean mass of the same mice as in (C) measured every 3 weeks starting from 14 weeks of age, WT n=14, *nonogt* n=13. (J) Left panel: respiratory exchange ratio (15 minutes bin), average of 4 consecutive days. Right panel: histogram representing day and night average RER, n=4 per group. (K) Adipocyte size distribution and average adipocyte diameter (right panel) calculated from the epididymal fat H&E staining images, n=5. Statistical analysis for (A), (B), (E), (J) and (K) Student t-test. Statistical analysis for (C), (D), (H), and (I) 2-way ANOVA. *p<0.05, **p<0.01, ***p<0.001 (for B), ***p<0.0001 (for C and H). Results are represented as mean±SEM.

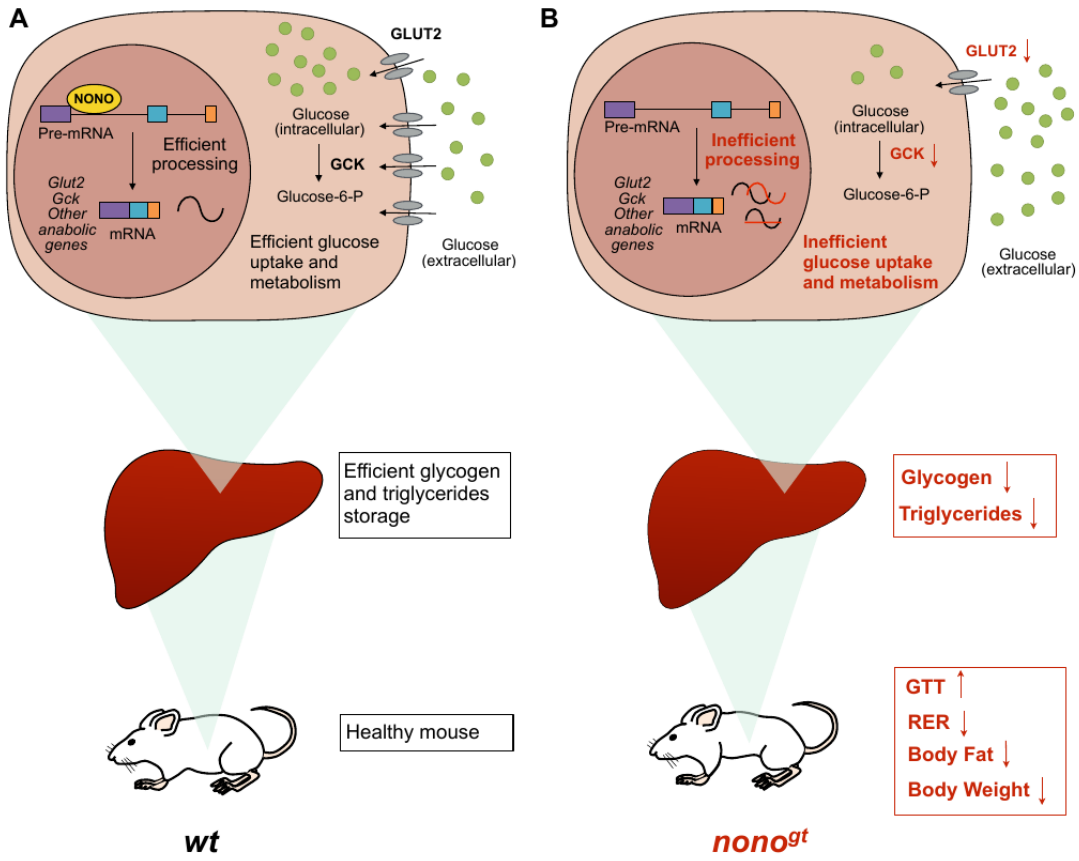

Figure 8. Proposed model of how NONO regulates gene expression in the liver and its physiological consequences
(A) In the presence of NONO, NONO-target RNAs involved in glucose metabolism and other anabolic pathways are efficiently processed to allow robust and in phase oscillation and normal glucose uptake and storage in the hepatocytes. (B) When NONO is absent, pre-mRNA processing of its target genes is less efficient and this leads to loss of oscillation or delay in the phase of oscillation. Altered expression expression pattern of NONO-target genes has a profound metaboloic impact; inefficient glucose uptake that leads to impaired glucose tolerance, reduced glucose and fat storage and increased fat breakdown.

Supplementary Figures

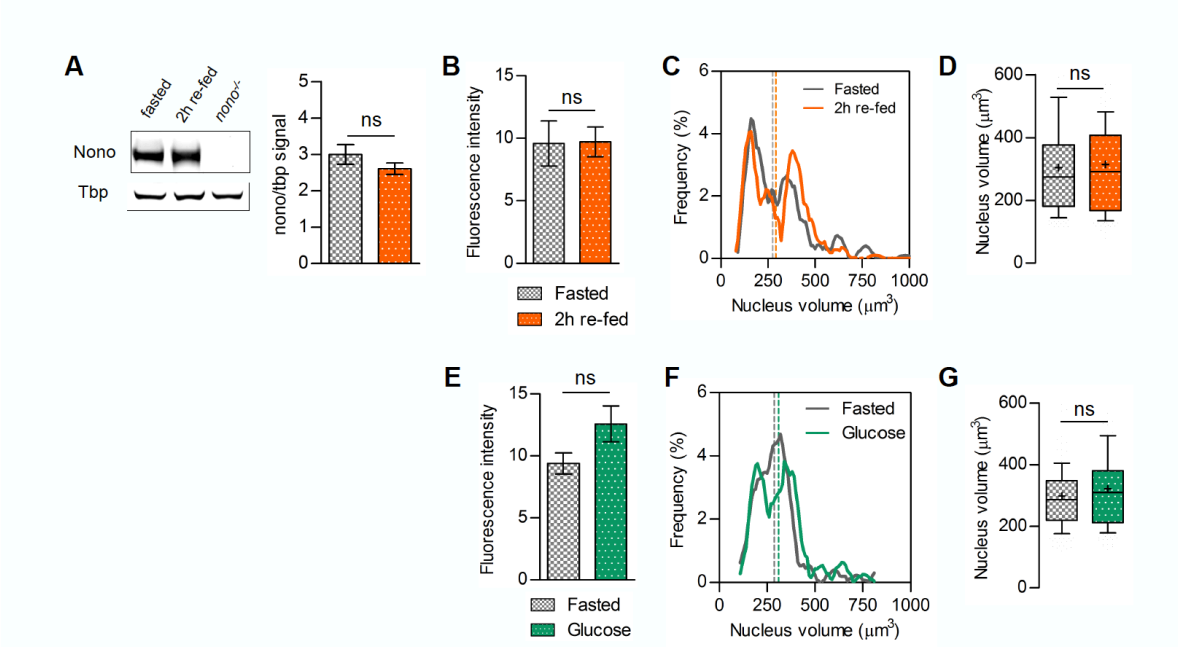

Figure S1. NONO protein abundance in the nucleus and liver nuclei size are unchanged upon feeding.
A) Representative western blot of NONO expression, n=5. (B) and (E) Average fluorescence intensity normalised to background; (C) and (F) distribution of the nucleus volume; (D) and (G) average nucleus volume; (C), (D), (F), and (G) n>170 nuclei; (B) and (E) n=12 images per group; For (D) and (G) results are represented as box and whiskers: 10-90 percentile range, '+' sign represents mean. For (A), (B) and (D) results are represented as mean±SEM. Statistical analysis student t test.

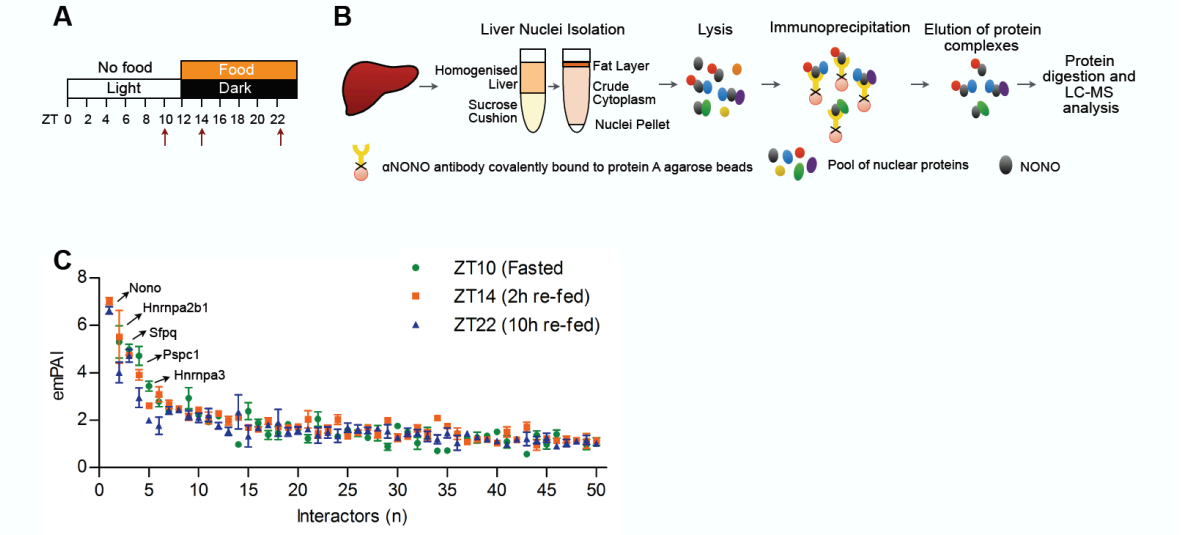

Figure S2. Characterization of NONO interactors by IP-MS.
(A) Experimental scheme indicating the time points at which liver were collected for IP-mass spectrometry analysis. Livers were collected at the end of the fasting phase (ZT10), 2h after the start of the feeding phase (ZT14) and at the end of the feeding phase (ZT22). (B) Outline of the experimental methods for the NONO IP-MS in liver nuclei. Liver was homogenized and ultracentrifuged on a sucrose cushion to isolate liver nuclei. Nuclear lysates were incubated with agarose beads cross-linked to anti-NONO antibody. NONO and NONO interactors were eluted and identified by mass spectrometry. (C) 50 most abundant NONO interactors sorted by average emPAI value. N=3 per group. Data are represented as mean±SEM.

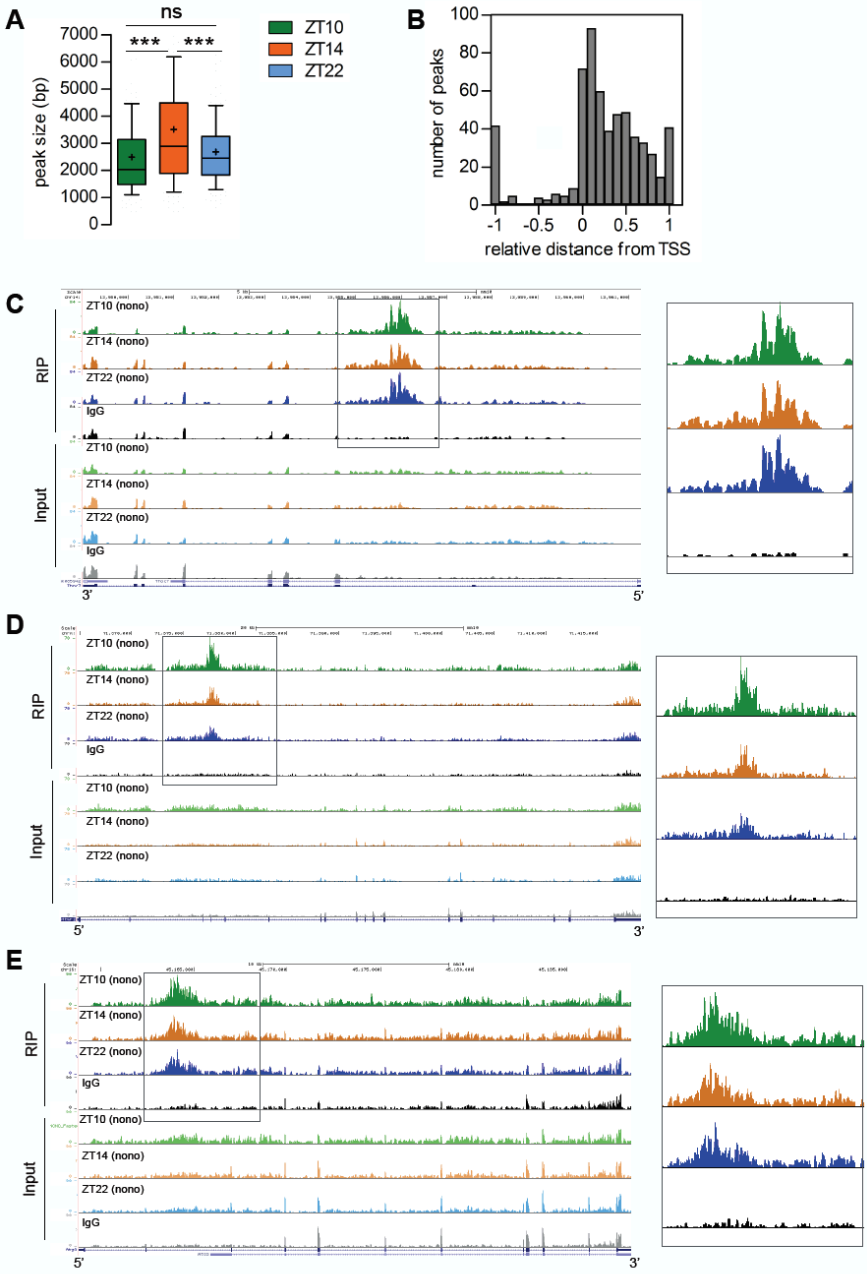

Figure S3. NONO binds promoter-proximal introns and its binding activity increases upon feeding. Related to Figure 2.
(A) Average RIP-seq peak size for the 134 common targets at each indicated time point. (B) Relative distance of NONO RIP-seq peaks (ZT14) from the TSS normalized to gene size. (C), (D) and (E) UCSC genome browser view of the RIP-seq reads mapping to Thoc7 (C), Mtmr1 (D) and Atg3 (E) genes, the right panels highlight the NONO RIP-seq peaks in Thoc7 intron 1, and Mtmr1 intron 2 and Atg3 intron 2. Each time point is a pool of 2 independent RIP experiments. In (A) results are represented as box and whiskers: 10-90 percentile range, '+' sign represents mean. Statistical analysis one-way ANOVA, ***p<0.0001.

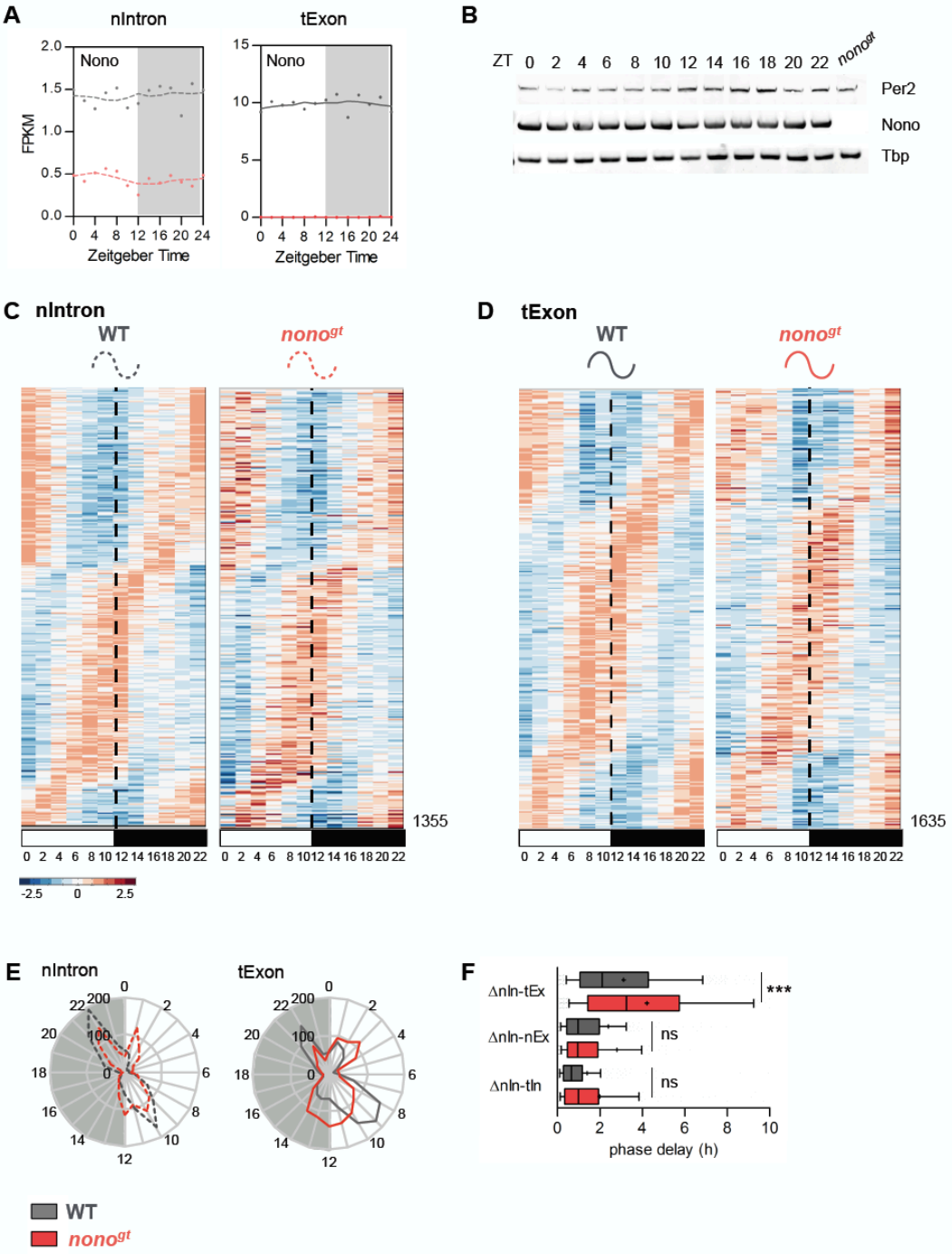

Figure S4. Mature mRNA peak phase of expression is delayed in *nono*^{gt} mice at genome wide level.
(A) Nono mRNA expression (FPKM) at the transcription level (nIntron) and at the mature mRNA level (tExon) across a 24 h cycle, samples were collected every 2 h starting at ZT0. Each time point is a pool of 2 mice. (B) NONO, PER2 and TBP protein expression in liver nuclei across a 24 h cycle, samples were collected every 2 h starting at ZT0. (C) Normalized profile of expression of genes cycling at the pre-mRNA level (nIntron) in both WT and *nono*^{gt} mice at the indicated time points. (D) Normalized profile of expression of genes cycling at the mature mRNA level (tExon) in both WT and *nono*^{gt} mice at the indicated time points. High expression is displayed in orange, low expression in blue. (E) Peak phase distribution of the same genes as in (C) and (D) separated by bins of 1h: left panel pre-mRNA peak phases (nIntron, n=1355), right panel mature mRNA peak phases (tExon, n=1635). (F) Phase delay between nIntrons and tExon, nIntron and nExon, nIntron and tIntron in WT and *nono*^{gt} livers. Only genes with a positive delay (phase difference≥0) were considered for this analysis. Statistical analysis one-way ANOVA, ***p<0,0001.

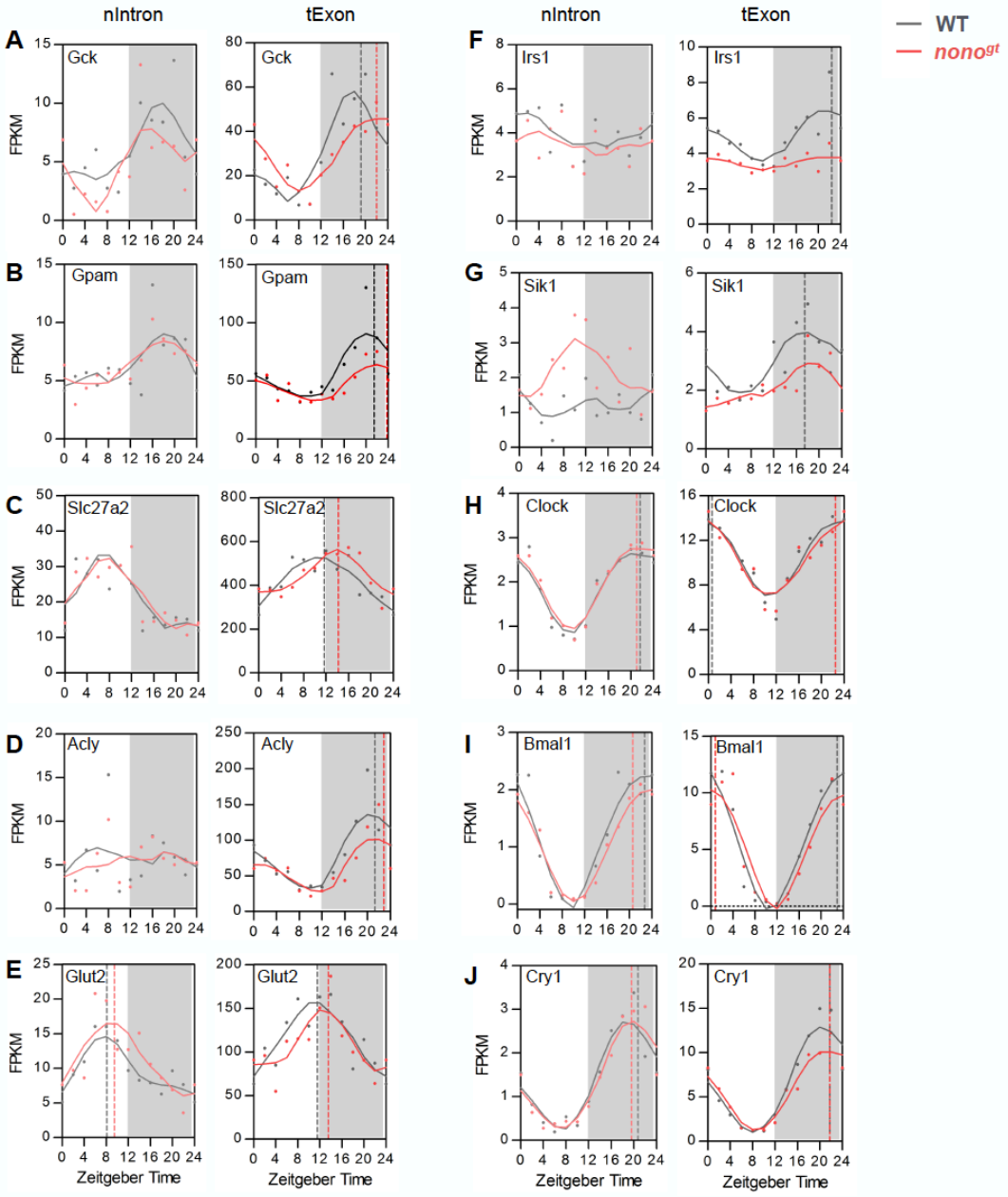

Figure S5. Examples of transcription and mature mRNA rhythms in *wt* and *nono*^{gt} livers.
Examples of gene expression at the transcription level (nIntron) and at the mature mRNA level (tExon) in the mouse liver, samples were collected every 2h starting at ZT0. When a gene is considered cycling its peak phase of expression calculated using metacycle (see STAR METHODS for details) is indicated as a dashed line. Each time point is a pool of 2 mice. (A-D) Examples of genes that are bound by NONO in the RIP-seq dataset and are rhythmic at the mRNA level but not at the transcription level in both genotypes. These genes are delayed in their phase of oscillation in *nono*^{gt} livers. Phase delay: 2.9h (Gck), 2.3h (Gpam), 2.5h (Slc27a2), 1.6h (Acly). (E) Example of a gene that is bound by NONO in the RIP-seq dataset and is rhyhtmic both at the transcription and mRNA level in both genotypes. For this group of genes *nono*^{gt} liver have a longer delay in the mRNA phase compared to the transcription phase. Glut2 gene phase delay: 1.4h (nIntron), 2h (tExon). (F-G) Examples of genes that are bound by NONO in the RIP-seq dataset, are not rhythmic at the transcription level and are rhythmic at the mRNA level only in the WT mice (loss of mRNA rhythmicity in *nono*^{gt} mice). (H-J) Examples of clock genes profile of expression. Clock genes are rhythmic both at the transcription (nIntron) and mature mRNA (tExon) level and are expressed at the expected phases in both geneotypes.

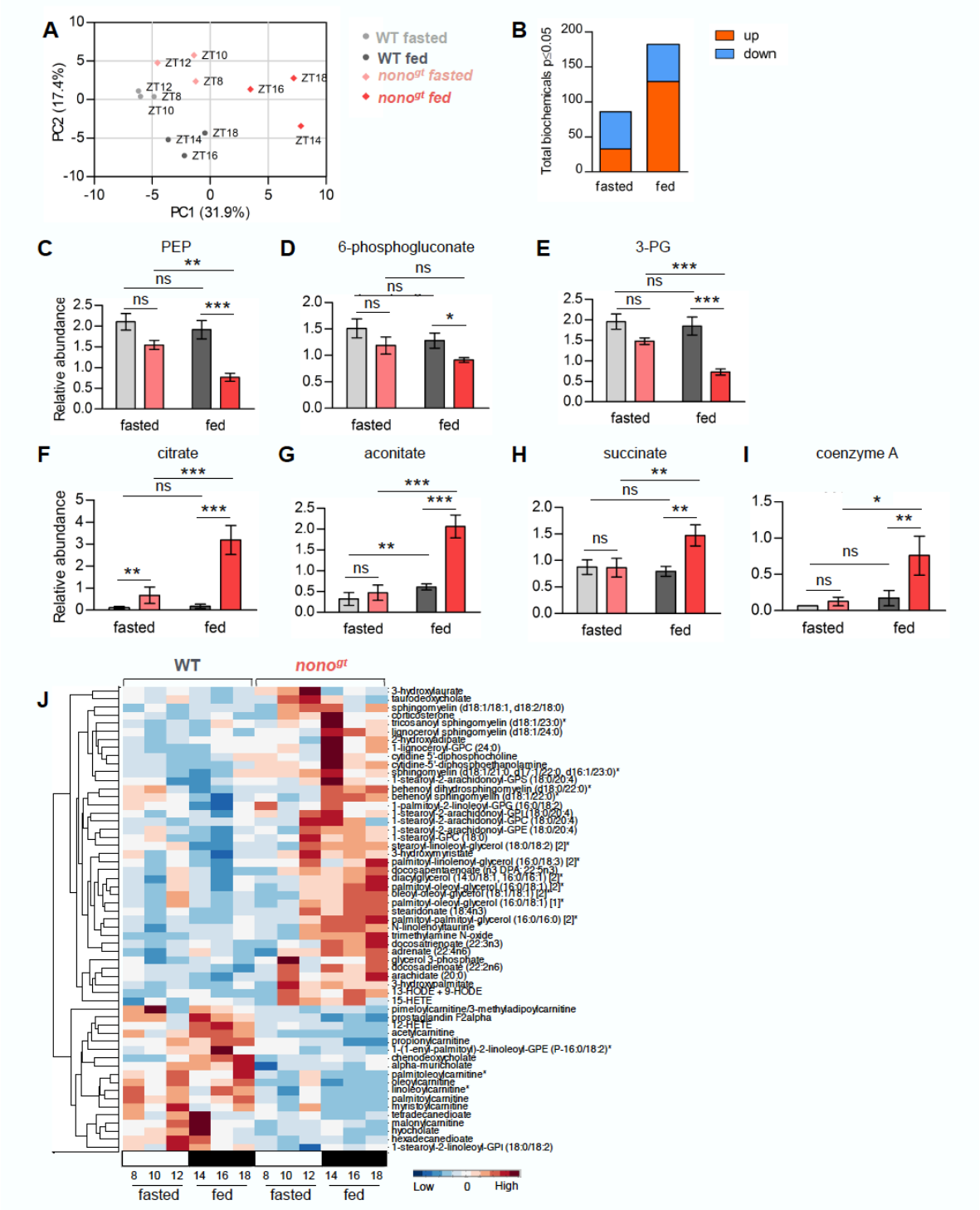

Figure S6. Upon feeding several metabolites involved in glucose metabolism, lipid metabolism and the TCA cycle are changed in *nonogt* livers. Related to Figure 6.
(A) PCA analysis of the metabolomics profile of WT and *nonogt* mice in fasted and re-fed conditions. (B) Number of significantly up and down-regulated metabolites in *nonogt* mice compared to *wt* in fasted and re-fed conditions. (C-I) Relative abundance (median normalized) of selected liver metabolites involved in glycolysis (C-E) and the TCA cycle (F-I). (J) Normalized quantification of lipid metabolites significantly altered between *wt* and *nonogt* mice. For metabolomics analysis liver samples were collected at 3 and 4 different time points respectively, fasted: ZT8, ZT10, ZT12; fed: ZT14, ZT16, ZT18, ZT20 (2 mice per time point). Statistical analyses were performed comparing fasted and fed groups of the two genotypes: fasted n=6, fed n=8. Statistical analysis for (C-I) ANOVA contrasts, *p<0.05, **p<0.01, ***p<0.0001.

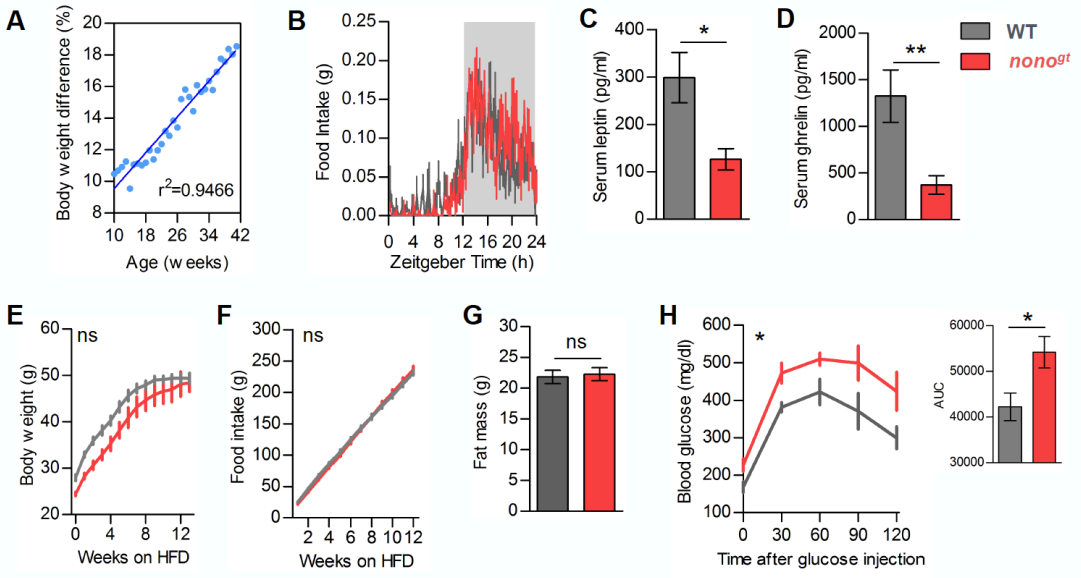

Figure S7. An high fat diet can compensate for defective glucose uptake and storage in *nono*^{gt} mice. Related to Figure 6.

(A) Percent body weight difference between *wt* and *nono*^{gt} mice from 10 to 42 weeks of age. When mice are on normal chow the body weight difference increases linearly with age (r^2=0.9466). (B) Food intake during 24 h (15 minutes bin) average of 4 consecutive days, n=4 per group. (C) Serum leptin levels after 12h of light-phase fasting, WT n=6, *nono*^{gt} n=6. (D) Serum ghrelin levels after 12h of light-phase fasting, WT n=8, *nono*^{gt} n=8. (E) Body weight curve during 12 weeks of HFD. (F) Cumulative food consumption of the same mice as in (E). (G) Fat mass of the same mice after 12 weeks on high fat diet. (H) Glucose tolerance test after 12 weeks on high fat diet, glucose (1g/kg), right panel AUC. For panels E-H WT n=6, *nono*^{gt} n=5. Results are represented as mean±SEM. Statistical analysis for (E), (F) and (H) 2-way ANOVA, Bonferroni posttest. Statistical analysis for (C), (D), (G) and AUC student t test. *p<0.05, **p<0.01.

Materials and Methods

Key resources table

REAGENT or RESOURCE	SOURCE	IDENTIFIER
Antibodies		
Normal rabbit IgG	Santa Cruz	Sc-2027
Rabbit anti-GCK	Santa Cruz	Sc-7908
Rabbit anti-TBP	Santa Cruz	Sc-273
Rabbit anti-GLUT2	ThermoFisher	720238
Rabbit anti-NONO	Steven A. Brown Laboratory	N/A
Alexa Fluor 680 conjugate anti-rabbit IgG	ThermoFisher	A-10043
Alexa Fluor 488 conjugate anti-rabbit IgG	ThermoFisher	A-11008
Bacterial and Virus Strains		
AAV2/8.TBG.NONO	This study	N/A
AAV2/8.TBG.NONOmut	This study	N/A
Chemicals, Peptides, and Recombinant Proteins		
Insulin	Novo Nordisk	NDC 0169-3473-18
D-Glucose	Sigma	G8270
Protein A agarose beads	Roche	11134515001
Vanadyl Ribonucleoside Complex (VRC)	NEB	S1402S
RNAse OUT	Invitrogen	10777019
Octyl β-D-glucopyranoside (NOG)	Sigma	O8001
Spermine	Sigma	S3256
Spermidine	Sigma	S2626
Trizol	Invitrogen	15596018
Bolt LDS Sample Buffer	Invitrogen	B0008
Bolt Sample Reducing Agent	Invitrogen	B0009
Bolt 4-12% Bis-Tris Plus Gels	Invitrogen	NW04125BOX
1x Phosphate Buffered Saline (PBS) with 1% Casein	BioRad	1610783
MluI	NEB	R0198S
SalI-HF	NEB	R3138S
T4 ligase	NEB	M0202S
Critical Commercial Assays		
Pierce BCA assay	ThermoFisher	23225
Triglyceride Quantification Kit	Abcam	ab65336
Ultra Sensitive Mouse Insulin ELISA kit	CrystalChem	90080
Glucose (HK) Assay Kit	Sigma	GAHK20-1KT
qScript cDNA SuperMix	Quantabio	95048
FastStart Universal SYBR Green Master Mix	Roche	04913914001
Ribo-Zero Magnetic Gold Kit	Illumina	MRZG12324
Deposited Data		
RIP-seq and liver nuclear and total transcriptome	This study	GEO: GSE98042
Experimental Models: Organisms/Strains		
C57BL/6-nono^{gt}	(Kowalska et al., 2012)	N/A
Oligonucleotides		
Primers for RT-PCR		
mGck_Intron	GGGAAGCTACTTGAGAGAGCA (Fwd)	This study; synthesized by N/A

	ACTCTGCATGGCCTCAAACT (Rev)	Integrated DNA Technologies	
mGck_Spliced	TCTGACTTCCTGGACAAGCA (Fwd)	This study; synthesized by Integrated DNA Technologies	N/A
	CCACGATGTTGTTCCCTTCT (Rev)		
mGlut2_Intron	CCCCAATTCCAACAGAAGAA (Fwd)	This study; synthesized by Integrated DNA Technologies	N/A
	TGGCCAACATGAAAACTCAA (Rev)		
mGlut2_Spliced	GCCTGTGTATGCAACCATTG (Fwd)	This study; synthesized by Integrated DNA Technologies	N/A
	CGTAACTCATCCAGGCGAAT (Rev)		
mActin	GGCTGTATTCCCCTCCATCG (Fwd)	This study; synthesized by Integrated DNA Technologies	N/A
	CCAGTTGGTAACAATGCCATGT (Rev)		
m18S rRNA	TCAAGAACGAAAGTCGGAGG (Fwd)	This study; synthesized by Integrated DNA Technologies	N/A
	GGACATCTAAGGGCATCAC (Rev)		
Primers for genotyping			
mNono wt	TTAGGGGGCCGAACTACTTGAATTG	This study; synthesized by Integrated DNA Technologies	N/A
	GGGCCGGGCAGATTTACTAGTTTTT		
b-GEO cassette	CAAATGGCGATTACCGTTGA	This study; synthesized by Integrated DNA Technologies	N/A
	TGCCCAGTCATAGCCGAATA		

Recombinant DNA		
pUC57.NONO	This study; synthesized by GenScript	N/A
pUC57.NONOmut	This study; synthesized by GenScript	N/A
pENN.AAV.TBG.PI	(Hogan et al., 2015)	N/A

Software and Algorithms		
ImageJ	NIH	https://imagej.nih.gov/ij/
ZEN Imaging Software	Carl Zeiss	https://www.zeiss.com/microscopy/int/products/microscope-software/zen.html
Imaris Image Analysis Software	Bitplane	http://www.bitplane.com
Prism	GraphPad	https://www.graphpad.com/scientific-software/prism/#1
Matlab	MathWorks	https://www.mathworks.com/products/matlab.html
R	R Foundation for Statistical Computing	https://www.r-project.org
FastQC	Babraham Bioinformatics	http://www.bioinformatics.babraham.ac.uk/projects/fastqc
STAR aligner	(Dobin et al., 2013)	http://code.google.com/p/rna-star/
HOMER	(Heinz et al., 2010)	http://homer.ucsd.edu/homer/
GO-Elite	(Zambon et al., 2012)	http://www.genmapp.org/go_elite/
Image Studio	LI-COR	https://www.licor.com/bio/products/software/image_studio/

Other		
Normal Chow Diet	LabDiet	5001
High Fat Diet	LabDiet	58Y1

Mouse models

All animal experiments were carried out in accordance with the guidelines of the IACUC of the Salk Institute, and the approval of the Zürich Cantonal Veterinary Authority. All mice were maintained in a pathogen-free environment and housed in clear shoebox cages in groups of five animals per cage with constant temperature and humidity and 12h:12h light-dark cycle. All animals had access to water at all times. Unless otherwise indicated, mice were fed ad libitum with a normal chow diet (LabDiet-5010). For the fasting/feeding experiments mice were fasted for 12h during the light phase (ZT0-ZT12) and fed for 12h during the dark phase (ZT12-ZT24). For the HFD experiments mice were fed ad libitum with a diet containing 60% fat (58Y1). *Nono*^{gt} mice were obtained as described previously (Kowalska et al., 2012). Briefly, chimeric mice were obtained from *Nono* gene-trapped embryonic stem (ES) cells (C57BL/6J genotype) via standard blastocyst injection of the ES cell clone YHA266 into SV129 mice by the University of California, Davis. Individual chimeric mice were backcrossed for 10 generations against the C57BL/6J background. All experiments were performed by comparing wild type and mutant male littermates.

Liver immunostaining

The livers were perfused with 2 ml of ice-cold PBS through the spleen and immediately collected. Pieces of the main liver lobes were embedded in optimal cutting temperature (O.C.T.) compound (Tissue-Plus, Scigen, 4583) and frozen at -80° C. For cryosectioning the embedded liver was equilibrated at -20° C in a cryostat chamber and 10 μm thick sections were cut. Liver slices were collected on 25x75x1.0mm microscope slides (Superfrost Plus, Fisherbrand) and stored at -80° C. For immunostaining frozen sections were thawed in a sealed environment to avoid damage by frozen water crystals. Liver sections were fixed at room temperature for 10 minutes in 4% PFA diluted in PBS. Sections were then washed 3 times in TBS-T (50mM Tris, 150mM NaCl, 0.05% Tween-20). The tissue sections were permeabilized in 1% Triton-X 100 diluted in TBS (50mM Tris, 150mM NaCl) for 30 minutes at room temperature. The sections were then incubated in blocking buffer (1% BSA, 0.5% Triton-X 100 in TBS) for 30 minutes. After the blocking step, liver sections were incubated for 1h with rabbit anti-NONO antibody (Kowalska et al., 2012) diluted 1:500 in blocking buffer. After 3 washes in TBS-T, the sections were incubated with the secondary antibody Alexa Fluor 488 conjugate anti-rabbit IgG

(Thermo Fisher) diluted 1:1000 in blocking buffer for 30 minutes. Sections were washed three times with TBS-T. At the first wash DAPI was added to the washing buffer at a concentration of 0.5 μg/ml. Sections were then mounted and imaged. Images were acquired with a 63x/1.4 NA Apochromat oil objective on an LSM 880 using the Airyscan detector (Carl Zeiss Microscopy). The images were acquired in "SR mode", which configures the 32 GaAsP detectors on the Airyscan detector as equivalent to 0.2 Airy Units. The 32-channel data was then processed using Zen software (Carl Zeiss Microscopy) (Huff, 2015). All images were acquired with a 63X objective, using 1.8% laser, 750 gain, and 0.97 μs pixel dwell time, and they were all processed with an "Airyscan parameter" (Wiener filter strength) of 4.1.

Speckle-like structures and fluorescence quantification

For image analysis Imaris software (Bitplane) was used. For the speckle-like structures quantification we used the 'spots' option. We considered 'speckle-like structures' objects within the nuclei (identified by DAPI stained areas) with an estimated diameter of 0.3 μm, 'quality' above 900 and 'intensity' above 924. For fluorescence intensity quantification, average intensity within the nuclei was normalized to average intensity outside the nuclei (background).

Immunoprecipitation from liver nuclear lysates

Immunoprecipitation of NONO complexes was performed from mouse liver nuclear extracts. The livers were perfused with 2 ml of ice-cold PBS through the spleen and immediately collected. Liver nuclei were isolated from an entire mouse liver as previously described (Ripperger and Schibler, 2006). Briefly the dissected mouse liver was rapidly homogenized in 5ml of ice cold PBS and mixed to 25ml of 2.4M sucrose buffer (2.4M sucrose, 150mM glycine, 10mM Hepes pH7.6, 15mM KCl, 2mM EDTA, 0.5mM spermidine, 0.15mM spermine, 1mM PMSF, 5mM β-mercaptoethanol and protease inhibitors (pepstatin A, leupeptin, aprotinin, trypsin inhibitor)). The homogenate was layered on top of a 10ml cushion of 2M sucrose buffer (2M sucrose, 10% glycerol, 125mM glycine, 10mM Hepes pH7.6, 15mM KCl, 2mM EDTA, 0.5mM spermidine, 0.15mM spermine, 1mM PMSF, 5mM β-mercaptoethanol and protease inhibitors) and centrifuged for 45min at 24,000rpm at 4° C in a Beckmann SW28 rotor. Isolated liver nuclei were resuspended in 800 μl of Nuclei Dilution Buffer (100mM KCl, 0.2mM EDTA, 20% glycerol, 20mM Hepes

pH7.6, 1mM PMSF, 5mM β-mercaptoethanol and protease inhibitors) and centrifuged at 5000rpm for 30 seconds. The nuclei pellet was lysed in nuclei lysis buffer (25mM Tris:HCl pH7.4, 187.5mM NaCl, 2.5mM EDTA, 10% NOG and protease inhibitors) and incubated for 20 minutes on ice. Lysates were centrifuged at 10000rpm for 10 minutes at 4° C and the protein concentration in the supernatant was measured with Pierce BCA assay (Thermofisher) following manufacturer's instructions. To immunoprecipitate NONO complexes, 600 μg of nuclear protein lysate were incubated with 10ul of protein A agarose beads cross-linked to polyclonal rabbit anti-NONO antibody (Kowalska et al., 2012) for 2h at 4°C. Immunoprecipitated NONO complexes were washed 3 times with IP washing buffer (75mM Tris:HCl pH7.4, 150mM NaCl, 1mM EDTA, 10% glycerol, 0.1% NOG and protease inhibitors) and eluted with 0.1M glycine pH 2.5. After elution the acidic glycine was neutralized with tris-base.

Mass spectrometry analysis (as described in (Ma et al., 2016)

Samples were precipitated by methanol/chloroform. Dried pellets were dissolved in 8M urea/100mM TEAB, pH 8.5. Proteins were reduced with 5mM tris(2-carboxyethyl)phosphine hydrochloride (TCEP, Sigma-Aldrich) and alkylated with 50mM chloroacetamide (Sigma-Aldrich). Proteins were digested overnight at 37°C in 2M urea/100mM TEAB, pH 8.5, with trypsin (Promega). Digestion was quenched with formic acid, 5% final concentration. The digested samples were analyzed on a Fusion Orbitrap tribrid mass spectrometer (Thermo). The digest was injected directly onto a 30cm, 75um ID column packed with BEH 1.7 μm C18 resin (Waters). Samples were separated at a flow rate of 200nl/min on a nLC 1000 (Thermo). Buffer A and B were 0.1% formic acid in water and acetonitrile, respectively. A gradient of 1-25%B over 90min, an increase to 40%B over 30min, an increase to 90%B over another 10min and held at 90%B for a final 10min of washing was used for 140min total run time. Column was re-equilibrated with 20ul of buffer A prior to the injection of sample. Peptides were eluted directly from the tip of the column and nanosprayed directly into the mass spectrometer by application of 2.5kV voltage at the back of the column. The Orbitrap Fusion was operated in a data dependent mode. Full MS^1 scans were collected in the Orbitrap at 120K resolution with a mass range of 400 to 1600m/z and an AGC target of $5e^5$. The cycle time was set to 3 seconds, and within

this 3 seconds the most abundant ions per scan were selected for CID MS/MS in the ion trap with an AGC target of $1e^4$ and minimum intensity of 5000. Maximum fill times were set to 50ms and 100ms for MS and MS/MS scans respectively. Quadrupole isolation at 1.6m/z was used, monoisotopic precursor selection was enabled and dynamic exclusion was used with exclusion duration of 5 seconds. Protein and peptide identification were done with Integrated Proteomics Pipeline – IP2 (Integrated Proteomics Applications). Tandem mass spectra were extracted from raw files using RawConverter (He et al., 2015) and searched with ProLuCID (Xu et al., 2015) against mouse UniProt database. The search space included all fully-tryptic and half-tryptic peptide candidates. Carbamidomethylation on cysteine was considered as a static modification. Data was searched with 50ppm precursor ion tolerance and 600ppm fragment ion tolerance. Data was filtered to 10ppm precursor ion tolerance post search. Identified proteins were filtered using DTASelect (Tabb et al., 2002) and utilizing a target-decoy database search strategy to control the false discovery rate to 1% at the protein level. Interactors were sorted by average emPAI (Ishihama et al., 2005). The top 50 proteins (excluding contaminants and ribosomal proteins) were selected.

Native RNA-immunoprecipitation (RIP)

RIP was performed in native conditions as previously described (Keene et al., 2006; Zhao et al., 2008, 2010), using one mouse liver nuclear lysate per IP. The livers were perfused with 2 ml of ice-cold PBS through the spleen and immediately collected. Liver nuclei isolation from mouse liver has been previously described (Ripperger and Schibler, 2006); briefly the dissected mouse liver was rapidly homogenized in 5ml of ice cold PBS and mixed to 25ml of 2.4M sucrose buffer (2.4M sucrose, 150mM glycine, 10mM Hepes pH7.6, 15mM KCl, 2mM EDTA, 0.5mM spermidine, 0.15mM spermine, 1mM PMSF, 1mM DTT, 400 μM VRC and protease inhibitors (pepstatin A, leupeptin, aprotinin, trypsin inhibitor)). The homogenate was layered on top of a 10ml cushion of 2M sucrose buffer (2M sucrose, 10% glycerol, 125mM glycine, 10mM Hepes pH7.6, 15mM KCl, 2mM EDTA, 0.5mM spermidine, 0.15mM spermine, 1mM PMSF, 1mM DTT, 400 μM VRC and protease inhibitors) and centrifuged for 45min at 24,000rpm at 4°C in a Beckmann SW28 rotor. Isolated liver nuclei were resuspended in Nuclei Dilution Buffer (100mM KCl, 0.2mM EDTA, 20% glycerol, 20mM Hepes pH7.6, 1mM PMSF, 1mM DTT, 400 μM VRC, 80U/ml

RNAse OUT and protease inhibitors). Liver nuclei were lysed in Polysome lysis buffer (100mM KCl, 5mM $MgCl_2$, 10mM HEPES pH 7.0, 0.5% NP40, 1mM DTT, 80U/ml RNAse OUT, 400uM VRC and protease inhibitors) and incubated 20 minutes on ice. Lysate was centrifuged and protein concentration in the supernatant was measured with Pierce BCA assay (Thermofisher). 0.5mg of protein were incubated with 40ul of protein A agarose beads pre-coated with 10µg of polyclonal rabbit anti-NONO antibody (Kowalska et al., 2012) or normal rabbit IgG (sc-2027) for 2h at 4°C. Before the incubation, 1/10 of the supernatant was put aside to be used as input. After incubation samples were washed 4 times with NT2 buffer (50mM Tris-HCl pH 7.4, 150 mM NaCl, 1mM MgCl2, 1% Triton-X 100). Immunoprecipitated RNA and input RNA were extracted using Trizol reagent (Invitrogen).

RNA extraction

For RNA extraction the livers were perfused with 2 ml of ice-cold PBS through the spleen and immediately collected. For total liver RNA extraction pieces from the main liver lobes were ground to a powder in liquid nitrogen. About 10mg of tissue were used for RNA extraction using Trizol reagent (Invitrogen). For nuclear RNA extraction liver nuclei were isolated as described above (see Native RNA-immunoprecipitation section). The nuclei pellet was rapidly resuspended in Trizol reagent (invitrogen) and purified.

High-throughput RNA sequencing (RNA-seq)

Liver total, nuclear and RIP purified RNA were used for RNA-seq. RNA from two biological replicates per time point was pooled prior to library preparation. Libraries were prepared using Illumina's TruSeq Stranded Total RNA Library Prep Kit with Ribo-Zero Gold according to manufacturer's instructions. In brief, rRNA was depleted from total RNA (1 μ g) by using subtractive hybridization. The RNA was then fragmented by metal-ion hydrolysis and subsequently converted to cDNA using SuperScript II. The cDNA was then end-repaired, adenylated and ligated with Illumina sequencing adapters. Finally, the libraries were enriched by PCR amplification. All sequencing libraries were then quantified, pooled and sequenced at single-end 50 base-pair (bp) on Illumina HiSeq 2500 at the Salk NGS Core. Each library was sequenced on average 20 million reads. Raw sequencing data was demultiplexed and converted into FASTQ files using CASAVA (v1.8.2).

RNA-seq and RIP-seq data analysis

Sequenced reads were quality-tested using FASTQC (available online at: http://www.bioinformatics.babraham.ac.uk/projects/fastqc) and aligned to the mm10 mouse genome using the STAR aligner (Dobin et al., 2013) version 2.4.0k. Mapping was carried out using default parameters (up to 10 mismatches per read, and up to 9 multi-mapping locations per read). For transcriptome data analysis, nuclear RNA-Seq and total RNA-Seq normalized gene expression (FPKM) was quantified across all gene exons and introns separately, using the top-expressed isoform as a proxy for gene expression. For the RIP-seq analysis, reads uniquely mapping to the genome were used for peak calling with Homer (Heinz et al., 2010) assuming the size of 500, extending the peaks to cover the full enriched region, assuming a fold enrichment of at least 2 over input reads, a poisson p-value threshold relative to input count of 1e-4. The peaks that had less then 1.5 fold enrichment over IgG control and less the 200 tag count were filtered out. Homer was also used to generate normalized read count density tracks for visualization of peaks, motif enrichment analysis, and peak annotation. Motif enrichment analysis was carried out for the peak regions found in introns, searching for motif lengths of 8, 10, and 12, or using a set of all vertebrate motifs known to Homer and using default values for all other parameters.

Statistical analysis of rhythmic gene expression

All RNA-Seq samples exhibited a relatively similar expression profile, reflecting the low variation in sequencing depth between the samples (total RNA-seq samples $17.4x10^6 \pm 4.1x10^6$ uniquely mapped reads, nuclear RNA-seq samples $19.7x10^6 \pm 4.4x10^6$ uniquely mapped reads). We compared FPKM values from nuclear Introns and Exons as well as total Introns and Exons separately in both *WT* and *nono*^{gt} animals based on a common list of 20770 genes. Only genes with an average FPKM value ≥0.3 over the 12 time points were considered as expressed. We then used meta2d, a function of the R package MetaCycle, to evaluate periodicity in the RNA seq data (Wu et al., 2016). Briefly, meta2D incorporates ARSER (Yang and Su, 2010), JTK_CYCLE (Hughes et al., 2010), and Lomb-Scargle (Glynn et al., 2006) and it implements N-version programming concepts to integrate their results (p and q values, period, phase and amplitude). Transcripts were considered to be rhythmically expressed when the integrated p value was <0.05. The

different analyses were run on homemade MATLAB (MathWorks) programs.

Gene ontology and pathway over-representation analysis (ORA) (as described in Zambon et al., 2012)

For gene ontology and pathway ORA analysis GO-Elite was used as previously described (Zambon et al., 2012). Each analyzed term was ranked according to a Z-score. We used 2000 permutations, Z-score cut-off of 1.96, permuted p-value cut-off of 0.05. Ontology terms were sorted by Z-score.

Gene Expression Analysis by RT-qPCR

Total RNA was prepared from WT and *nono*^{gt} livers as described above and quantified using Nanodrop 2000 spectrophotometer (ThermoFisher). 1 μg of RNA was reverse transcribed using qScript cDNA SuperMix (QuantaBio) in a final volume of 20 μl, according to manufacturer's instructions. Reverse transcribed RNA was diluted 1:6 and 25ng of cDNA were used in qPCR reactions. qPCR reactions were prepared using the FastStart Universal SYBR Green Master Mix (Roche). The sequences of the primers used are listed in the key resources table. Reactions were run on a 7900HT Fast Real-Time PCR System (ThermoFisher) by the Functional Genomics Core Facility of the Salk Institute. Gene expression was normalized to 18S RNA and quantified using the comparative CT method.

Western Blotting

For protein extraction, 10-20mg of frozen liver powder was homogenized in RIPA lysis buffer (10mM Tris-HCl pH8.0, 1mM EDTA, 1% Triton-X 100, 0.1% SDS, 140mM NaCl and protease inhibitor cocktail). Samples were incubated with agitation for 30 minutes at 4° C and clarified by centrifugation and at 13000rpm for 10 minutes at 4° C. The protein concentration in the supernatant was determined using the BCA assay (Pierce). Equal amounts of protein (40 μg) were heat-denatured in Bolt LDS Sample Buffer (after addition of Bolt Sample Reducing Agent, ThermoFisher), resolved by SDS-PAGE using Bolt 4-12% Bis-Tris Plus Gels (ThermoFisher), and transferred to a nitrocellulose membrane using the iBlot Dry Blotting system (ThermoFisher). The membranes were blocked in 1XPBS 1% Casein Blocker (BioRad) diluted 1:10 for 1h at room temperature and then incubated with antibodies against NONO (rabbit polyclonal (Kowalska et al., 2012)), GCK (rabbit polyclonal, sc-7908), GLUT2 (rabbit polyclonal, ThermoFisher 720238) and

TBP (rabbit polyclonal, sc-273). Alexa Fluor 680 conjugate anti-Rabbit IgG (ThermoFisher, A-10043) was used as secondary antibody. Membrane-bound immune complexes were detected by Odyssey Imaging Systems (LI-COR Biosciences). Quantification was performed using Image Studio software (LI-COR Biosciences). Data were normalized to TBP protein expression.

GTT and ITT

For GTT and ITT mice were fasted for 12h during the light phase (ZT0-ZT12). Glucose (2g/kg for mice on normal chow, 1g/kg for mice on HFD) or insulin (0.5U/kg body weight) was injected intraperitoneally. Blood glucose level was measured using Nova Max plus glucose meter prior to injection and after 15, 30, 60, 90 and 120 minutes after injection.

Blood measurements

For all blood measurements mice were fasted for 12h during the light phase (ZT0-ZT12). Blood glucose content was measured through tail vein bleeding using the Nova Max plus glucose meter. Serum insulin levels were determined using Ultra Sensitive Mouse Insulin ELISA Kit (Crystal Chem), according to manufacturer's instructions. Whole blood was withdrawn from the tail vein, and serum was separated by centrifugation. 5 μl of serum were used for quantification. Leptin and ghrelin levels were determined using Bio-Plex Pro Mouse Diabetes 8-Plex Assay (Bio-rad) following manufacturer's instructions. Whole blood was withdrawn from the tail vein, and serum was separated by centrifugation and diluted 4-fold for quantification.

Liver glycogen quantification

Liver glycogen content was assayed as previously described (Passonneau and Lauderdale, 1974). Liver samples were ground in liquid nitrogen and 15-20mg of liver powder was placed in 0.5ml of 2M HCl and incubated at 100°C for 1h. After neutralization with an equal volume of 2M NaOH, the liberated glucose units were assayed enzymatically using the glucose (hk) assay kit (GAHK20, sigma). Glycogen content was expressed as micromoles of glucosyl units liberated per gram wet liver weight.

Adeno-associated Viruses (AAV) Strains, Propagation and Injection

Viruses were derived from pENN.AAV.TBG.PI; an adeno-associated virus, serotype

8 with a TBG promoter (Hogan et al., 2015). Briefly, 1-2µg of pENN.AAV.TBG.PI was digested with enzymes MluI and SalI (New England Biolabs). Meanwhile, the same amount of pUC57 constructs expressing either WT NONO (pUC57.NONO) or NONO with mutations F113A, F115A, K192A and I194A (pUC57.NONOmut) were also digested with MluI and SalI. The pUC57.NONO and pUC57.NONOmut constructs were produced by GenScript. The digested pENN.AAV.TBG.PI was ligated with the WT or mutant NONO inserts using T4 ligase (New England Biolabs) and transformed in One Shot TOP10 Chemically Competent *E. coli* (Invitrogen). The vectors were amplified using endotoxin-free maxi prep kit (Qiagen). The amplified vector sequences were verified by sequencing and checked for recombination prior to virus packaging. The resulting vectors (pENN.AAV.TBG.PI.NONO and pENN.AAV.TBG.PI.NONOmut) were packaged by the Salk Institute Gene Transfer Targeting and Therapeutics Core. The amplified viruses are referred to as AAV8.NONO and AAV8.NONOmut. Mice received a single tail vein injection of 10^{11} genome copies of either one of the described viral vectors.

Oil-Red-O staining

Oil-red-o staining was performed as previously described (Mehlem et al., 2013). Briefly, mice were sacrificed and the liver was perfused with ice-cold 1XPBS to remove the excess of blood. Pieces from the main liver lobes were embedded in optimal cutting temperature (O.C.T.) compound (Tissue-Plus, Scigen, 4583) and frozen at -80°C. For cryosectioning the embedded liver was equilibrated at -20°C in a cryostat chamber and 14 μm thick sections were cut. Unfixed tissue slides were stained with ORO and images were taken with a Zeiss VivaTome microscope at a 20X magnification. 10 images were taken per mouse and ImageJ was used for quantification of liver lipid content.

Liver triglycerides quantification

Livers were collected from ad libitum fed mice. The livers were perfused with 2 ml of ice-cold PBS through the spleen and immediately collected. For triglycerides quantification, Triglyceride Quantification kit (abcam) was used, following manufacturer's instructions. Briefly 100mg of liver powder were homogenized in 5% NP-40 using a dounce homogenizer. The samples were then heated to 80-100°C for 2-5 minutes and cooled down to room temperature. The heating step was repeated one more time and the samples were centrifuged at top speed for 2 minutes.

Supernatants were diluted 1:10 before proceeding with the assay.

Body composition

Magnetic resonance imaging scans for fat and lean mass were performed using an Echo MRI-100 instrument according to the manufacturer's instructions.

Indirect calorimetry

Mice were individually housed for at least 3 days before calorimetry experiments. Food intake, locomotor activity, oxygen consumption and carbon dioxide production were simultaneously measured for individually housed mice with a LabMaster system (TSE Systems). Data were collected for 3-4 days and analyzed.

Histology

Mouse abdominal fat tissue was fixed in 10% formalin and paraffin embedded. Sections (6 μ m) were used for haematoxylin and eosin staining.

Metabolomics analysis

Frozen liver powder aliquots were used for detection and relative quantification of metabolites by Metabolon as described (Evans et al., 2009). The dataset comprises a total of 588 compounds of known identity (named biochemical). An identical mass-equivalent of each liver was extracted and run across the platform; no additional normalization was applied prior to statistical analysis. Following log transformation and imputation of missing values, if any, with the minimum observed value for each compound, ANOVA contrasts were used to identify biochemicals that differed significantly between experimental groups. Only biochemicals with $p \leq 0.05$ were considered statistically significant. Analysis by two-way ANOVA identified biochemicals exhibiting significant interaction and main effects for experimental parameters of genotype and treatment.

Quantification and statistical analysis

Statistical parameters, including the exact value of n, descriptive statistics and statistical significance are reported in the method details, figures and the figure legends. All samples represent biological replicates. Unless otherwise specified in figure legends, all values shown in graphs are represented as mean±SEM. For statistical significance of the differences between the means of two groups, we used Student's t test. Statistical significance of differences among multiple groups (≥3) was calculated by performing ANOVA multiple comparisons. Statistical tests were

performed using Graph Pad Prism 5.

Data and software availability

The data discussed in this study have been deposited in NCBI's Gene Expression Omnibus (Edgar et al., 2002) and are accessible through GEO Series accession number GSE98042 (https://www.ncbi.nlm.nih.gov/geo/query/acc.cgi?acc=GSE98042).

Authors contribution

GB designed and performed the experiments, analyzed and interpreted the results and wrote the manuscript. SP supervised the study, designed the experiments, interpreted the results and wrote the manuscript. SAB supervised the study, designed the experiments, interpreted the results and reviewed the manuscript. LSM assisted in designing and performing experiments, analyzed RIP-seq, RNA-seq and metabolomics data and edited the manuscript. GE analyzed RIP-seq and RNA-seq data. HDL produced RIP-seq and RNA-seq libraries. EM performed experiments and provided technical support.

Acknowledgements

GB is a member of the Molecular Life Sciences Program of the Life Sciences Zurich graduate School. GB was partially supported by fellowships from Glenn Center for Aging Research and the Swiss National Science Foundation (SNF). This work was partially supported by Paul F. Glenn Center for Biology of Aging Research at the Salk Institute, the Helmsley Foundation, the American Federation for Aging Research grant M14322 (to SP). This work was partially supported by the Waitt Advanced Biophotonics Core, the GT3 Core, The Razavi Newman Integrative Genomics and Bioinformatics Core, the Mass Spectrometry Core and the NGS Core of the Salk Institute with funding from NIH-NCI CCSG: P30 014195, NINDS Neuroscience Core Grant: NS072031, the Waitt Foundation, NINDS R24 Core Grant, NEI, the Chapman Foundation and the Helmsley Center for Genomic Medicine. SAB and EM were supported by SNF and the Hartmann-Mueller Foundation. We thank Dr. Marc Montminy for sharing equipment and reagents. We thank Sam Van De Velde for reagents. We thank Uri Manor, Puifai Santisakultarm, Manching Ku, Max Shokhirev, James Moresco and Jolene Diedrich for technical

support; Amandine Chaix for technical support and comments on the manuscript; Emily Manoogian, Gabriele Sulli and David O'Keefe for comments and editing the manuscript.

4. GENERAL DISCUSSION AND OUTLOOK

In this work we report a novel role for the nuclear RNA-binding protein NONO in metabolic homeostasis. Specifically, NONO binds to pre-mRNAs encoding several key regulators of liver anabolic metabolism and enhances the processing of these pre-mRNAs, allowing for robust daily oscillation in mRNA levels. This facilitates subsequent translation of these anabolic regulators, which is necessary to store excess nutrients (as glycogen and triglycerides) during the postprandial period. Mice that lack NONO expression exhibit disruptions in this temporal regulation, such that animals shift from storing glucose as glycogen and fat to fat oxidation. This results in reduced glucose tolerance, reduced levels of glycogen and triglycerides in the liver, and reduced levels of body fat and body weight.

The liver is the central tissue maintaining metabolic homeostasis as the animal shifts between fed and fasted states. Indeed, the liver has first access to most ingested nutrients by virtue of their absorption into the hepatic portal vein. As a result the liver is exposed to higher nutrient levels than are other peripheral tissues (Moore et al., 2012). Fasting induces hepatic glycogen depletion, and glucose and ketone body production. Feeding a carbohydrate containing meal stimulates hepatic glucose uptake and glycolysis, replenishes glycogen stores, and induces fatty acid synthesis, while inhibiting β-oxidation and ketogenesis (Geisler et al., 2016). Understanding the elasticity of hepatic metabolite flux and the central role of the liver in providing nutrients to peripheral tissues is essential to studies of metabolic perturbation. In opposition to the relatively slow metabolic adaptation to fasting, feeding of a meal results in rapid metabolic changes. These metabolic changes require rapid changes in gene expression. As gene lengths vary by many orders of magnitude, their transcription would require highly variable amount of time assuming constant transcription rate. It is thus likely that for genes that require fast activation, like in case of response to feeding, modulation of both transcription and processing rates might play a role in fine tuning gene expression. In this work, we showed that NONO act as a post-transcriptional regulator to synchronize expression of mature mRNA with the fasting/feeding cycle.

NONO is one of the main components of nuclear paraspeckles and is essential for paraspeckle integrity (Sasaki et al., 2009). Paraspeckles are RNAse-sensitive structures whose formation depends on transcription by RNA polymerase II (Fox et al., 2002, 2005). It has been recently shown that liver weight, protein and

RNA content oscillate in a circadian fashion with maximum amounts overlapping with the mouse active/feeding phase (Sinturel et al., 2017). This suggests that feeding triggers a general increase in RNA and protein synthesis. It is likely that a general increase in transcription requires a parallel increase in pre-mRNA processing; we can hypothesize that the increased number of NONO-containing speckles might be due to increased recruitment of NONO and NONO-interacting factors to actively transcribed pre-mRNAs. Alternatively, specific phosphorylation events could play a role, as suggested in the case of MNK kinases (Buxadé et al., 2008) or during mitosis (Proteau et al., 2005). However, we speculate that the feeding-induced speckle-like structures we describe here are spatially and functionally distinct from paraspeckles. Recent research suggests that several different classes of NONO-containing nuclear speckles may exist (Li et al., 2017). Although the function of paraspeckles is still unclear, they have been shown to retain mRNAs that have undergone A-to-I editing by dsRNA-dependent adenosine deaminases (ADARs). mRNAs subject to this type of regulation include those with inverted repeated *Alu (*IR*Alu)* elements within their 3'UTR. Previous studies also showed that a NONO-containing complex specifically interacts with mRNAs having structured or edited 3'-UTRs to prevent their nuclear export (Chen and Carmichael, 2009; Chen et al., 2008; Zhang and Carmichael, 2001). One example of RNA regulated in this way is the mouse nuclear transcript CTN-RNA, which is edited within its 3'UTR and localizes to paraspeckles. During stress, CTN-RNA is cleaved and released into the cytoplasm as *mCat2* mRNA (Prasanth et al., 2005). In this work we found that NONO binds to introns and may instead function as a molecular scaffold to assemble the mRNA processing machinery on target RNAs and enhance pre-mRNA processing and mRNA stability. For example, levels of *Gck* mature mRNA peak toward the end of the night, yet NONO binds to *Gck* pre-mRNA at all time points tested (ZT10, ZT14 and ZT22). Thus, we hypothesize that NONO may prime its target pre-mRNAs for processing. In the absence of NONO, this recruitment is less efficient, leading to delays in the phase of oscillation or loss of rhythmicity.

In agreement with what has been demonstrated for NonA, the *Drosophila* homolog of NONO (McMahon et al., 2016), we found that NONO bound primarily to introns. Only 5% of the average, 27-kilobase (kb) human gene encodes protein; the majority is intronic sequence (Venter et al., 2001). Thus, transcription represents a

significant commitment of both energy and time (Swinburne and Silver, 2008). The number and size of introns contribute to the high variability observed in gene lengths (Heyn et al., 2015). How long it takes to transcribe a eukaryotic gene will be significantly affected by the gene architecture, in particular by the presence and abundance of introns. At one end, highly expressed genes tend to have short introns (Castillo-Davis et al., 2002; Jeffares et al., 2008), while in the opposite extreme, such as for the 2400 kb human dystrophin gene that is 99% intronic, transcription can take more than 16 h due to the gene's excessive length (Tennyson et al., 1995). Despite intron causing significant delay in transcription, the size of introns varies widely and there is a general trend for shorter introns in more basal species and longer ones in primates (Gelfman et al., 2012). The reason why evolution favored larger introns is a subject of debate. There is evidence that the presence of introns in genes enhances their transcription (Brinster et al., 1988; Furger et al., 2002). Possible mechanisms are that co-transcriptional processes feedback to the promoter or change the processivity of RNAPII (Heyn et al., 2015). Furthermore, the presence of long introns may serve as a timing mechanism for biological signals in feedback regulatory networks (Lewis, 2003; Oswald and Oates, 2011; Swinburne et al., 2008). Since transcription takes time, the expression of a gene will be significantly delayed if it contains long introns in comparison to shorter ones, this phenomenon is called intron delay (Swinburne and Silver, 2008). Delays might be important to generate oscillations in gene expression (Lewis, 2003). It was reported that intron length can indeed increase the period of oscillation (Swinburne et al., 2008). We can hypothesize that in the circadian clock system introns may play a role in modulating the period and phase of oscillation of the genes. NONO might be one of the factors involved in this modulation. Indeed absence on NONO leads to either loss of rhythmicity or significant phase delay in its target genes.

In particular, our data show that NONO preferentially bound promoter-proximal introns. It was postulated that introns have different functions according to their relative position on the DNA and mRNA. In particular, promoter-proximal introns are more likely to contain signal sequences responsible for intron-mediated enhancement (IME) (Rose et al., 2008), a mechanism by which introns positively affect gene expression. In this model: 1) the intron increases mRNA accumulation; 2) large portions of the intron can be deleted without eliminating its effect on

expression; and 3) the intron only increases mRNA levels when downstream of, and close to, the start of transcription. It is possible that the unusual characteristics of IME and the very large effect that some introns have on mRNA production reflect a major unrecognized method of gene regulation. IME has been described in diverse organisms, suggesting that it is a fundamental feature of gene expression (Gallegos and Rose, 2015). The mechanism of IME is largely unknown, but one possibility is that introns may increase gene expression by recruiting components of the splicing and mRNA export machineries. Indeed, studies over the past few years have revealed that virtually all of the steps in the gene expression pathway are extensively coupled to one another (Bentley, 1999; Hirose and Manley, 2000; Proudfoot et al., 2002). Consistent with this emerging concept, pre-mRNA splicing is thought to be coupled to transcription, mRNA export, and other steps in gene expression (Reed and Hurt, 2002). Assembly of specific factors in a specific order on the nascent mRNA might thus affect transcription as well as several other downstream steps regulating gene expression.

NONO and its paralogues, SFPQ and PSPC1, often function as heterodimers, and have been described as multifunctional proteins whose specific role in cellular processes may depend on the molecular and cellular context (Knott et al., 2016). Further studies will be required to assess whether the PSPC1 and SFPQ play a similar role or cooperate with NONO to regulate metabolic homeostasis. Recent studies have shown that PSPC1 plays a role in adipose tissue development (Wang et al., 2017). It is therefore likely that DBHS proteins play complementary roles in different organs to regulate different aspects of metabolism. In this respect, NONO itself has been shown to: 1) regulate phosphodiesterase mRNA splicing and degradation in human adrenocortical cells to affect glucocorticoids production (Lu and Sewer, 2015), 2) positively regulate lipogenesis in breast cancer cells through SREBP1 (Zhu et al., 2015), and 3) act as an mTOR cofactor (Amelio et al., 2007). We predict that each member of the DBHS family will have unique and common targets in each tissue, and mediate both unique and redundant functions.

DBHS proteins are emerging to be clinically relevant also in the context of development, immunity and cancer. DBHS proteins belong to the group human genes with the lowest tolerance for mutations. This suggests their strong involvement in disease phenotypes in humans (Knott et al., 2016). Mutations in

NONO have been identified in patients with intellectual disability, and neither PSPC1 nor SFPQ can compensate for these defects. Consistent with this, NONO-deficient mice exhibit a similar neurological defect (Mircsof et al., 2015). NONO and SFPQ directly interact with the c-Jun N-terminal Kinase (JNK1) in an RNA-dependent manner and they are necessary for neuronal growth (Sury et al., 2015). Similarly, in neuronal cells, NONO and SFPQ directly interact with Protein degylcase-1 (DJ-1) and display a neuroprotective role (Xu et al., 2005). In photoreceptor development, NONO acts as an enhancer and post-transcriptional splicing regulator for rod-specific genes such as rhodopsin (Yadav et al., 2014). As many gene regulators DBHS protein can act either as tumor suppressors or as oncogenes depending on the contexts. Breast cancers with loss of NONO were associated with increased tumor size, likely due to increased proliferation (Traish et al., 1997). This is in line with NONO acting as a regulator of the cell cycle (Kowalska et al., 2013). In contrast, increased NONO abundance has been associated with enhanced melanoma progression (Schiffner et al., 2011), and malignant progression of breast tumors (Pavao et al., 2001). It is likely that the association of NONO with active transcription alters gene expression in these examples. NONO can facilitate interaction with the long noncoding RNA lncUSMycN and the N-Myc mRNA and leads to post-transcriptional up-regulation of the oncoprotein N-Myc (Liu et al., 2014).

Given the widespread role of DBHS proteins in both transcriptional and post-transcriptional regulation in many cell types, it is possible that additional clinical roles may be hidden by the functional redundancy of the three DBHS proteins. Here we demonstrated that NONO functions specifically in the liver to maintain whole-organism glucose homeostasis. We found that NONO-deficient mice have impaired glucose tolerance but similar insulin sensitivity compared to *wt* mice. The cause of the reduced glucose tolerance in NONO-deficient mice could thus be either a reduced glucose uptake from the liver and other tissues, or a reduced insulin secretion from the pancreas. After a carbohydrate meal, ~33% of the glucose is taken up by the liver, another ~33% is taken up by muscle and adipose tissue, and the remaining glucose is taken up by the brain, kidney and RBCs (Moore et al., 2012). By re-expressing NONO specifically in the liver we were able to rescue, at least in part, the glucose intolerance in NONO-deficient mice. This demonstrated that NONO expression in the liver is important for efficient glucose uptake. However, we

cannot exclude that insulin secretion in response to glucose might be impaired. We predict that NONO might play a similar function in other organs involved in the regulation of glucose homeostasis (like the adipose tissue and the muscle). It will be interesting in the future, using tissue specific NONO-deficient mouse models, to assess tissue specific functions of NONO both in regulating response to nutritional stimuli and circadian gene expression.

In this work we characterized NONO protein interactors in the mouse liver at different times of the day. We did not find significant differences between time points, but future investigations should adopt a more quantitative approach, like SILAC proteomics, in order to accurately determine whether time-dependent differences in the pool of NONO interactors exist. Our data suggest that there are at least two main classes of NONO interactors: (1) RNA-binding proteins involved RNA metabolism, and (2) components of chromatin modifying complexes. Previous studies have shown that NONO and related factors function as transcriptional cofactors, binding to histone modifiers to regulate chromatin structure and circadian function (Brown et al., 2005; Duong et al., 2011). Gel filtration analyses suggest that only a subset of NONO-containing speckle-like structures are circadian in nature (Brown et al., 2005). It is thus tempting to speculate that NONO might be part of at least two distinct macromolecular complexes with roles in either RNA-processing or transcription. In the future it will be interesting to investigate whether one or the other function is predominant at certain times of the day. NONO and SFPQ were also found to interact with RNAPII CTD. Both hypo- and hyperphosphorylated CTD matrices bound these proteins with similar selectivity. NONO and SFPQ can interact with the CTD and RNA simultaneously, therefore they may provide a direct physical link between the RNAPII CTD and pre-mRNA processing components, at both the initiation and elongation phases of transcription (Emili et al., 2002). More recently, NONO and SFPQ were identified as a components of chromatin-associated mRNP particles integrating transcript elongation with the regulation of splicing (Close et al., 2012). Similarly, NONO and SFPQ were identified as component of RALY-containing ribonucleoprotein particles, known to be involved in several aspects of RNA metabolism (Tenzer et al., 2013). Several interactors identified in these studies were also present in our dataset. To summarize, current evidences suggest that NONO might be acting at the interface of transcription and other downstream mRNA

processing events in macromolecular complexes whose composition and specific function may be context-dependent.

Several studies have shown that DBHS proteins may play an important role to adapt to different cellular stress conditions. Evidence suggests that NONO:SFPQ dimers have function in DNA repair. Purified NONO:SFPQ dimers stimulate DNA end joining by ten-fold or more in a reconstituted in vitro assay system (Bladen et al., 2005; Udayakumar and Dynan, 2015; Udayakumar et al., 2003). Deficiency in NONO and SFPQ in cultured cell models is associated with radiosensitivity and delayed double strand break repair (Ha et al., 2011; Krietsch et al., 2012; Li et al., 2009, 2014). Various lines of evidence also link NONO and SFPQ to homologous recombination repair, nucleotide excision repair, interstrand cross-link repair, and DNA damage-dependent cell cycle checkpoint control (Alfano et al., 2016; Jaafar et al., 2017; Kowalska et al., 2013; Morozumi et al., 2009). Furthermore, DBHS proteins have been implicated in the immune response to viruses and can bind viral RNAs, bind to host ncRNAs, or interact with other proteins to regulate the transcription of immune related genes upon immune stimuli (Cao et al., 2015; Emmott et al., 2010; Greco-Stewart et al., 2006; Imamura et al., 2014; Kula et al., 2013; Landeras-Bueno et al., 2011; Lee et al., 2016; St Gelais et al., 2015). Feeding can be regarded as a stress stimulus for the cell. Nutrients have to be kept within a narrow concentration range in the blood to avoid tissue damage. Furthermore, nutrient metabolism generates oxidative stress. Indeed fasting and caloric restriction have been associated with several health benefits (Froy and Miskin, 2010; Kopeina et al., 2017; Mattson et al., 2017). As mentioned above, the liver has first access to most ingested nutrients by virtue of their absorption into the hepatic portal vein and is exposed to higher nutrient levels than are other peripheral tissues. Our data provide evidence that the RNA-binding protein NONO is important for coordinating hepatic gene expression with the feeding/fasting cycle, and for efficient nutrient uptake and metabolism. Indeed, absence of NONO affects whole-organism metabolic homeostasis and leads to impaired glucose tolerance and reduced body weight due to increased utilization of fat deposits as energy source. Disruption of the temporal coordination between metabolic demand and gene expression leads to the development of metabolic diseases, like obesity and diabetes. The role of RNA-binding proteins in regulating gene expression under diverse environmental

conditions is only now beginning to be elucidated. Our findings help to better understand how metabolic homeostasis is maintained in mammals, and identify novel therapeutic targets for treating diabetes and other associated metabolic dysfunctions.

5. ACKNOWLEDGEMENTS

First of all I would like to thank my thesis supervisor prof. Steven A. Brown for giving me the opportunity to perform my PhD project in his lab. In particular I would like to thank him for being always eager to discuss about science and ideas and for being so supportive. Whenever there is a problem he always has a good answer and a good solution. He is for me an example of fairness and good leadership.

I also would like to thank my thesis supervisor at the Salk Institute, prof. Satchidananda Panda for accepting me in his lab, for encouraging me to try new things and follow my ideas and for granting me freedom and independence in the lab.

I am very grateful also to my committee members prof. Michael Arand and prof. Christian Wolfrum for their help and guidance over the years.

Many thanks also to all my lab colleagues at the University of Zurich and at the Salk Institute for their support and useful scientific and non-scientific discussions. I have been so lucky to have the opportunity to interact with two different labs in two different continents and get in touch with so diverse cultures, scientific projects personalities and points of view.

Many many thanks to all the staff of the core facilities at the University of Zurich and at the Salk Institute, their help and expertise has been instrumental for the progress of my project.

I would also like to thank all my friends in Zurich and in San Diego; Arianna Mei, Gabriele Sulli, Maryna Mosalenko, Paola Orsolini, Stefano Malvezzi, Andrea Arcifa, Michela Puddu, Giuseppe De Gregorio, Sergio Leone and many many others. In particular I would like to thank Paola that is always there whenever I need anything! Many thanks also to Gabriele that has been a great colleague as well as a great friend!

I want to express all my gratitude especially to my life partner and colleague Ludovic, for his invaluable help, advice and support over the years.

Last but not least I would like to thank all my family. Thanks to my sisters for all their support and help. Many thanks also to my wonderful parents, I can never thank them enough for being so supportive and loving.

6. LIST OF ABBREVIATIONS

AANAT	Arylalkylamine N-acetyltransferase
AAV	Adeno-Associated Virus
ACLY	ATP-Citrate Lyase
ADAR	Adenosine Deaminase, RNA specific
AMP	Adenosine Monophosphate
AMPK	AMP Kinase
ANOVA	Analysis Of Variance
ATP	Adenosine Triphosphate
BCA	Bicinchoninic Acid
BMAL1	Brain and Muscle ARNT-Like Protein 1
BSA	Bovine Serum Albumin
cAMP	Cyclic Adenosine Monophosphate
CCG	Clock Controlled Gene
cDNA	Complementary Deoxyribonucleic Acid
ChIP-Seq	Chromatin Immuno-Precipitation followed by Sequencing
CIRBP	Cold Inducible RNA Binding Protein
CLOCK	Circadian Locomoter Output Cycles Kaput Protein
CoA	Coenzyme A
CPEB2	Cytoplasmic Polyadenylation Element Binding Protein 2
CPEB4	Cytoplasmic Polyadenylation Element Binding Protein 4
CPT1A	Carnitine Palmitoyltransferase 1A
CRY1	Cryptochrome 1
CRY2	Cryptochrome 2
CT	Circadian Time
CTD	Carboxy-Terminal Domain
DAPI	4',6-diamidino-2-phenylindole
DBHS	Drosophila Behavior Human Splicing
DBP	D-box Binding PAR BZIP Transcription Factor
2D-DIGE	Two Dimensional Difference Gel Electrophoresis
DDX5	Dead-box polypeptide 5
DHX9	DEAH-box protein 9
DNA	Deoxyribonucleic Acid

dsRNA	Double Strand RNA
DTT	Dithiothreitol
4E-BP	4E Binding Protein
EDTA	Ethylenediaminetetraacetic acid
E2F1	E2F Transcription Factor 1
E2F2	E2F Transcription Factor 2
EIF4A	Eukaryotic Translation Initiation Factor 4A
EIF4B	Eukaryotic Translation Initiation Factor 4B
EIF4E	Eukaryotic Translation Initiation Factor 4E
EIF4F	Eukaryotic Translation Initiation Factor 4F
EIF4G	Eukaryotic Translation Initiation Factor 4G
EIF4H	Eukaryotic Translation Initiation Factor 4H
ELISA	Enzyme-Linked Immunosorbent Assay
eRNA	Enhancer RNA
FAA	Food Anticipatory Activity
FFA	Free Fatty Acid
FAD	Flavin Adenine Dinucleotide
FBXL3	F-Box And Leucine Rich Repeat Protein 3
FPKM	Fragments Per Kilobase per Million mapped reads
GCK	Glucokinase
GEO	Gene Expression Omnibus
GLUT2	Glucose Transporter 2
GPAM	Glycerol-3-Phosphate Acyltransferase, Mitochondrial
GRO-Seq	Global-Run-On sequencing
GSK-3	Glycogen Synthase Kinase 3
GTT	Glucose Tolerance Test
GYS2	Glycogen Synthase 2
HCl	Hydrogen Chloride
HEPES	4-(2-hydroxyethyl)-1-piperazineethanesulfonic acid
HFD	High Fat Diet
HGP	Hepatic Glucose Production
H3K9ac	Histone 3-Lysine 9 acetylation
H3K27ac	Histone 3-Lysine 27 acetylation
H3K4me1	Histone 3-Lysine 4 monomethylation
H3K4me3	Histone 3-Lysine 4 trimethylation
H3K36me3	Histone 3-Lysine 36 trimethylation

H3K79me2	Histone 3-Lysine 79 dimethylation
HMGCS2	Hydroxy-Methylglutaryl-CoA Synthase 2
hnRNP	Heterogeneous Nuclear Ribonucleoprotein
hnRNPI	Heterogeneous Nuclear Ribonucleoprotein I
hnRNPD	Heterogeneous Nuclear Ribonucleoprotein D
hnRNPQ	Heterogeneous Nuclear Ribonucleoprotein Q
IgG	Immunoglobulin G
ILF3	Interleukin Enhancer Binding Factor 3
IME	Intron-Mediated Enhancement
IP	Immunoprecipitation
IP-MS	Immunoprecipitation followed by Mass Spectrometry
IR*Alu*	Inverted Repeated Alu
IRES	Internal Ribosome Entry Site
ITT	Insulin Tolerance Test
KEGG	Kyoto Encyclopedia of Genes and Genomes
KCl	Potassium Chloride
LDS	Lithium Dodecyl Sulfate
mCAT2	Mouse Cationic Amino acid Transporter 2
MgCl2	Magnesium Chloride
MODY2	Maturity Onset Diabetes of the Young 2
mRNA	Messenger Ribonucleic Acid
mRNP	Messenger Ribonucleoprotein
mTOR	Mechanistic Target Of Rapamycin
NaCl	Sodium Chloride
NAD^+/NADH	Nicotinamide Adenine Dinucleotide
NAMPT	Nicotinamide Phosphoribosyltransferase
NaOH	Sodium Hydroxide
NEAT1	Nuclear Enriched Abundant Transcript 1
NOC	Nocturnin
NOG	n-Octylglucoside
NonA	no on or off transient A
NONO	Non-POU Domain Containing Octamer Binding
NOPS	NonA/paraspeckle
OCT	Optimal Cutting Temperature
ORA	Over-Representation Analysis
ORO	Oil-Red-O

PAR	Polyadenylate Rhythmic
PARN	Polyadenylate Specific Ribonuclease
PBS	Phosphate Buffered Saline
PEP	Phosphoenol pyruvate
PER1	Period 1
PER2	Period 2
PER3	Period 3
PFA	Paraformaldehyde
3-PG	3-Phosphoglycerate
PHAX	Phosphorylated Adaptor For RNA Export
PKA	Protein Kinase A
PMSF	Phenylmethylsulfonyl Fluoride
p54nrb	54 KDa Nuclear RNA- And DNA-Binding Protein
Poly(A)	Polyadenylate
pre-mRNA	Premature Messenger Ribonucleic Acid
PSF	PTB associated Splicing Factor
PSP1	Paraspeckle Protein 1
PSPC1	Paraspeckle Protein Component 1
PTB	Polypyrimidine Tract Binding Protein
qPCR	Quantitative Polymerase Chain Reaction
RIP	RNA Immunoprecipitation
RIPA	Radioimmunoprecipitation Assay
RIP-Seq	RNA Immunoprecipitation followed by Sequencing
RBC	Red Blood Cell
RBM4	RNA Binding Motif Protein 4
RBP	RNA Binding Protein
RER	Respiratory Exchange Ratio
RNA	Ribonucleic Acid
RNAPII	RNA polymerase II
RNA-Seq	RNA Sequencing
ROR	RAR Related Orphan Receptor
RP	Ribosomal Protein
RPF-Seq	Ribosome Profiling coupled with RNA Sequencing
RRM	RNA Recognition Motif
rRNA	Ribosomal RNA
RT-PCR	Reverse Transcription Polymerase Chain Reaction

SCN	Suprachiasmatic Nucleus
SDS	Sodium Dodecyl Sulfate
SDS-PAGE	Sodium Dodecyl Sulfate Polyacrylamide Gel Electrophoresis
Ser5	Serine 5
SETX	Senataxin
SFPQ	Splicing Factor Proline and Glutamine rich
SIRT	Sirtuin
SILAC	Stable Isotope Labeling with Amino acids in Cell culture
siRNA	Small Interfering RNA
snRNA	Small Nuclear Ribonucleic Acid
SREBP1	Sterol Regulatory Element Binding Protein 1
TBG	Thyroxine Binding Globulin
TBP	TATA Binding Protein
TBS	Tris-Buffered Saline
TCA	Tricarboxylic Acid
TIM	Timeless
TNF α	Tumor Necrosis Factor Alpha
TPA	Tetradecanoylphorbol Acetate
Tris	Tris(hydroxymethyl)aminomethane
Tris-HCl	Tris(hydroxymethyl)aminomethane Hydrochloride
TSS	Transcription Start Site
U2AF26	U2-auxiliary-factor 26
U2AF26ΔE67	U2-auxiliary-factor 26 exon 6/7 deleted
UTR	Untranslated Region
VRC	Vanadyl Ribonucleoside Complex
WT	Wild-Type
XRN2	5'-3' Exoribonuclease 2
ZT	Zeitgeber Time

7. REFERENCES

Agius, L. (2008). Glucokinase and molecular aspects of liver glycogen metabolism. Biochem. J. *414*, 1–18.

Alfano, L., Costa, C., Caporaso, A., Altieri, A., Indovina, P., Macaluso, M., Giordano, A., and Pentimalli, F. (2016). NONO regulates the intra-S-phase checkpoint in response to UV radiation. Oncogene *35*, 567–576.

Amelio, A.L., Miraglia, L.J., Conkright, J.J., Mercer, B.A., Batalov, S., Cavett, V., Orth, A.P., Busby, J., Hogenesch, J.B., and Conkright, M.D. (2007). A coactivator trap identifies NONO (p54nrb) as a component of the cAMP-signaling pathway. Proc. Natl. Acad. Sci. U. S. A. *104*, 20314–20319.

Arble, D.M., Bass, J., Laposky, A.D., Vitaterna, M.H., and Turek, F.W. (2009). Circadian timing of food intake contributes to weight gain. Obes. Silver Spring Md *17*, 2100–2102.

Arble, D.M., Ramsey, K.M., Bass, J., and Turek, F.W. (2010). Circadian disruption and metabolic disease: findings from animal models. Best Pract. Res. Clin. Endocrinol. Metab. *24*, 785–800.

Asher, G., Gatfield, D., Stratmann, M., Reinke, H., Dibner, C., Kreppel, F., Mostoslavsky, R., Alt, F.W., and Schibler, U. (2008). SIRT1 regulates circadian clock gene expression through PER2 deacetylation. Cell *134*, 317–328.

Atger, F., Gobet, C., Marquis, J., Martin, E., Wang, J., Weger, B., Lefebvre, G., Descombes, P., Naef, F., and Gachon, F. (2015). Circadian and feeding rhythms differentially affect rhythmic mRNA transcription and translation in mouse liver. Proc. Natl. Acad. Sci. U. S. A.

Atger, F., Mauvoisin, D., Weger, B., Gobet, C., and Gachon, F. (2017). Regulation of Mammalian Physiology by Interconnected Circadian and Feeding Rhythms. Front. Endocrinol. *8*, 42.

Balsalobre, A., Brown, S.A., Marcacci, L., Tronche, F., Kellendonk, C., Reichardt, H.M., Schütz, G., and Schibler, U. (2000). Resetting of circadian time in peripheral tissues by glucocorticoid signaling. Science *289*, 2344–2347.

Barger, L.K., Lockley, S.W., Rajaratnam, S.M.W., and Landrigan, C.P. (2009). Neurobehavioral, health, and safety consequences associated with shift work in safety-sensitive professions. Curr. Neurol. Neurosci. Rep. *9*, 155–164.

Baron, K.G., and Reid, K.J. (2014). Circadian misalignment and health. Int. Rev. Psychiatry Abingdon Engl. *26*, 139–154.

Bass, J., and Takahashi, J.S. (2010). Circadian integration of metabolism and energetics. Science *330*, 1349–1354.

Bell-Pedersen, D., Cassone, V.M., Earnest, D.J., Golden, S.S., Hardin, P.E., Thomas, T.L., and Zoran, M.J. (2005). Circadian rhythms from multiple oscillators: lessons from diverse organisms. Nat. Rev. Genet. *6*, 544–556.

Benegiamo, G., Brown, S.A., and Panda, S. (2016). RNA Dynamics in the Control of

Circadian Rhythm. Adv. Exp. Med. Biol. *907*, 107–122.

Bentley, D. (1999). Coupling RNA polymerase II transcription with pre-mRNA processing. Curr. Opin. Cell Biol. *11*, 347–351.

Bladen, C.L., Udayakumar, D., Takeda, Y., and Dynan, W.S. (2005). Identification of the polypyrimidine tract binding protein-associated splicing factor.p54(nrb) complex as a candidate DNA double-strand break rejoining factor. J. Biol. Chem. *280*, 5205–5210.

Bond, C.S., and Fox, A.H. (2009). Paraspeckles: nuclear bodies built on long noncoding RNA. J. Cell Biol. *186*, 637–644.

Brinster, R.L., Allen, J.M., Behringer, R.R., Gelinas, R.E., and Palmiter, R.D. (1988). Introns increase transcriptional efficiency in transgenic mice. Proc. Natl. Acad. Sci. U. S. A. *85*, 836–840.

Brown, S.A. (2016). Circadian Metabolism: From Mechanisms to Metabolomics and Medicine. Trends Endocrinol. Metab. TEM *27*, 415–426.

Brown, S.A., Zumbrunn, G., Fleury-Olela, F., Preitner, N., and Schibler, U. (2002). Rhythms of mammalian body temperature can sustain peripheral circadian clocks. Curr. Biol. CB *12*, 1574–1583.

Brown, S.A., Ripperger, J., Kadener, S., Fleury-Olela, F., Vilbois, F., Rosbash, M., and Schibler, U. (2005). PERIOD1-associated proteins modulate the negative limb of the mammalian circadian oscillator. Science *308*, 693–696.

Brum, M.C.B., Filho, F.F.D., Schnorr, C.C., Bottega, G.B., and Rodrigues, T.C. (2015). Shift work and its association with metabolic disorders. Diabetol. Metab. Syndr. *7*, 45.

Buhr, E.D., Yoo, S.-H., and Takahashi, J.S. (2010). Temperature as a universal resetting cue for mammalian circadian oscillators. Science *330*, 379–385.

Buijs, R.M., Wortel, J., Van Heerikhuize, J.J., Feenstra, M.G., Ter Horst, G.J., Romijn, H.J., and Kalsbeek, A. (1999). Anatomical and functional demonstration of a multisynaptic suprachiasmatic nucleus adrenal (cortex) pathway. Eur. J. Neurosci. *11*, 1535–1544.

Buxadé, M., Morrice, N., Krebs, D.L., and Proud, C.G. (2008). The PSF.p54nrb complex is a novel Mnk substrate that binds the mRNA for tumor necrosis factor alpha. J. Biol. Chem. *283*, 57–65.

Canuto, R., Garcez, A.S., and Olinto, M.T.A. (2013). Metabolic syndrome and shift work: a systematic review. Sleep Med. Rev. *17*, 425–431.

Cao, S., Moss, W., O'Grady, T., Concha, M., Strong, M.J., Wang, X., Yu, Y., Baddoo, M., Zhang, K., Fewell, C., et al. (2015). New Noncoding Lytic Transcripts Derived from the Epstein-Barr Virus Latency Origin of Replication, oriP, Are Hyperedited, Bind the Paraspeckle Protein, NONO/p54nrb, and Support Viral Lytic Transcription. J. Virol. *89*, 7120–7132.

Castillo-Davis, C.I., Mekhedov, S.L., Hartl, D.L., Koonin, E.V., and Kondrashov, F.A. (2002). Selection for short introns in highly expressed genes. Nat. Genet. *31*, 415–418.

Chapman, R.D., Heidemann, M., Albert, T.K., Mailhammer, R., Flatley, A.,

Meisterernst, M., Kremmer, E., and Eick, D. (2007). Transcribing RNA polymerase II is phosphorylated at CTD residue serine-7. Science *318*, 1780–1782.

Chavan, R., Feillet, C., Costa, S.S.F., Delorme, J.E., Okabe, T., Ripperger, J.A., and Albrecht, U. (2016). Liver-derived ketone bodies are necessary for food anticipation. Nat. Commun. *7*, 10580.

Chen, L.-L., and Carmichael, G.G. (2009). Altered nuclear retention of mRNAs containing inverted repeats in human embryonic stem cells: functional role of a nuclear noncoding RNA. Mol. Cell *35*, 467–478.

Chen, L.-L., DeCerbo, J.N., and Carmichael, G.G. (2008). Alu element-mediated gene silencing. EMBO J. *27*, 1694–1705.

Close, P., East, P., Dirac-Svejstrup, A.B., Hartmann, H., Heron, M., Maslen, S., Chariot, A., Söding, J., Skehel, M., and Svejstrup, J.Q. (2012). DBIRD complex integrates alternative mRNA splicing with RNA polymerase II transcript elongation. Nature *484*, 386–389.

Core, L.J., Waterfall, J.J., and Lis, J.T. (2008). Nascent RNA sequencing reveals widespread pausing and divergent initiation at human promoters. Science *322*, 1845–1848.

D'Ambrogio, A., Nagaoka, K., and Richter, J.D. (2013). Translational control of cell growth and malignancy by the CPEBs. Nat. Rev. Cancer *13*, 283–290.

Damiola, F., Le Minh, N., Preitner, N., Kornmann, B., Fleury-Olela, F., and Schibler, U. (2000). Restricted feeding uncouples circadian oscillators in peripheral tissues from the central pacemaker in the suprachiasmatic nucleus. Genes Dev. *14*, 2950–2961.

Dibner, C., Sage, D., Unser, M., Bauer, C., d'Eysmond, T., Naef, F., and Schibler, U. (2009). Circadian gene expression is resilient to large fluctuations in overall transcription rates. EMBO J. *28*, 123–134.

Dibner, C., Schibler, U., and Albrecht, U. (2010). The mammalian circadian timing system: organization and coordination of central and peripheral clocks. Annu. Rev. Physiol. *72*, 517–549.

Dobin, A., Davis, C.A., Schlesinger, F., Drenkow, J., Zaleski, C., Jha, S., Batut, P., Chaisson, M., and Gingeras, T.R. (2013). STAR: ultrafast universal RNA-seq aligner. Bioinforma. Oxf. Engl. *29*, 15–21.

Dodd, A.N., Salathia, N., Hall, A., Kévei, E., Tóth, R., Nagy, F., Hibberd, J.M., Millar, A.J., and Webb, A.A.R. (2005). Plant circadian clocks increase photosynthesis, growth, survival, and competitive advantage. Science *309*, 630–633.

Dong, B., Horowitz, D.S., Kobayashi, R., and Krainer, A.R. (1993). Purification and cDNA cloning of HeLa cell p54nrb, a nuclear protein with two RNA recognition motifs and extensive homology to human splicing factor PSF and Drosophila NONA/BJ6. Nucleic Acids Res. *21*, 4085–4092.

Dong, X., Shylnova, O., Challis, J.R.G., and Lye, S.J. (2005). Identification and characterization of the protein-associated splicing factor as a negative co-regulator of the progesterone receptor. J. Biol. Chem. *280*, 13329–13340.

Dong, X., Sweet, J., Challis, J.R.G., Brown, T., and Lye, S.J. (2007). Transcriptional activity of androgen receptor is modulated by two RNA splicing factors, PSF and

p54nrb. Mol. Cell. Biol. *27*, 4863–4875.

Dong, X., Yu, C., Shynlova, O., Challis, J.R.G., Rennie, P.S., and Lye, S.J. (2009). p54nrb is a transcriptional corepressor of the progesterone receptor that modulates transcription of the labor-associated gene, connexin 43 (Gja1). Mol. Endocrinol. Baltim. Md *23*, 1147–1160.

van Drongelen, A., Boot, C.R.L., Merkus, S.L., Smid, T., and van der Beek, A.J. (2011). The effects of shift work on body weight change - a systematic review of longitudinal studies. Scand. J. Work. Environ. Health *37*, 263–275.

Dunlap, J.C. (1999). Molecular bases for circadian clocks. Cell *96*, 271–290.

Duong, H.A., Robles, M.S., Knutti, D., and Weitz, C.J. (2011). A molecular mechanism for circadian clock negative feedback. Science *332*, 1436–1439.

Dupuis, J., Langenberg, C., Prokopenko, I., Saxena, R., Soranzo, N., Jackson, A.U., Wheeler, E., Glazer, N.L., Bouatia-Naji, N., Gloyn, A.L., et al. (2010). New genetic loci implicated in fasting glucose homeostasis and their impact on type 2 diabetes risk. Nat. Genet. *42*, 105–116.

Edgar, R., Domrachev, M., and Lash, A.E. (2002). Gene Expression Omnibus: NCBI gene expression and hybridization array data repository. Nucleic Acids Res. *30*, 207–210.

Emili, A., Shales, M., McCracken, S., Xie, W., Tucker, P.W., Kobayashi, R., Blencowe, B.J., and Ingles, C.J. (2002). Splicing and transcription-associated proteins PSF and p54nrb/nonO bind to the RNA polymerase II CTD. RNA N. Y. N *8*, 1102–1111.

Emmott, E., Wise, H., Loucaides, E.M., Matthews, D.A., Digard, P., and Hiscox, J.A. (2010). Quantitative proteomics using SILAC coupled to LC-MS/MS reveals changes in the nucleolar proteome in influenza A virus-infected cells. J. Proteome Res. *9*, 5335–5345.

Evans, A.M., DeHaven, C.D., Barrett, T., Mitchell, M., and Milgram, E. (2009). Integrated, nontargeted ultrahigh performance liquid chromatography/electrospray ionization tandem mass spectrometry platform for the identification and relative quantification of the small-molecule complement of biological systems. Anal. Chem. *81*, 6656–6667.

Fang, B., Everett, L.J., Jager, J., Briggs, E., Armour, S.M., Feng, D., Roy, A., Gerhart-Hines, Z., Sun, Z., and Lazar, M.A. (2014). Circadian enhancers coordinate multiple phases of rhythmic gene transcription in vivo. Cell *159*, 1140–1152.

Feillet, C.A., Ripperger, J.A., Magnone, M.C., Dulloo, A., Albrecht, U., and Challet, E. (2006). Lack of food anticipation in Per2 mutant mice. Curr. Biol. CB *16*, 2016–2022.

Fonken, L.K., Workman, J.L., Walton, J.C., Weil, Z.M., Morris, J.S., Haim, A., and Nelson, R.J. (2010). Light at night increases body mass by shifting the time of food intake. Proc. Natl. Acad. Sci. U. S. A. *107*, 18664–18669.

Fox, A.H., and Lamond, A.I. (2010). Paraspeckles. Cold Spring Harb. Perspect. Biol. *2*, a000687.

Fox, A.H., Lam, Y.W., Leung, A.K.L., Lyon, C.E., Andersen, J., Mann, M., and Lamond, A.I. (2002). Paraspeckles: a novel nuclear domain. Curr. Biol. CB *12*, 13–25.

Fox, A.H., Bond, C.S., and Lamond, A.I. (2005). P54nrb forms a heterodimer with PSP1 that localizes to paraspeckles in an RNA-dependent manner. Mol. Biol. Cell *16*, 5304–5315.

Froy, O., and Miskin, R. (2010). Effect of feeding regimens on circadian rhythms: implications for aging and longevity. Aging *2*, 7–27.

Fujino, Y., Iso, H., Tamakoshi, A., Inaba, Y., Koizumi, A., Kubo, T., Yoshimura, T., and Japanese Collaborative Cohort Study Group (2006). A prospective cohort study of shift work and risk of ischemic heart disease in Japanese male workers. Am. J. Epidemiol. *164*, 128–135.

Furger, A., O'Sullivan, J.M., Binnie, A., Lee, B.A., and Proudfoot, N.J. (2002). Promoter proximal splice sites enhance transcription. Genes Dev. *16*, 2792–2799.

Gaidatzis, D., Burger, L., Florescu, M., and Stadler, M.B. (2015). Analysis of intronic and exonic reads in RNA-seq data characterizes transcriptional and post-transcriptional regulation. Nat. Biotechnol. *33*, 722–729.

Gallegos, J.E., and Rose, A.B. (2015). The enduring mystery of intron-mediated enhancement. Plant Sci. Int. J. Exp. Plant Biol. *237*, 8–15.

Garaulet, M., Corbalán-Tutau, M.D., Madrid, J.A., Baraza, J.C., Parnell, L.D., Lee, Y.-C., and Ordovas, J.M. (2010). PERIOD2 variants are associated with abdominal obesity, psycho-behavioral factors, and attrition in the dietary treatment of obesity. J. Am. Diet. Assoc. *110*, 917–921.

Garaulet, M., Smith, C.E., Gomez-Abellán, P., Ordovás-Montañés, M., Lee, Y.-C., Parnell, L.D., Arnett, D.K., and Ordovás, J.M. (2014). REV-ERB-ALPHA circadian gene variant associates with obesity in two independent populations: Mediterranean and North American. Mol. Nutr. Food Res. *58*, 821–829.

Garbarino-Pico, E., Niu, S., Rollag, M.D., Strayer, C.A., Besharse, J.C., and Green, C.B. (2007). Immediate early response of the circadian polyA ribonuclease nocturnin to two extracellular stimuli. RNA N. Y. N *13*, 745–755.

Gehring, N.H., Wahle, E., and Fischer, U. (2017). Deciphering the mRNP Code: RNA-Bound Determinants of Post-Transcriptional Gene Regulation. Trends Biochem. Sci.

Geisler, C.E., Hepler, C., Higgins, M.R., and Renquist, B.J. (2016). Hepatic adaptations to maintain metabolic homeostasis in response to fasting and refeeding in mice. Nutr. Metab. *13*, 62.

Gelfman, S., Burstein, D., Penn, O., Savchenko, A., Amit, M., Schwartz, S., Pupko, T., and Ast, G. (2012). Changes in exon-intron structure during vertebrate evolution affect the splicing pattern of exons. Genome Res. *22*, 35–50.

Gerich, J.E. (2010). Role of the kidney in normal glucose homeostasis and in the hyperglycaemia of diabetes mellitus: therapeutic implications. Diabet. Med. J. Br. Diabet. Assoc. *27*, 136–142.

Glynn, E.F., Chen, J., and Mushegian, A.R. (2006). Detecting periodic patterns in unevenly spaced gene expression time series using Lomb-Scargle periodograms. Bioinforma. Oxf. Engl. *22*, 310–316.

Gotic, I., Omidi, S., Fleury-Olela, F., Molina, N., Naef, F., and Schibler, U. (2016). Temperature regulates splicing efficiency of the cold-inducible RNA-binding protein

gene Cirbp. Genes Dev. *30*, 2005–2017.

Gozani, O., Patton, J.G., and Reed, R. (1994). A novel set of spliceosome-associated proteins and the essential splicing factor PSF bind stably to pre-mRNA prior to catalytic step II of the splicing reaction. EMBO J. *13*, 3356–3367.

Greco-Stewart, V.S., Thibault, C.S.-L., and Pelchat, M. (2006). Binding of the polypyrimidine tract-binding protein-associated splicing factor (PSF) to the hepatitis delta virus RNA. Virology *356*, 35–44.

Green, C.B., and Besharse, J.C. (1996). Identification of a novel vertebrate circadian clock-regulated gene encoding the protein nocturnin. Proc. Natl. Acad. Sci. U. S. A. *93*, 14884–14888.

Green, C.B., Douris, N., Kojima, S., Strayer, C.A., Fogerty, J., Lourim, D., Keller, S.R., and Besharse, J.C. (2007). Loss of Nocturnin, a circadian deadenylase, confers resistance to hepatic steatosis and diet-induced obesity. Proc. Natl. Acad. Sci. U. S. A. *104*, 9888–9893.

Guhaniyogi, J., and Brewer, G. (2001). Regulation of mRNA stability in mammalian cells. Gene *265*, 11–23.

Ha, K., Takeda, Y., and Dynan, W.S. (2011). Sequences in PSF/SFPQ mediate radioresistance and recruitment of PSF/SFPQ-containing complexes to DNA damage sites in human cells. DNA Repair *10*, 252–259.

Hallier, M., Tavitian, A., and Moreau-Gachelin, F. (1996). The transcription factor Spi-1/PU.1 binds RNA and interferes with the RNA-binding protein p54nrb. J. Biol. Chem. *271*, 11177–11181.

Hall-Pogar, T., Liang, S., Hague, L.K., and Lutz, C.S. (2007). Specific trans-acting proteins interact with auxiliary RNA polyadenylation elements in the COX-2 3'-UTR. RNA N. Y. N *13*, 1103–1115.

He, L., Diedrich, J., Chu, Y.-Y., and Yates, J.R. (2015). Extracting Accurate Precursor Information for Tandem Mass Spectra by RawConverter. Anal. Chem. *87*, 11361–11367.

Heinz, S., Benner, C., Spann, N., Bertolino, E., Lin, Y.C., Laslo, P., Cheng, J.X., Murre, C., Singh, H., and Glass, C.K. (2010). Simple combinations of lineage-determining transcription factors prime cis-regulatory elements required for macrophage and B cell identities. Mol. Cell *38*, 576–589.

Heyn, P., Kalinka, A.T., Tomancak, P., and Neugebauer, K.M. (2015). Introns and gene expression: cellular constraints, transcriptional regulation, and evolutionary consequences. BioEssays News Rev. Mol. Cell. Dev. Biol. *37*, 148–154.

Hirano, A., Braas, D., Fu, Y.-H., and Ptáček, L.J. (2017). FAD Regulates CRYPTOCHROME Protein Stability and Circadian Clock in Mice. Cell Rep. *19*, 255–266.

Hirose, Y., and Manley, J.L. (2000). RNA polymerase II and the integration of nuclear events. Genes Dev. *14*, 1415–1429.

Hogan, M.F., Ravnskjaer, K., Matsumura, S., Huising, M.O., Hull, R.L., Kahn, S.E., and Montminy, M. (2015). Hepatic Insulin Resistance Following Chronic Activation of the CREB Coactivator CRTC2. J. Biol. Chem. *290*, 25997–26006.

Hogenesch, J.B., and Herzog, E.D. (2011). Intracellular and intercellular processes determine robustness of the circadian clock. FEBS Lett. *585*, 1427–1434.

Huff, J. (2015). The Airyscan detector from ZEISS: confocal imaging with improved signal-to-noise ratio and super-resolution. Nat Meth *12*.

Hughes, M.E., DiTacchio, L., Hayes, K.R., Vollmers, C., Pulivarthy, S., Baggs, J.E., Panda, S., and Hogenesch, J.B. (2009). Harmonics of circadian gene transcription in mammals. PLoS Genet. *5*, e1000442.

Hughes, M.E., Hogenesch, J.B., and Kornacker, K. (2010). JTK_CYCLE: an efficient nonparametric algorithm for detecting rhythmic components in genome-scale data sets. J. Biol. Rhythms *25*, 372–380.

Imamura, K., Imamachi, N., Akizuki, G., Kumakura, M., Kawaguchi, A., Nagata, K., Kato, A., Kawaguchi, Y., Sato, H., Yoneda, M., et al. (2014). Long noncoding RNA NEAT1-dependent SFPQ relocation from promoter region to paraspeckle mediates IL8 expression upon immune stimuli. Mol. Cell *53*, 393–406.

Ishida, A., Mutoh, T., Ueyama, T., Bando, H., Masubuchi, S., Nakahara, D., Tsujimoto, G., and Okamura, H. (2005). Light activates the adrenal gland: timing of gene expression and glucocorticoid release. Cell Metab. *2*, 297–307.

Ishihama, Y., Oda, Y., Tabata, T., Sato, T., Nagasu, T., Rappsilber, J., and Mann, M. (2005). Exponentially modified protein abundance index (emPAI) for estimation of absolute protein amount in proteomics by the number of sequenced peptides per protein. Mol. Cell. Proteomics MCP *4*, 1265–1272.

Izumi, H., McCloskey, A., Shinmyozu, K., and Ohno, M. (2014). p54nrb/NonO and PSF promote U snRNA nuclear export by accelerating its export complex assembly. Nucleic Acids Res. *42*, 3998–4007.

Jaafar, L., Li, Z., Li, S., and Dynan, W.S. (2017). SFPQ•NONO and XLF function separately and together to promote DNA double-strand break repair via canonical nonhomologous end joining. Nucleic Acids Res. *45*, 1848–1859.

Janich, P., Arpat, A.B., Castelo-Szekely, V., Lopes, M., and Gatfield, D. (2015). Ribosome profiling reveals the rhythmic liver translatome and circadian clock regulation by upstream open reading frames. Genome Res.

Jeffares, D.C., Penkett, C.J., and Bähler, J. (2008). Rapidly regulated genes are intron poor. Trends Genet. TIG *24*, 375–378.

Jones, J.G. (2016). Hepatic glucose and lipid metabolism. Diabetologia *59*, 1098–1103.

Jones, J.C., Phatnani, H.P., Haystead, T.A., MacDonald, J.A., Alam, S.M., and Greenleaf, A.L. (2004). C-terminal repeat domain kinase I phosphorylates Ser2 and Ser5 of RNA polymerase II C-terminal domain repeats. J. Biol. Chem. *279*, 24957–24964.

Jouffe, C., Cretenet, G., Symul, L., Martin, E., Atger, F., Naef, F., and Gachon, F. (2013). The circadian clock coordinates ribosome biogenesis. PLoS Biol. *11*, e1001455.

Kameoka, S., Duque, P., and Konarska, M.M. (2004). p54(nrb) associates with the 5' splice site within large transcription/splicing complexes. EMBO J. *23*, 1782–1791.

Kanai, Y., Dohmae, N., and Hirokawa, N. (2004). Kinesin transports RNA: isolation and characterization of an RNA-transporting granule. Neuron *43*, 513–525.

Kaneko, S., Rozenblatt-Rosen, O., Meyerson, M., and Manley, J.L. (2007). The multifunctional protein p54nrb/PSF recruits the exonuclease XRN2 to facilitate pre-mRNA 3' processing and transcription termination. Genes Dev. *21*, 1779–1789.

Kawaguchi, T., Tanigawa, A., Naganuma, T., Ohkawa, Y., Souquere, S., Pierron, G., and Hirose, T. (2015). SWI/SNF chromatin-remodeling complexes function in noncoding RNA-dependent assembly of nuclear bodies. Proc. Natl. Acad. Sci. U. S. A. *112*, 4304–4309.

Keene, J.D., Komisarow, J.M., and Friedersdorf, M.B. (2006). RIP-Chip: the isolation and identification of mRNAs, microRNAs and protein components of ribonucleoprotein complexes from cell extracts. Nat. Protoc. *1*, 302–307.

Kettner, N.M., Mayo, S.A., Hua, J., Lee, C., Moore, D.D., and Fu, L. (2015). Circadian Dysfunction Induces Leptin Resistance in Mice. Cell Metab. *22*, 448–459.

Kim, T.-K., and Shiekhattar, R. (2015). Architectural and Functional Commonalities between Enhancers and Promoters. Cell *162*, 948–959.

Kim, D.-Y., Woo, K.-C., Lee, K.-H., Kim, T.-D., and Kim, K.-T. (2010). hnRNP Q and PTB modulate the circadian oscillation of mouse Rev-erb alpha via IRES-mediated translation. Nucleic Acids Res. *38*, 7068–7078.

Kim, D.-Y., Kwak, E., Kim, S.-H., Lee, K.-H., Woo, K.-C., and Kim, K.-T. (2011). hnRNP Q mediates a phase-dependent translation-coupled mRNA decay of mouse Period3. Nucleic Acids Res. *39*, 8901–8914.

Kim, T.-D., Woo, K.-C., Cho, S., Ha, D.-C., Jang, S.K., and Kim, K.-T. (2007). Rhythmic control of AANAT translation by hnRNP Q in circadian melatonin production. Genes Dev. *21*, 797–810.

Knott, G.J., Bond, C.S., and Fox, A.H. (2016). The DBHS proteins SFPQ, NONO and PSPC1: a multipurpose molecular scaffold. Nucleic Acids Res. *44*, 3989–4004.

Koike, N., Yoo, S.-H., Huang, H.-C., Kumar, V., Lee, C., Kim, T.-K., and Takahashi, J.S. (2012). Transcriptional architecture and chromatin landscape of the core circadian clock in mammals. Science *338*, 349–354.

Kojima, S., and Green, C.B. (2015). Circadian genomics reveal a role for post-transcriptional regulation in mammals. Biochemistry (Mosc.) *54*, 124–133.

Kojima, S., Matsumoto, K., Hirose, M., Shimada, M., Nagano, M., Shigeyoshi, Y., Hoshino, S., Ui-Tei, K., Saigo, K., Green, C.B., et al. (2007). LARK activates posttranscriptional expression of an essential mammalian clock protein, PERIOD1. Proc. Natl. Acad. Sci. U. S. A. *104*, 1859–1864.

Kojima, S., Sher-Chen, E.L., and Green, C.B. (2012). Circadian control of mRNA polyadenylation dynamics regulates rhythmic protein expression. Genes Dev. *26*, 2724–2736.

Kopeina, G.S., Senichkin, V.V., and Zhivotovsky, B. (2017). Caloric restriction - A promising anti-cancer approach: From molecular mechanisms to clinical trials. Biochim. Biophys. Acta *1867*, 29–41.

Kowalska, E., Ripperger, J.A., Muheim, C., Maier, B., Kurihara, Y., Fox, A.H.,

Kramer, A., and Brown, S.A. (2012). Distinct roles of DBHS family members in the circadian transcriptional feedback loop. Mol. Cell. Biol. *32*, 4585–4594.

Kowalska, E., Ripperger, J.A., Hoegger, D.C., Bruegger, P., Buch, T., Birchler, T., Mueller, A., Albrecht, U., Contaldo, C., and Brown, S.A. (2013). NONO couples the circadian clock to the cell cycle. Proc. Natl. Acad. Sci. U. S. A. *110*, 1592–1599.

Krieger, D.T. (1974). Food and water restriction shifts corticosterone, temperature, activity and brain amine periodicity. Endocrinology *95*, 1195–1201.

Krieger, D.T., Hauser, H., and Krey, L.C. (1977). Suprachiasmatic nuclear lesions do not abolish food-shifted circadian adrenal and temperature rhythmicity. Science *197*, 398–399.

Krietsch, J., Caron, M.-C., Gagné, J.-P., Ethier, C., Vignard, J., Vincent, M., Rouleau, M., Hendzel, M.J., Poirier, G.G., and Masson, J.-Y. (2012). PARP activation regulates the RNA-binding protein NONO in the DNA damage response to DNA double-strand breaks. Nucleic Acids Res. *40*, 10287–10301.

Kula, A., Gharu, L., and Marcello, A. (2013). HIV-1 pre-mRNA commitment to Rev mediated export through PSF and Matrin 3. Virology *435*, 329–340.

Kuwahara, S., Ikei, A., Taguchi, Y., Tabuchi, Y., Fujimoto, N., Obinata, M., Uesugi, S., and Kurihara, Y. (2006). PSPC1, NONO, and SFPQ are expressed in mouse Sertoli cells and may function as coregulators of androgen receptor-mediated transcription. Biol. Reprod. *75*, 352–359.

Laermans, J., Vancleef, L., Tack, J., and Depoortere, I. (2015). Role of the clock gene Bmal1 and the gastric ghrelin-secreting cell in the circadian regulation of the ghrelin-GOAT system. Sci. Rep. *5*, 16748.

Lamia, K.A., Storch, K.-F., and Weitz, C.J. (2008). Physiological significance of a peripheral tissue circadian clock. Proc. Natl. Acad. Sci. U. S. A. *105*, 15172–15177.

Lamia, K.A., Sachdeva, U.M., DiTacchio, L., Williams, E.C., Alvarez, J.G., Egan, D.F., Vasquez, D.S., Juguilon, H., Panda, S., Shaw, R.J., et al. (2009). AMPK regulates the circadian clock by cryptochrome phosphorylation and degradation. Science *326*, 437–440.

Landeras-Bueno, S., Jorba, N., Pérez-Cidoncha, M., and Ortín, J. (2011). The splicing factor proline-glutamine rich (SFPQ/PSF) is involved in influenza virus transcription. PLoS Pathog. *7*, e1002397.

Landgraf, D., Tsang, A.H., Leliavski, A., Koch, C.E., Barclay, J.L., Drucker, D.J., and Oster, H. (2015). Oxyntomodulin regulates resetting of the liver circadian clock by food. eLife *4*, e06253.

Le Martelot, G., Canella, D., Symul, L., Migliavacca, E., Gilardi, F., Liechti, R., Martin, O., Harshman, K., Delorenzi, M., Desvergne, B., et al. (2012). Genome-wide RNA polymerase II profiles and RNA accumulation reveal kinetics of transcription and associated epigenetic changes during diurnal cycles. PLoS Biol. *10*, e1001442.

Le Minh, N., Damiola, F., Tronche, F., Schütz, G., and Schibler, U. (2001). Glucocorticoid hormones inhibit food-induced phase-shifting of peripheral circadian oscillators. EMBO J. *20*, 7128–7136.

Lee, C., Etchegaray, J.P., Cagampang, F.R., Loudon, A.S., and Reppert, S.M. (2001). Posttranslational mechanisms regulate the mammalian circadian clock. Cell

107, 855–867.

Lee, K.-H., Woo, K.-C., Kim, D.-Y., Kim, T.-D., Shin, J., Park, S.M., Jang, S.K., and Kim, K.-T. (2012). Rhythmic interaction between Period1 mRNA and hnRNP Q leads to circadian time-dependent translation. Mol. Cell. Biol. *32*, 717–728.

Lee, N., Yario, T.A., Gao, J.S., and Steitz, J.A. (2016). EBV noncoding RNA EBER2 interacts with host RNA-binding proteins to regulate viral gene expression. Proc. Natl. Acad. Sci. U. S. A. *113*, 3221–3226.

LeSauter, J., Hoque, N., Weintraub, M., Pfaff, D.W., and Silver, R. (2009). Stomach ghrelin-secreting cells as food-entrainable circadian clocks. Proc. Natl. Acad. Sci. U. S. A. *106*, 13582–13587.

Lewis, J. (2003). Autoinhibition with transcriptional delay: a simple mechanism for the zebrafish somitogenesis oscillator. Curr. Biol. CB *13*, 1398–1408.

Li, J., Grant, G.R., Hogenesch, J.B., and Hughes, M.E. (2015). Considerations for RNA-seq analysis of circadian rhythms. Methods Enzymol. *551*, 349–367.

Li, R., Harvey, A.R., Hodgetts, S.I., and Fox, A.H. (2017). Functional dissection of NEAT1 using genome editing reveals substantial localisation of the NEAT1_1 isoform outside paraspeckles. RNA N. Y. N.

Li, S., Kuhne, W.W., Kulharya, A., Hudson, F.Z., Ha, K., Cao, Z., and Dynan, W.S. (2009). Involvement of p54(nrb), a PSF partner protein, in DNA double-strand break repair and radioresistance. Nucleic Acids Res. *37*, 6746–6753.

Li, S., Li, Z., Shu, F.-J., Xiong, H., Phillips, A.C., and Dynan, W.S. (2014). Double-strand break repair deficiency in NONO knockout murine embryonic fibroblasts and compensation by spontaneous upregulation of the PSPC1 paralog. Nucleic Acids Res. *42*, 9771–9780.

Liang, S., and Lutz, C.S. (2006). p54nrb is a component of the snRNP-free U1A (SF-A) complex that promotes pre-mRNA cleavage during polyadenylation. RNA N. Y. N *12*, 111–121.

Libert, S., Bonkowski, M.S., Pointer, K., Pletcher, S.D., and Guarente, L. (2012). Deviation of innate circadian period from 24 h reduces longevity in mice. Aging Cell *11*, 794–800.

Lim, C., and Allada, R. (2013). Emerging roles for post-transcriptional regulation in circadian clocks. Nat. Neurosci. *16*, 1544–1550.

Liu, P.Y., Erriquez, D., Marshall, G.M., Tee, A.E., Polly, P., Wong, M., Liu, B., Bell, J.L., Zhang, X.D., Milazzo, G., et al. (2014). Effects of a novel long noncoding RNA, lncUSMycN, on N-Myc expression and neuroblastoma progression. J. Natl. Cancer Inst. *106*.

Lowrey, P.L., and Takahashi, J.S. (2011). Genetics of circadian rhythms in Mammalian model organisms. Adv. Genet. *74*, 175–230.

Lu, J.Y., and Sewer, M.B. (2015). p54nrb/NONO regulates cyclic AMP-dependent glucocorticoid production by modulating phosphodiesterase mRNA splicing and degradation. Mol. Cell. Biol. *35*, 1223–1237.

Luco, R.F., Allo, M., Schor, I.E., Kornblihtt, A.R., and Misteli, T. (2011). Epigenetics in alternative pre-mRNA splicing. Cell *144*, 16–26.

Lutz, C.S., Cooke, C., O'Connor, J.P., Kobayashi, R., and Alwine, J.C. (1998). The snRNP-free U1A (SF-A) complex(es): identification of the largest subunit as PSF, the polypyrimidine-tract binding protein-associated splicing factor. RNA N. Y. N *4*, 1493–1499.

Ma, J., Diedrich, J.K., Jungreis, I., Donaldson, C., Vaughan, J., Kellis, M., Yates, J.R., and Saghatelian, A. (2016). Improved Identification and Analysis of Small Open Reading Frame Encoded Polypeptides. Anal. Chem. *88*, 3967–3975.

Machicao, F., Peter, A., Machann, J., Königsrainer, I., Böhm, A., Lutz, S.Z., Heni, M., Fritsche, A., Schick, F., Königsrainer, A., et al. (2016). Glucose-Raising Polymorphisms in the Human Clock Gene Cryptochrome 2 (CRY2) Affect Hepatic Lipid Content. PloS One *11*, e0145563.

Mann, M. (2006). Functional and quantitative proteomics using SILAC. Nat. Rev. Mol. Cell Biol. *7*, 952–958.

Mannen, T., Yamashita, S., Tomita, K., Goshima, N., and Hirose, T. (2016). The Sam68 nuclear body is composed of two RNase-sensitive substructures joined by the adaptor HNRNPL. J. Cell Biol. *214*, 45–59.

Mao, Y.S., Sunwoo, H., Zhang, B., and Spector, D.L. (2011). Direct visualization of the co-transcriptional assembly of a nuclear body by noncoding RNAs. Nat. Cell Biol. *13*, 95–101.

Marcheva, B., Ramsey, K.M., Buhr, E.D., Kobayashi, Y., Su, H., Ko, C.H., Ivanova, G., Omura, C., Mo, S., Vitaterna, M.H., et al. (2010). Disruption of the clock components CLOCK and BMAL1 leads to hypoinsulinaemia and diabetes. Nature *466*, 627–631.

Masri, S., Rigor, P., Cervantes, M., Ceglia, N., Sebastian, C., Xiao, C., Roqueta-Rivera, M., Deng, C., Osborne, T.F., Mostoslavsky, R., et al. (2014). Partitioning circadian transcription by SIRT6 leads to segregated control of cellular metabolism. Cell *158*, 659–672.

Massa, M.L., Gagliardino, J.J., and Francini, F. (2011). Liver glucokinase: An overview on the regulatory mechanisms of its activity. IUBMB Life *63*, 1–6.

Mattson, M.P., Longo, V.D., and Harvie, M. (2017). Impact of intermittent fasting on health and disease processes. Ageing Res. Rev. *39*, 46–58.

Mauvoisin, D., Wang, J., Jouffe, C., Martin, E., Atger, F., Waridel, P., Quadroni, M., Gachon, F., and Naef, F. (2014). Circadian clock-dependent and -independent rhythmic proteomes implement distinct diurnal functions in mouse liver. Proc. Natl. Acad. Sci. U. S. A. *111*, 167–172.

Mayeuf-Louchart, A., Zecchin, M., Staels, B., and Duez, H. (2017). Circadian control of metabolism and pathological consequences of clock perturbations. Biochimie.

McGlincy, N.J., Valomon, A., Chesham, J.E., Maywood, E.S., Hastings, M.H., and Ule, J. (2012). Regulation of alternative splicing by the circadian clock and food related cues. Genome Biol. *13*, R54.

McHill, A.W., Melanson, E.L., Higgins, J., Connick, E., Moehlman, T.M., Stothard, E.R., and Wright, K.P. (2014). Impact of circadian misalignment on energy metabolism during simulated nightshift work. Proc. Natl. Acad. Sci. U. S. A. *111*, 17302–17307.

McMahon, A.C., Rahman, R., Jin, H., Shen, J.L., Fieldsend, A., Luo, W., and Rosbash, M. (2016). TRIBE: Hijacking an RNA-Editing Enzyme to Identify Cell-Specific Targets of RNA-Binding Proteins. Cell *165*, 742–753.

Mehlem, A., Hagberg, C.E., Muhl, L., Eriksson, U., and Falkevall, A. (2013). Imaging of neutral lipids by oil red O for analyzing the metabolic status in health and disease. Nat. Protoc. *8*, 1149–1154.

Menet, J.S., Rodriguez, J., Abruzzi, K.C., and Rosbash, M. (2012). Nascent-Seq reveals novel features of mouse circadian transcriptional regulation. eLife *1*, e00011.

Mircsof, D., Langouët, M., Rio, M., Moutton, S., Siquier-Pernet, K., Bole-Feysot, C., Cagnard, N., Nitschke, P., Gaspar, L., Žnidarič, M., et al. (2015). Mutations in NONO lead to syndromic intellectual disability and inhibitory synaptic defects. Nat. Neurosci.

Mohawk, J.A., Green, C.B., and Takahashi, J.S. (2012). Central and peripheral circadian clocks in mammals. Annu. Rev. Neurosci. *35*, 445–462.

Mollet, I.G., Ben-Dov, C., Felício-Silva, D., Grosso, A.R., Eleutério, P., Alves, R., Staller, R., Silva, T.S., and Carmo-Fonseca, M. (2010). Unconstrained mining of transcript data reveals increased alternative splicing complexity in the human transcriptome. Nucleic Acids Res. *38*, 4740–4754.

Montes, M., Becerra, S., Sánchez-Álvarez, M., and Suñé, C. (2012). Functional coupling of transcription and splicing. Gene *501*, 104–117.

Moore, M.C., Coate, K.C., Winnick, J.J., An, Z., and Cherrington, A.D. (2012). Regulation of hepatic glucose uptake and storage in vivo. Adv. Nutr. Bethesda Md *3*, 286–294.

Morozumi, Y., Takizawa, Y., Takaku, M., and Kurumizaka, H. (2009). Human PSF binds to RAD51 and modulates its homologous-pairing and strand-exchange activities. Nucleic Acids Res. *37*, 4296–4307.

Muhammad Z. Shrayyef, J.E.G. Normal Glucose Homeostasis.

Nagai, K., Nishio, T., Nakagawa, H., Nakamura, S., and Fukuda, Y. (1978). Effect of bilateral lesions of the suprachiasmatic nuclei on the circadian rhythm of food-intake. Brain Res. *142*, 384–389.

Naganuma, T., Nakagawa, S., Tanigawa, A., Sasaki, Y.F., Goshima, N., and Hirose, T. (2012). Alternative 3'-end processing of long noncoding RNA initiates construction of nuclear paraspeckles. EMBO J. *31*, 4020–4034.

Nakagawa, S., and Hirose, T. (2012). Paraspeckle nuclear bodies--useful uselessness? Cell. Mol. Life Sci. CMLS *69*, 3027–3036.

Nakagawa, S., Naganuma, T., Shioi, G., and Hirose, T. (2011). Paraspeckles are subpopulation-specific nuclear bodies that are not essential in mice. J. Cell Biol. *193*, 31–39.

Nakahata, Y., Kaluzova, M., Grimaldi, B., Sahar, S., Hirayama, J., Chen, D., Guarente, L.P., and Sassone-Corsi, P. (2008). The NAD+-dependent deacetylase SIRT1 modulates CLOCK-mediated chromatin remodeling and circadian control. Cell *134*, 329–340.

Nakahata, Y., Sahar, S., Astarita, G., Kaluzova, M., and Sassone-Corsi, P. (2009). Circadian control of the NAD+ salvage pathway by CLOCK-SIRT1. Science *324*,

654–657.

Nicolaides, N.C., Charmandari, E., Chrousos, G.P., and Kino, T. (2014). Circadian endocrine rhythms: the hypothalamic-pituitary-adrenal axis and its actions. Ann. N. Y. Acad. Sci. *1318*, 71–80.

Nilsen, T.W., and Graveley, B.R. (2010). Expansion of the eukaryotic proteome by alternative splicing. Nature *463*, 457–463.

O'Neill, J.S., and Reddy, A.B. (2011). Circadian clocks in human red blood cells. Nature *469*, 498–503.

Oswald, A., and Oates, A.C. (2011). Control of endogenous gene expression timing by introns. Genome Biol. *12*, 107.

Padmanabhan, K., Robles, M.S., Westerling, T., and Weitz, C.J. (2012). Feedback regulation of transcriptional termination by the mammalian circadian clock PERIOD complex. Science *337*, 599–602.

Panda, S. (2016). Circadian physiology of metabolism. Science *354*, 1008–1015.

Panda, S., Hogenesch, J.B., and Kay, S.A. (2002a). Circadian rhythms from flies to human. Nature *417*, 329–335.

Panda, S., Antoch, M.P., Miller, B.H., Su, A.I., Schook, A.B., Straume, M., Schultz, P.G., Kay, S.A., Takahashi, J.S., and Hogenesch, J.B. (2002b). Coordinated transcription of key pathways in the mouse by the circadian clock. Cell *109*, 307–320.

Paschos, G.K., Ibrahim, S., Song, W.-L., Kunieda, T., Grant, G., Reyes, T.M., Bradfield, C.A., Vaughan, C.H., Eiden, M., Masoodi, M., et al. (2012). Obesity in mice with adipocyte-specific deletion of clock component Arntl. Nat. Med. *18*, 1768–1777.

Passonneau, J.V., and Lauderdale, V.R. (1974). A comparison of three methods of glycogen measurement in tissues. Anal. Biochem. *60*, 405–412.

Pavao, M., Huang, Y.H., Hafer, L.J., Moreland, R.B., and Traish, A.M. (2001). Immunodetection of nmt55/p54nrb isoforms in human breast cancer. BMC Cancer *1*, 15.

Peng, R., Dye, B.T., Pérez, I., Barnard, D.C., Thompson, A.B., and Patton, J.G. (2002). PSF and p54nrb bind a conserved stem in U5 snRNA. RNA N. Y. N *8*, 1334–1347.

Peng, R., Hawkins, I., Link, A.J., and Patton, J.G. (2006). The splicing factor PSF is part of a large complex that assembles in the absence of pre-mRNA and contains all five snRNPs. RNA Biol. *3*, 69–76.

Perelis, M., Marcheva, B., Ramsey, K.M., Schipma, M.J., Hutchison, A.L., Taguchi, A., Peek, C.B., Hong, H., Huang, W., Omura, C., et al. (2015). Pancreatic β cell enhancers regulate rhythmic transcription of genes controlling insulin secretion. Science *350*, aac4250.

Petersen, M.C., Vatner, D.F., and Shulman, G.I. (2017). Regulation of hepatic glucose metabolism in health and disease. Nat. Rev. Endocrinol. *13*, 572–587.

Pitts, S., Perone, E., and Silver, R. (2003). Food-entrained circadian rhythms are sustained in arrhythmic Clk/Clk mutant mice. Am. J. Physiol. Regul. Integr. Comp.

Physiol. *285*, R57-67.

Prasanth, K.V., Prasanth, S.G., Xuan, Z., Hearn, S., Freier, S.M., Bennett, C.F., Zhang, M.Q., and Spector, D.L. (2005). Regulating gene expression through RNA nuclear retention. Cell *123*, 249–263.

Preitner, N., Damiola, F., Lopez-Molina, L., Zakany, J., Duboule, D., Albrecht, U., and Schibler, U. (2002). The orphan nuclear receptor REV-ERBalpha controls circadian transcription within the positive limb of the mammalian circadian oscillator. Cell *110*, 251–260.

Preußner, M., Wilhelmi, I., Schultz, A.-S., Finkernagel, F., Michel, M., Möröy, T., and Heyd, F. (2014). Rhythmic U2af26 alternative splicing controls PERIOD1 stability and the circadian clock in mice. Mol. Cell *54*, 651–662.

Proteau, A., Blier, S., Albert, A.L., Lavoie, S.B., Traish, A.M., and Vincent, M. (2005). The multifunctional nuclear protein p54nrb is multiphosphorylated in mitosis and interacts with the mitotic regulator Pin1. J. Mol. Biol. *346*, 1163–1172.

Proudfoot, N.J., Furger, A., and Dye, M.J. (2002). Integrating mRNA processing with transcription. Cell *108*, 501–512.

Rabani, M., Raychowdhury, R., Jovanovic, M., Rooney, M., Stumpo, D.J., Pauli, A., Hacohen, N., Schier, A.F., Blackshear, P.J., Friedman, N., et al. (2014). High-resolution sequencing and modeling identifies distinct dynamic RNA regulatory strategies. Cell *159*, 1698–1710.

Ramsey, K.M., Yoshino, J., Brace, C.S., Abrassart, D., Kobayashi, Y., Marcheva, B., Hong, H.-K., Chong, J.L., Buhr, E.D., Lee, C., et al. (2009). Circadian clock feedback cycle through NAMPT-mediated NAD+ biosynthesis. Science *324*, 651–654.

Reddy, A.B., and O'Neill, J.S. (2010). Healthy clocks, healthy body, healthy mind. Trends Cell Biol. *20*, 36–44.

Reddy, A.B., Karp, N.A., Maywood, E.S., Sage, E.A., Deery, M., O'Neill, J.S., Wong, G.K.Y., Chesham, J., Odell, M., Lilley, K.S., et al. (2006). Circadian orchestration of the hepatic proteome. Curr. Biol. CB *16*, 1107–1115.

Reddy, A.B., Maywood, E.S., Karp, N.A., King, V.M., Inoue, Y., Gonzalez, F.J., Lilley, K.S., Kyriacou, C.P., and Hastings, M.H. (2007). Glucocorticoid signaling synchronizes the liver circadian transcriptome. Hepatol. Baltim. Md *45*, 1478–1488.

Reed, R., and Hurt, E. (2002). A conserved mRNA export machinery coupled to pre-mRNA splicing. Cell *108*, 523–531.

Rey, G., Cesbron, F., Rougemont, J., Reinke, H., Brunner, M., and Naef, F. (2011). Genome-wide and phase-specific DNA-binding rhythms of BMAL1 control circadian output functions in mouse liver. PLoS Biol. *9*, e1000595.

Ripperger, J.A., and Schibler, U. (2006). Rhythmic CLOCK-BMAL1 binding to multiple E-box motifs drives circadian Dbp transcription and chromatin transitions. Nat. Genet. *38*, 369–374.

Robinson, B.G., Frim, D.M., Schwartz, W.J., and Majzoub, J.A. (1988). Vasopressin mRNA in the suprachiasmatic nuclei: daily regulation of polyadenylate tail length. Science *241*, 342–344.

Robles, M.S., Cox, J., and Mann, M. (2014). In-vivo quantitative proteomics reveals

a key contribution of post-transcriptional mechanisms to the circadian regulation of liver metabolism. PLoS Genet. *10*, e1004047.

Rose, A.B., Elfersi, T., Parra, G., and Korf, I. (2008). Promoter-proximal introns in Arabidopsis thaliana are enriched in dispersed signals that elevate gene expression. Plant Cell *20*, 543–551.

Rudic, R.D., McNamara, P., Curtis, A.-M., Boston, R.C., Panda, S., Hogenesch, J.B., and Fitzgerald, G.A. (2004). BMAL1 and CLOCK, two essential components of the circadian clock, are involved in glucose homeostasis. PLoS Biol. *2*, e377.

Sachs, A. (1990). The role of poly(A) in the translation and stability of mRNA. Curr. Opin. Cell Biol. *2*, 1092–1098.

Sadacca, L.A., Lamia, K.A., deLemos, A.S., Blum, B., and Weitz, C.J. (2011). An intrinsic circadian clock of the pancreas is required for normal insulin release and glucose homeostasis in mice. Diabetologia *54*, 120–124.

Saini, C., Morf, J., Stratmann, M., Gos, P., and Schibler, U. (2012). Simulated body temperature rhythms reveal the phase-shifting behavior and plasticity of mammalian circadian oscillators. Genes Dev. *26*, 567–580.

Saini, C., Liani, A., Curie, T., Gos, P., Kreppel, F., Emmenegger, Y., Bonacina, L., Wolf, J.-P., Poget, Y.-A., Franken, P., et al. (2013). Real-time recording of circadian liver gene expression in freely moving mice reveals the phase-setting behavior of hepatocyte clocks. Genes Dev. *27*, 1526–1536.

Salgado-Delgado, R., Angeles-Castellanos, M., Buijs, M.R., and Escobar, C. (2008). Internal desynchronization in a model of night-work by forced activity in rats. Neuroscience *154*, 922–931.

Sánchez-Jiménez, F., and Sánchez-Margalet, V. (2013). Role of Sam68 in post-transcriptional gene regulation. Int. J. Mol. Sci. *14*, 23402–23419.

Sasaki, Y.T.F., and Hirose, T. (2009). How to build a paraspeckle. Genome Biol. *10*, 227.

Sasaki, Y.T.F., Ideue, T., Sano, M., Mituyama, T., and Hirose, T. (2009). MENepsilon/beta noncoding RNAs are essential for structural integrity of nuclear paraspeckles. Proc. Natl. Acad. Sci. U. S. A. *106*, 2525–2530.

Sato, T.K., Panda, S., Miraglia, L.J., Reyes, T.M., Rudic, R.D., McNamara, P., Naik, K.A., FitzGerald, G.A., Kay, S.A., and Hogenesch, J.B. (2004). A functional genomics strategy reveals Rora as a component of the mammalian circadian clock. Neuron *43*, 527–537.

Scadden, D. (2009). A NEAT way of regulating nuclear export of mRNAs. Mol. Cell *35*, 395–396.

Scheer, F.A.J.L., Hilton, M.F., Mantzoros, C.S., and Shea, S.A. (2009). Adverse metabolic and cardiovascular consequences of circadian misalignment. Proc. Natl. Acad. Sci. U. S. A. *106*, 4453–4458.

Schiffner, S., Zimara, N., Schmid, R., and Bosserhoff, A.-K. (2011). p54nrb is a new regulator of progression of malignant melanoma. Carcinogenesis *32*, 1176–1182.

Schmidt, E.E., and Schibler, U. (1995). Cell size regulation, a mechanism that controls cellular RNA accumulation: consequences on regulation of the ubiquitous

transcription factors Oct1 and NF-Y and the liver-enriched transcription factor DBP. J. Cell Biol. *128*, 467–483.

Schwartsburd, P.M. (2017). Catabolic and anabolic faces of insulin resistance and their disorders: a new insight into circadian control of metabolic disorders leading to diabetes. Future Sci. OA *3*, FSO201.

Scott, E.M., Carter, A.M., and Grant, P.J. (2008). Association between polymorphisms in the Clock gene, obesity and the metabolic syndrome in man. Int. J. Obes. 2005 *32*, 658–662.

Sharabi, K., Tavares, C.D.J., Rines, A.K., and Puigserver, P. (2015). Molecular pathophysiology of hepatic glucose production. Mol. Aspects Med. *46*, 21–33.

Shav-Tal, Y., and Zipori, D. (2002). PSF and p54(nrb)/NonO--multi-functional nuclear proteins. FEBS Lett. *531*, 109–114.

Shi, Y., Di Giammartino, D.C., Taylor, D., Sarkeshik, A., Rice, W.J., Yates, J.R., Frank, J., and Manley, J.L. (2009). Molecular architecture of the human pre-mRNA 3' processing complex. Mol. Cell *33*, 365–376.

Sinturel, F., Gerber, A., Mauvoisin, D., Wang, J., Gatfield, D., Stubblefield, J.J., Green, C.B., Gachon, F., and Schibler, U. (2017). Diurnal Oscillations in Liver Mass and Cell Size Accompany Ribosome Assembly Cycles. Cell *169*, 651–663.e14.

Skourti-Stathaki, K., Proudfoot, N.J., and Gromak, N. (2011). Human senataxin resolves RNA/DNA hybrids formed at transcriptional pause sites to promote Xrn2-dependent termination. Mol. Cell *42*, 794–805.

So, A.Y.-L., Bernal, T.U., Pillsbury, M.L., Yamamoto, K.R., and Feldman, B.J. (2009). Glucocorticoid regulation of the circadian clock modulates glucose homeostasis. Proc. Natl. Acad. Sci. U. S. A. *106*, 17582–17587.

Sobel, J.A., Krier, I., Andersin, T., Raghav, S., Canella, D., Gilardi, F., Kalantzi, A.S., Rey, G., Weger, B., Gachon, F., et al. (2017). Transcriptional regulatory logic of the diurnal cycle in the mouse liver. PLoS Biol. *15*, e2001069.

Sookoian, S., Gemma, C., Fernández Gianotti, T., Burgueño, A., Alvarez, A., González, C.D., and Pirola, C.J. (2007). Effects of rotating shift work on biomarkers of metabolic syndrome and inflammation. J. Intern. Med. *261*, 285–292.

St Gelais, C., Roger, J., and Wu, L. (2015). Non-POU Domain-Containing Octamer-Binding Protein Negatively Regulates HIV-1 Infection in CD4(+) T Cells. AIDS Res. Hum. Retroviruses *31*, 806–816.

Stephan, F.K. (2002). The "other" circadian system: food as a Zeitgeber. J. Biol. Rhythms *17*, 284–292.

Stephan, F.K., Swann, J.M., and Sisk, C.L. (1979). Entrainment of circadian rhythms by feeding schedules in rats with suprachiasmatic lesions. Behav. Neural Biol. *25*, 545–554.

Stokkan, K.A., Yamazaki, S., Tei, H., Sakaki, Y., and Menaker, M. (2001). Entrainment of the circadian clock in the liver by feeding. Science *291*, 490–493.

Storch, K.-F., and Weitz, C.J. (2009). Daily rhythms of food-anticipatory behavioral activity do not require the known circadian clock. Proc. Natl. Acad. Sci. U. S. A. *106*, 6808–6813.

Sury, M.D., McShane, E., Hernandez-Miranda, L.R., Birchmeier, C., and Selbach, M. (2015). Quantitative proteomics reveals dynamic interaction of c-Jun N-terminal kinase (JNK) with RNA transport granule proteins splicing factor proline- and glutamine-rich (Sfpq) and non-POU domain-containing octamer-binding protein (Nono) during neuronal differentiation. Mol. Cell. Proteomics MCP *14*, 50–65.

Swinburne, I.A., and Silver, P.A. (2008). Intron delays and transcriptional timing during development. Dev. Cell *14*, 324–330.

Swinburne, I.A., Miguez, D.G., Landgraf, D., and Silver, P.A. (2008). Intron length increases oscillatory periods of gene expression in animal cells. Genes Dev. *22*, 2342–2346.

Tabb, D.L., McDonald, W.H., and Yates, J.R. (2002). DTASelect and Contrast: tools for assembling and comparing protein identifications from shotgun proteomics. J. Proteome Res. *1*, 21–26.

Takahashi, J.S. (2017). Transcriptional architecture of the mammalian circadian clock. Nat. Rev. Genet. *18*, 164–179.

Takahashi, J.S., Hong, H.-K., Ko, C.H., and McDearmon, E.L. (2008). The genetics of mammalian circadian order and disorder: implications for physiology and disease. Nat. Rev. Genet. *9*, 764–775.

Tennyson, C.N., Klamut, H.J., and Worton, R.G. (1995). The human dystrophin gene requires 16 hours to be transcribed and is cotranscriptionally spliced. Nat. Genet. *9*, 184–190.

Tenzer, S., Moro, A., Kuharev, J., Francis, A.C., Vidalino, L., Provenzani, A., and Macchi, P. (2013). Proteome-wide characterization of the RNA-binding protein RALY-interactome using the in vivo-biotinylation-pulldown-quant (iBioPQ) approach. J. Proteome Res. *12*, 2869–2884.

Thorens, B., and Mueckler, M. (2010). Glucose transporters in the 21st Century. Am. J. Physiol. Endocrinol. Metab. *298*, E141-145.

Titchenell, P.M., Quinn, W.J., Lu, M., Chu, Q., Lu, W., Li, C., Chen, H., Monks, B.R., Chen, J., Rabinowitz, J.D., et al. (2016). Direct Hepatocyte Insulin Signaling Is Required for Lipogenesis but Is Dispensable for the Suppression of Glucose Production. Cell Metab. *23*, 1154–1166.

Torres, M., Becquet, D., Blanchard, M.-P., Guillen, S., Boyer, B., Moreno, M., Franc, J.-L., and François-Bellan, A.-M. (2016). Circadian RNA expression elicited by 3'-UTR IRAlu-paraspeckle associated elements. eLife *5*.

Traish, A.M., Huang, Y.H., Ashba, J., Pronovost, M., Pavao, M., McAneny, D.B., and Moreland, R.B. (1997). Loss of expression of a 55 kDa nuclear protein (nmt55) in estrogen receptor-negative human breast cancer. Diagn. Mol. Pathol. Am. J. Surg. Pathol. Part B *6*, 209–221.

Turek, F.W., Joshu, C., Kohsaka, A., Lin, E., Ivanova, G., McDearmon, E., Laposky, A., Losee-Olson, S., Easton, A., Jensen, D.R., et al. (2005). Obesity and metabolic syndrome in circadian Clock mutant mice. Science *308*, 1043–1045.

Udayakumar, D., and Dynan, W.S. (2015). Characterization of DNA binding and pairing activities associated with the native SFPQ·NONO DNA repair protein complex. Biochem. Biophys. Res. Commun. *463*, 473–478.

Udayakumar, D., Bladen, C.L., Hudson, F.Z., and Dynan, W.S. (2003). Distinct pathways of nonhomologous end joining that are differentially regulated by DNA-dependent protein kinase-mediated phosphorylation. J. Biol. Chem. *278*, 41631–41635.

Uren, P.J., Bahrami-Samani, E., Burns, S.C., Qiao, M., Karginov, F.V., Hodges, E., Hannon, G.J., Sanford, J.R., Penalva, L.O.F., and Smith, A.D. (2012). Site identification in high-throughput RNA-protein interaction data. Bioinforma. Oxf. Engl. *28*, 3013–3020.

Venter, J.C., Adams, M.D., Myers, E.W., Li, P.W., Mural, R.J., Sutton, G.G., Smith, H.O., Yandell, M., Evans, C.A., Holt, R.A., et al. (2001). The sequence of the human genome. Science *291*, 1304–1351.

Vollmers, C., Gill, S., DiTacchio, L., Pulivarthy, S.R., Le, H.D., and Panda, S. (2009). Time of feeding and the intrinsic circadian clock drive rhythms in hepatic gene expression. Proc. Natl. Acad. Sci. U. S. A. *106*, 21453–21458.

Vollmers, C., Schmitz, R.J., Nathanson, J., Yeo, G., Ecker, J.R., and Panda, S. (2012). Circadian oscillations of protein-coding and regulatory RNAs in a highly dynamic mammalian liver epigenome. Cell Metab. *16*, 833–845.

Vujovic, N., Davidson, A.J., and Menaker, M. (2008). Sympathetic input modulates, but does not determine, phase of peripheral circadian oscillators. Am. J. Physiol. Regul. Integr. Comp. Physiol. *295*, R355-360.

Wang, E.T., Sandberg, R., Luo, S., Khrebtukova, I., Zhang, L., Mayr, C., Kingsmore, S.F., Schroth, G.P., and Burge, C.B. (2008). Alternative isoform regulation in human tissue transcriptomes. Nature *456*, 470–476.

Wang, F., Zhang, L., Zhang, Y., Zhang, B., He, Y., Xie, S., Li, M., Miao, X., Chan, E.Y.Y., Tang, J.L., et al. (2014). Meta-analysis on night shift work and risk of metabolic syndrome. Obes. Rev. Off. J. Int. Assoc. Study Obes. *15*, 709–720.

Wang, J., Rajbhandari, P., Damianov, A., Han, A., Sallam, T., Waki, H., Villanueva, C.J., Lee, S.D., Nielsen, R., Mandrup, S., et al. (2017). RNA-binding protein PSPC1 promotes the differentiation-dependent nuclear export of adipocyte RNAs. J. Clin. Invest.

Wang, Y., Osterbur, D.L., Megaw, P.L., Tosini, G., Fukuhara, C., Green, C.B., and Besharse, J.C. (2001). Rhythmic expression of Nocturnin mRNA in multiple tissues of the mouse. BMC Dev. Biol. *1*, 9.

Weger, B.D., Weger, M., Görling, B., Schink, A., Gobet, C., Keime, C., Poschet, G., Jost, B., Krone, N., Hell, R., et al. (2016). Extensive Regulation of Diurnal Transcription and Metabolism by Glucocorticoids. PLoS Genet. *12*, e1006512.

Weidensdorfer, D., Stöhr, N., Baude, A., Lederer, M., Köhn, M., Schierhorn, A., Buchmeier, S., Wahle, E., and Hüttelmaier, S. (2009). Control of c-myc mRNA stability by IGF2BP1-associated cytoplasmic RNPs. RNA N. Y. N *15*, 104–115.

Witten, J.T., and Ule, J. (2011). Understanding splicing regulation through RNA splicing maps. Trends Genet. TIG *27*, 89–97.

Woelfle, M.A., Ouyang, Y., Phanvijhitsiri, K., and Johnson, C.H. (2004). The adaptive value of circadian clocks: an experimental assessment in cyanobacteria. Curr. Biol. CB *14*, 1481–1486.

Woo, K.-C., Kim, T.-D., Lee, K.-H., Kim, D.-Y., Kim, W., Lee, K.-Y., and Kim, K.-T. (2009). Mouse period 2 mRNA circadian oscillation is modulated by PTB-mediated rhythmic mRNA degradation. Nucleic Acids Res. *37*, 26–37.

Woo, K.-C., Ha, D.-C., Lee, K.-H., Kim, D.-Y., Kim, T.-D., and Kim, K.-T. (2010). Circadian amplitude of cryptochrome 1 is modulated by mRNA stability regulation via cytoplasmic hnRNP D oscillation. Mol. Cell. Biol. *30*, 197–205.

Woon, P.Y., Kaisaki, P.J., Bragança, J., Bihoreau, M.-T., Levy, J.C., Farrall, M., and Gauguier, D. (2007). Aryl hydrocarbon receptor nuclear translocator-like (BMAL1) is associated with susceptibility to hypertension and type 2 diabetes. Proc. Natl. Acad. Sci. U. S. A. *104*, 14412–14417.

Wu, G., Anafi, R.C., Hughes, M.E., Kornacker, K., and Hogenesch, J.B. (2016). MetaCycle: an integrated R package to evaluate periodicity in large scale data. Bioinforma. Oxf. Engl. *32*, 3351–3353.

Xu, J., Zhong, N., Wang, H., Elias, J.E., Kim, C.Y., Woldman, I., Pifl, C., Gygi, S.P., Geula, C., and Yankner, B.A. (2005). The Parkinson's disease-associated DJ-1 protein is a transcriptional co-activator that protects against neuronal apoptosis. Hum. Mol. Genet. *14*, 1231–1241.

Xu, T., Park, S.K., Venable, J.D., Wohlschlegel, J.A., Diedrich, J.K., Cociorva, D., Lu, B., Liao, L., Hewel, J., Han, X., et al. (2015). ProLuCID: An improved SEQUEST-like algorithm with enhanced sensitivity and specificity. J. Proteomics *129*, 16–24.

Yadav, S.P., Hao, H., Yang, H.-J., Kautzmann, M.-A.I., Brooks, M., Nellissery, J., Klocke, B., Seifert, M., and Swaroop, A. (2014). The transcription-splicing protein NonO/p54nrb and three NonO-interacting proteins bind to distal enhancer region and augment rhodopsin expression. Hum. Mol. Genet. *23*, 2132–2144.

Yamamoto, T., Nakahata, Y., Tanaka, M., Yoshida, M., Soma, H., Shinohara, K., Yasuda, A., Mamine, T., and Takumi, T. (2005). Acute physical stress elevates mouse period1 mRNA expression in mouse peripheral tissues via a glucocorticoid-responsive element. J. Biol. Chem. *280*, 42036–42043.

Yamauchi, T., Nakamura, N., Hiramoto, M., Yuri, M., Yokota, H., Naitou, M., Takeuchi, M., Yamanaka, K., Kita, A., Nakahara, T., et al. (2012). Sepantronium bromide (YM155) induces disruption of the ILF3/p54(nrb) complex, which is required for survivin expression. Biochem. Biophys. Res. Commun. *425*, 711–716.

Yamazaki, T., and Hirose, T. (2015). The building process of the functional paraspeckle with long non-coding RNAs. Front. Biosci. Elite Ed. *7*, 1–41.

Yamazaki, S., Numano, R., Abe, M., Hida, A., Takahashi, R., Ueda, M., Block, G.D., Sakaki, Y., Menaker, M., and Tei, H. (2000). Resetting central and peripheral circadian oscillators in transgenic rats. Science *288*, 682–685.

Yang, R., and Su, Z. (2010). Analyzing circadian expression data by harmonic regression based on autoregressive spectral estimation. Bioinforma. Oxf. Engl. *26*, i168-174.

Yoo, S.-H., Yamazaki, S., Lowrey, P.L., Shimomura, K., Ko, C.H., Buhr, E.D., Siepka, S.M., Hong, H.-K., Oh, W.J., Yoo, O.J., et al. (2004). PERIOD2::LUCIFERASE real-time reporting of circadian dynamics reveals persistent circadian oscillations in mouse peripheral tissues. Proc. Natl. Acad. Sci. U. S. A. *101*, 5339–5346.

Yoshitane, H., Ozaki, H., Terajima, H., Du, N.-H., Suzuki, Y., Fujimori, T., Kosaka, N., Shimba, S., Sugano, S., Takagi, T., et al. (2014). CLOCK-controlled polyphonic regulation of circadian rhythms through canonical and noncanonical E-boxes. Mol. Cell. Biol. *34*, 1776–1787.

Zambon, A.C., Gaj, S., Ho, I., Hanspers, K., Vranizan, K., Evelo, C.T., Conklin, B.R., Pico, A.R., and Salomonis, N. (2012). GO-Elite: a flexible solution for pathway and ontology over-representation. Bioinformatics *28*, 2209–2210.

Zarrinpar, A., Chaix, A., and Panda, S. (2016). Daily Eating Patterns and Their Impact on Health and Disease. Trends Endocrinol. Metab. TEM *27*, 69–83.

Zhang, Z., and Carmichael, G.G. (2001). The fate of dsRNA in the nucleus: a p54(nrb)-containing complex mediates the nuclear retention of promiscuously A-to-I edited RNAs. Cell *106*, 465–475.

Zhang, R., Lahens, N.F., Ballance, H.I., Hughes, M.E., and Hogenesch, J.B. (2014). A circadian gene expression atlas in mammals: implications for biology and medicine. Proc. Natl. Acad. Sci. U. S. A. *111*, 16219–16224.

Zhang, X., Virtanen, A., and Kleiman, F.E. (2010). To polyadenylate or to deadenylate: that is the question. Cell Cycle Georget. Tex *9*, 4437–4449.

Zhao, J., Sun, B.K., Erwin, J.A., Song, J.-J., and Lee, J.T. (2008). Polycomb proteins targeted by a short repeat RNA to the mouse X chromosome. Science *322*, 750–756.

Zhao, J., Ohsumi, T.K., Kung, J.T., Ogawa, Y., Grau, D.J., Sarma, K., Song, J.J., Kingston, R.E., Borowsky, M., and Lee, J.T. (2010). Genome-wide identification of polycomb-associated RNAs by RIP-seq. Mol. Cell *40*, 939–953.

Zhu, Z., Zhao, X., Zhao, L., Yang, H., Liu, L., Li, J., Wu, J., Yang, F., Huang, G., and Liu, J. (2015). p54(nrb)/NONO regulates lipid metabolism and breast cancer growth through SREBP-1A. Oncogene.

9. CURRICULUM VITAE

Name: Giorgia

Surname: Benegiamo

Date of Birth: 18/11/1986

Nationality: Italian

EDUCATION

Institution and location	*Degree*	*MM/YYYY*	*Field of Study*
- University of Zurich, Switzerland and Salk Institute for Biological Studies, La Jolla CA (joint PhD project)	PhD	10/2017 (planned)	Molecular Life Sciences
- University of Bologna, Italy	M.Sc.	03/2011	Medical Biotechnology
- University of Bologna, Italy	B.Sc.	11/2008	Biotechnology

RESEARCH EXPERIENCES

Institution and location	*Position*	*Duration (MM-YYYY)*
- University of Zürich, Switzerland AND Salk Institute for Biological Studies, La Jolla CA, USA Supervisors: Prof. Steven A. Brown, Prof. Satchidananda Panda Project Title: ''The role of the RNA-binding protein NONO in the regulation of circadian rhythms and metabolism''	PhD Student	11/2012 - present
- Laboratory of Immunology and biology of metastasis - University of Bologna, Italy Supervisors: Prof. Pier-Luigi Lollini, Prof. Carla DeGiovanni Project Title: ''Immunological prevention of mammary carcinogenesis in HER-2/neu IL15$^{-/-}$ mice''	Master Student	1/2010 – 3/2011
- Unit of Immunotherapy of Human Tumors - Istituto Nazionale Tumori – Milan, Italy Supervisors: Dr. Licia Rivoltini, Prof. Annalisa Pession Project Title: ''The effect of acidic pH on the tumor infiltrating T lymphocytes''	Bachelor Student	5/2008 – 8/2008

PROFESSIONAL DEVELOPMENT

Courses	*Location*	*MM/YYYY*
- NCCR RNA & Disease Summer School "RNA & RNP architecture: from structure to function to disease"	Saas-Fee (Switzerland)	08/2017
- CSHL Eukaryotic Gene Expression Summer School	CSHL (USA)	08/2014
Conferences with active participation	*Location*	*MM/YYYY*
- Short talk: European Biological Rhythms Society (EBRS) meeting	Amsterdam (Nederlands)	07/2017
- Short talk and poster presentation: Keystone Symposium 'Protein-RNA Interactions: Scale, Mechanisms, Structure and Function of Coding and Noncoding RNPs'	Banff, Alberta (Canada)	02/2017
- Poster presentation: 16th IGIS Symposium – 'The Islet and Metabolism Keep Time'	Saint-Jean-Cap-Ferrat (France)	04/2015

FINANCIAL SUPPORT

- Doc.Mobility Fellowship from the Swiss National Science Foundation (SNF)	July 2016 – June 2017
- Fellowship from the Glenn Foundation for Medical Research	May 2014 – April 2016

PUBLICATIONS

Benegiamo G, Mure LS, Erikson G, Le HD, Moriggi E, Brown SA, Panda S. The RNA-binding protein NONO coordinates hepatic adaptation to feeding. Cell Metab*., accepted*

Mure LS, Le HD, **Benegiamo G**, Chang MW, Jillani N, Maini N, Kariuki T, Dkhissi-Benyahya O, Cooper HM, Panda S. Diurnal transcriptome atlas of a primate across all major neural and peripheral tissues. *Under revision*

Mure LS, Hatori M, Ruda K, **Benegiamo G**, Demas J and Panda S. Deactivation and regeneration of melanopsin photoresponses by beta arrestin -1 and -2. *In preparation*

Benegiamo, G., Brown, S.A., and Panda, S. (2016). RNA Dynamics in the Control of Circadian Rhythm. Adv. Exp. Med. Biol. *907*, 107–122.

Cela, O., Scrima, R., Pazienza, V., Merla, G., **Benegiamo, G.**, Augello, B., Fugetto, S., Menga, M., Rubino, R., Fuhr, L., et al. (2015). Clock genes-dependent acetylation of

complex I sets rhythmic activity of mitochondrial OxPhos. Biochim. Biophys. Acta *1863*, 596–606.

Croci, S., Nanni, P., Palladini, A., Nicoletti, G., Grosso, V., **Benegiamo, G.**, Landuzzi, L., Lamolinara, A., Ianzano, M.L., Ranieri, D., et al. (2015). Interleukin-15 is required for immunosurveillance and immunoprevention of HER2/neu-driven mammary carcinogenesis. Breast Cancer Res. BCR *17*, 70.

Benegiamo, G., Mazzoccoli, G., Cappello, F., Rappa, F., Scibetta, N., Oben, J., Greco, A., Williams, R., Andriulli, A., Vinciguerra, M., et al. (2013). Mutual antagonism between circadian protein period 2 and hepatitis C virus replication in hepatocytes. PloS One *8*, e60527.

Panza, A., Pazienza, V., Ripoli, M., **Benegiamo, G.**, Gentile, A., Valvano, M.R., Augello, B., Merla, G., Prattichizzo, C., Tavano, F., et al. (2013). Interplay between SOX9, β-catenin and PPARγ activation in colorectal cancer. Biochim. Biophys. Acta *1833*, 1853–1865.

Benegiamo, G., Vinciguerra, M., Guarnieri, V., Niro, G.A., Andriulli, A., and Pazienza, V. (2013). Hepatitis delta virus induces specific DNA methylation processes in Huh-7 liver cancer cells. FEBS Lett. *587*, 1424–1428.

Mazzoccoli, G., Francavilla, M., Pazienza, V., **Benegiamo, G.**, Piepoli, A., Vinciguerra, M., Giuliani, F., Yamamoto, T., and Takumi, T. (2012). Differential patterns in the periodicity and dynamics of clock gene expression in mouse liver and stomach. Chronobiol. Int. *29*, 1300–1311.

Pazienza, V., Tavano, F., Francavilla, M., Fontana, A., Pellegrini, F., **Benegiamo, G.**, Corbo, V., di Mola, F.F., Di Sebastiano, P., Andriulli, A., et al. (2012). Time-Qualified Patterns of Variation of PPARγ, DNMT1, and DNMT3B Expression in Pancreatic Cancer Cell Lines. PPAR Res. *2012*, 890875.

Pazienza, V., Tavano, F., **Benegiamo, G.**, Vinciguerra, M., Burbaci, F.P., Copetti, M., di Mola, F.F., Andriulli, A., and di Sebastiano, P. (2012). Correlations among PPARγ, DNMT1, and DNMT3B Expression Levels and Pancreatic Cancer. PPAR Res. *2012*, 461784

Mazzoccoli, G., Francavilla, M., Giuliani, F., Aucella, F., Vinciguerra, M., Pazienza, V., Piepoli, A., **Benegiamo, G.**, Liu, S., and Cai, Y. (2012). Clock gene expression in mouse kidney and testis: analysis of periodical and dynamical patterns. J. Biol. Regul. Homeost. Agents *26*, 303–311.

Guarnieri, V., Valentina D'Elia, A., Baorda, F., Pazienza, V., **Benegiamo, G.**, Stanziale, P., Copetti, M., Battista, C., Grimaldi, F., Damante, G., et al. (2012). CASR gene activating mutations in two families with autosomal dominant hypocalcemia. Mol. Genet. Metab. *107*, 548–552.

Benegiamo, G., Vinciguerra, M., Mazzoccoli, G., Piepoli, A., Andriulli, A., and Pazienza, V. (2012). DNA methyltransferases 1 and 3b expression in Huh-7 cells expressing HCV core protein of different genotypes. Dig. Dis. Sci. *57*, 1598–1603.

Mazzoccoli, G., Piepoli, A., Carella, M., Panza, A., Pazienza, V., **Benegiamo, G.**, Palumbo, O., and Ranieri, E. (2012). Altered expression of the clock gene machinery in kidney cancer patients. Biomed. Pharmacother. Bioméd. Pharmacothérapie *66*, 175–179.

Mazzoccoli, G., Pazienza, V., Panza, A., Valvano, M.R., **Benegiamo, G.**, Vinciguerra, M., Andriulli, A., and Piepoli, A. (2012). ARNTL2 and SERPINE1: potential biomarkers for tumor aggressiveness in colorectal cancer. J. Cancer Res. Clin. Oncol. *138*, 501–511.

Pazienza, V., Piepoli, A., Panza, A., Valvano, M.R., **Benegiamo, G.**, Vinciguerra, M., Andriulli, A., and Mazzoccoli, G. (2012). SIRT1 and the clock gene machinery in colorectal cancer. Cancer Invest. *30*, 98–105.

10. APPENDIX

Chapter 5
RNA Dynamics in the Control of Circadian Rhythm

Giorgia Benegiamo, Steven A. Brown, and Satchidananda Panda

Abstract The circadian oscillator is based on transcription-translation feedback loops that generate 24 h oscillations in gene expression. Although circadian regulation of mRNA expression at the transcriptional level is one of the most important steps for the generation of circadian rhythms within the cell, multiple lines of evidence point to a disconnect between transcript oscillation and protein oscillation. This can be explained by regulatory RNA-binding proteins acting on the nascent transcripts to modulate their processing, export, translation and degradation rates. In this chapter we will review what is known about the different steps involved in circadian gene expression from transcription initiation to mRNA stability and translation efficiency. The role of ribonucleoprotein particles in the generation of rhythmic gene expression is only starting to be elucidated, but it is likely that they cooperate with the basal transcriptional machinery to help to maintain the precision of the clock under diverse cellular and environmental conditions.

Keywords eRNA • Chromatin modifications • Nascent-seq • RNA-seq • RNAPII • Exon array • IRES • Ribosome • PolyA tail length

G. Benegiamo
Institute of Pharmacology and Toxicology, University of Zürich,
Winterthurerstrasse 190, Zürich 8057, Switzerland

Salk Institute for Biological Studies,
10010, North Torrey Pines Road, La Jolla, CA 92037, USA

S.A. Brown
Institute of Pharmacology and Toxicology, University of Zürich,
Winterthurerstrasse 190, Zürich 8057, Switzerland

S. Panda (✉)
Salk Institute for Biological Studies,
10010, North Torrey Pines Road, La Jolla, CA 92037, USA
e-mail: satchin@salk.edu

G.W. Yeo (ed.), *RNA Processing*, Advances in Experimental Medicine
and Biology 907, DOI 10.1007/978-3-319-29073-7_5

1 Introduction

To adapt to predictable daily changes in the environment, organisms developed mechanisms to anticipate these changes and respond appropriately. Central to this coordination is an intrinsic *oscillator* that generates *circadian rhythms* of behavior, physiology and metabolism. Anatomically, in mammals, the hypothalamic Suprachiasmatic Nucleus (SCN) consisting of ~20,000 neurons functions is the master circadian oscillator. However, the molecular mechanism of the circadian clock is cell autonomous and is present in almost every cell of our body. The SCN oscillator uses synaptic and diffusible factors to orchestrate rhythms in peripheral tissues in appropriate phases.

The molecular circadian oscillator is based on transcription-translation feedback loops with time-delays that generate 24-h oscillations in many of its constituents. Circadian rhythms in animals are endogenous self-sustaining ~24 h rhythms generated by the basic mechanism of cell autonomous transcriptional feedback loops conserved from flies to human. Both components and mechanisms of circadian rhythms are largely conserved in animals [1]. The transcriptional activators CLOCK and BMAL1 dimerize and activate the transcription of Period (*per*) and Cryptochrome (*cry*). The PER/CRY heterodimer, in turn, represses the transcriptional activities of CLOCK/BMAL1 [2]. In an interconnected loop, nuclear hormone receptors REV-ERB and ROR act as repressors and activators to drive rhythmic transcription of several clock components [3, 4].

The molecular circadian clock drives rhythmic transcription from a large number of genes by (a) directly binding to the respective *cis*-regulatory sites, (b) indirectly by their immediate targets that are also transcription factors, (c) by post transcriptional regulations, and (d) by functional interactions with several signaling and transcriptional regulators. In any given tissue in insects and mammals, up to 15 % of the expressed genome exhibit a circadian expression pattern, with peak levels of expression of different transcripts timed to different times of the day or night [1].

Genomics studies have shown that the steady-state levels of a large number of transcripts show daily oscillations. Immediately after transcription initiation and throughout their life cycles, RNAs are bound by a large number of proteins, some of which remain stably bound while others are subject to dynamic exchange. These complexes containing RNAs and their associated proteins constitute the ribonucleoprotein particles (RNPs). The combination of factors binding to a particular RNA and their position along the transcript determines every step of RNA regulation throughout its lifetime. Given the large number of protein coding, small RNAs, miRNAs, ncRNAs that show circadian rhythm in different tissues, and the indirect evidence for circadian rhythm in ribosome turnover, proteins that bind to these RNAs to process, transport, stabilize, translate or degrade can have a profound impact on circadian rhythms in cellular and organismal function.

Upon transcription, not all mRNAs immediately enter the translationally active pool. Some destined for a particular subcellular location travel in multi-mRNA packets or particles and are held in a quiescent state awaiting either proper subcellular localization or a signal that timing is now right to make protein [5]. Similarly it is

also conceivable that some RNAs accumulate in ribonucleoprotein bodies inside the nucleus waiting to be processed or exported until a second signal is received. This integrated model for the regulation of gene expression fits very well to the features of biological clocks, whose function is to synchronize and adapt internal biological processes to environmental stimuli. Furthermore, the time lag between nascent RNA and mRNA for many of the circadian transcripts is specific to the transcript, which suggests that some type of post-transcriptional regulation at splicing or polyadenylation must play a role to maintain such phase relationship. Posttranscriptional events can also buffer variable transcriptional output to generate robust and reproducible rhythms of mRNA expression and protein synthesis. Overall, there is ample evidence for potential roles of RBPs in circadian organization; however, there are very few RBPs with known function in the circadian function. We will review all the different levels at which gene expression shows circadian variation, from transcription initiation to mRNA stability and translation efficiency and cite specific examples of RBPs regulating circadian function.

2 Circadian Regulation of Transcription Initiation

With increased understanding of the mechanism of transcription initiation, it is becoming apparent that in addition to the RNA polymerase complex, several proteins involved in chromatin modification and several RNAs, including enhancer RNAs, non-coding RNAs, and antisense RNAs, play an integral role in initiation and initiation rate. Transcription is the first step of gene expression, and it starts with the binding of the enzyme RNA polymerase II to a segment of DNA. Of particular importance for transcription initiation is the carboxy-terminal domain (CTD) of RNA polymerase II.

The RNA polymerase II CTD typically consists of up to 52 repeats of the sequence Tyr-Ser-Pro-Thr-Ser-Pro-Ser and it serves as a flexible binding scaffold for numerous nuclear factors, determined by the phosphorylation patterns on the CTD repeats. RNA polymerase II can exist in two main forms: RNAPII0, with a highly phosphorylated CTD, and RNAPIIA, with a nonphosphorylated or hypophosphorylated CTD. The phosphorylation state changes as RNAPII progresses through the transcription cycle: the initiating RNAPII is form IIA, and the elongating enzyme is form II0. The phosphorylated CTD physically links pre-mRNA processing to transcription by tethering processing factors to elongating RNAPII, e.g., 5′-end capping, 3′-end cleavage, and polyadenylation. Nearly all of our knowledge of genome-wide transcriptional and post-transcriptional regulation of circadian transcription comes from experiments done in several labs on male mouse liver. In these experiments the adult mice are fed a normal diet ad libitum and entrained to 12 h light: 12 h dark (LD) cycle for a few days. If the mice are held under LD cycle conditions during sample collection, the sampling times are represented as Zeitgeiber time (ZT), where the time of lights-on is considered ZT0. If the mice are transferred to constant darkness prior to sample collection, the timing is represented as Circadian time (CT), where CT0 roughly corresponds to the subjective time of lights-on (or equivalent to ZT0). The

data collected from different times of at least a full day is analyzed by fitting to a wave function, so that the probability values related to robustness of oscillation, peak and trough time/phase of oscillation can be derived. Detected oscillation in given molecules or their activities and the associated phase or time of peak or trough level can be used to explain potential sequence of regulatory events. Due to changes in experimental conditions and sampling frequency, the circadian rhythm parameters might be slightly different in different manuscripts. Therefore, it is relevant to compare the phase information from the same experiment.

Among several published circadian ChIP-seq experiments, the large number of histone modifications, oscillator components binding to chromatin, RNA pol binding, and transcripts from mouse liver reported in Koike *et al*. makes this study relevant to compare the timing of various steps in circadian transcription regulation. In this study CTD phosphorylation status shows a circadian variation, with RNAPIIA signal reaching its peak level at CT14.5 and the RNAPII0 signal peaking at CT0.6. The hypophosphorylated RNAPIIA peak at CT14.5 coincides closely with the peak of intron-containing or nascent transcripts at CT15.1. On the other hand, the peak of hyperphosphorylated RNAPII0 signal coincides with the peak of CRY1 occupancy at CT0.4. At this time CLOCK and BMAL1 are beginning a new cycle of binding but are transcriptionally silent, likely because CRY1 is bound at the same sites. One possible scenario is that RNAPII can be recruited by CLOCK:BMAL and that RNAPII initiation occurs but then pauses or stalls and accumulates at CT0. Alternatively, RNAPII0 occupancy at CT0 could be independent of CLOCK:BMAL1 and could reflect a peak of transcription at CT0 [6].

In addition to circadian oscillations at promoter activity, oscillations in enhancer activities are also found. Fang et al. recently identified circadian transcriptional activity at enhancer regions in mouse liver. This transcriptional activity produces cycling enhancer associated non-coding RNAs called enhancer RNAs (eRNAs; [7, 8]). The circadian eRNAs oscillate in diverse phases and each phase group is enriched in binding motives for different classes of clock transcription factors. The motif enrichment in a given eRNA group is predictive of the specific transcription factor binding. Moreover, circadian eRNAs transcription correlates and can predict rhythmic transcription of nearby genes. The authors propose that circadian transcription factors like CLOCK/BMAL and Rev-erba can bind multiples sites in the genome; however, many of these genes are bound but not controlled, due to inactive binding or long distance looping at different genes. Transcriptional activity at enhancers can be used as markers to assess where a transcription factor is actually functional and they suggest that only the genes that are expressed in phase with CLOCK/BMAL binding are true BMAL1/CLOCK targets [9].

Also chromatin modifications associated with transcription initiation and elongation show circadian variations. Histone H3K4me3, H3K9ac, and H3K27ac are enriched at promoters and show robust circadian rhythms in occupancy at transcription starting sites (TSSs). Histone H3K4me1, a marker that is characteristic of enhancer sites and gene bodies, exhibits a very subtle circadian modulation. There is an antiphase rhythm in H3K4me1 and H3K4me3 occupancy at the Dbp intron1 site. Histone H3K27ac is also highly enriched at both intragenic and intergenic enhancer

sites. The elongation marks, H3K36me3 and H3K79me2, also express very low-amplitude circadian modulation. On a genome-wide level, circadian rhythms in RNAPIIA, RNAPII0, H3K4me3, H3K9ac, and H3K27ac occupancy at TSSs can be seen in all classes of expressed genes and are stronger in intron RNA cycling genes. Unexpectedly, noncycling intron expressed genes also show circadian modulation of RNAPII occupancy and histone modifications. Genome-wide analysis of the periodicity and phase of these histone marks reveals that large number of genes exhibit circadian rhythms in histone modifications. The overall number of histone modification sites does not appear to vary on a circadian basis; rather the recruitment (and initiation) of RNAPII appears to underlie the variation in the amplitude on histone marks. Circadian modulation of RNAPII occupancy and histone modifications occurs not only at promoter proximal regions but also at distal intergenic enhancer sites. Thus, circadian transcriptional regulation appears to be involved in the initial stages of RNAPII recruitment and initiation and the histone modification associated with these events to set the stage for gene expression on a global scale [6].

3 Circadian Regulation of Transcription Termination

Although most focus in circadian regulation has been on daily oscillations in transcription initiation by alternating action of activators and suppressors, recent results have indicated that transcription termination may also be rhythmic. In mammals, PER and CRY proteins accumulate, form a large nuclear complex, and associate with the dimeric transcription factor CLOCK-BMAL at *Per* and *Cry* promoters, repressing their own transcription. PER complexes include the RNA-binding protein NONO and the histone methyltransferase WDR5 [10], and they function in part by recruiting a SIN3 histone deacetylase complex to clock gene promoters [11]. In addition to known PER-associated proteins, Padmanabahn et al. identified the RNA helicases DDX5, DHX9 and SETX in mouse PER complexes. DDX5 and DHX9 function in transcription and pre-mRNA processing [12]. Both are associated with elongating RNA polymerase II [13] and are components of the 3′ transcriptional termination complex [14]. After cleavage of the nascent transcript, unwinding of the RNA-DNA duplex by SETX at the 3′ termination site permits the XRN2 nuclease to degrade the downstream 3′ RNA and thereby release the polymerase [15]. PER complex inhibits SETX activity, blocking subsequent processing by XRN2 and thus blocking transcription termination. Inhibition of termination reduces the rate of transcription, and as a consequence during the negative feedback, RNA polymerase II accumulates at the 5′ site as well as at the 3′ site of *Per* and *Cry* genes [16]. The mammalian PER complex has at least two actions in circadian feedback. It represses transcription by recruiting a SIN3 hystone deacetylase complex to clock gene promoters [11], and it inhibits termination by antagonizing the action of SETX at the 3′ termination site. Both processes contribute to circadian Per gene repression, but one or the other could predominate at different target genes [16].

4 Evidence for the Relevance of Posttranscriptional Events on Circadian Gene Expression

Although circadian regulation of mRNA expression at the transcriptional level is one of the important steps for circadian rhythms in cellular function, multiple lines of evidence point to a disconnect between transcript oscillation and protein oscillation, which can be explained by regulatory RNA-binding proteins acting on the transcripts. The transcription rate itself varies significantly in cells from different tissues [17], yet the free-running endogenous circadian oscillator shows remarkable stability in period length among tissue types. Thus it is likely that the oscillator possesses a mechanism that allows compensating for differences in transcription rates. Indeed, partial inhibition of transcription by a-amanitin treatment in mouse fibroblasts reduces RNA PolII dependent transcription rate by up to threefolds, but doesn't stop cell-autonomous oscillator. The circadian oscillator as measured by translated protein continues to oscillate, albeit with dampened amplitude and slightly shorter periodicity [18]. Similarly, in *Drosophila*, constitutively high mRNA expression of a circadian clock component does not stop the clock; rather, the translated protein level continues to oscillate. These results suggest a posttranscriptional mechanism potentially involving mRNA-binding proteins that can support translational rhythm even when transcriptional oscillation is blunted or inhibited [18, 19].

Furthermore a systematic analysis of the mammalian "circadian proteome" revealed that up to 20 % of soluble proteins in mouse liver are subject to circadian control; however, almost half of the cycling proteins lack a corresponding cycling transcript, further supporting the hypothesis that posttranscriptional mechanisms play a significant role in mammalian circadian rhythms [20, 21]. Interestingly, human red blood cells, which have no nucleus (or DNA) and therefore cannot perform transcription, display robust, temperature-entrainable and temperature-compensated circadian rhythms in peroxiredoxin redox cycles, consistent with the presence of a circadian clock within these cells despite the lack of ability to make new RNA [22].

More recently, additional evidence underlined the importance of posttranscriptional regulation in circadian gene expression. Through high-throughput sequencing or Nascent-Seq and RNA-Seq, Rodriguez at al. identified 136 robust "nascent cyclers" and 237 robust mRNA cyclers in fly heads. Despite a highly significant overlap, most genes in the two data sets are distinct. They propose a model in which transcriptionally active genes can be organized in four groups: genes with both robust nascent and robust mRNA cycling, genes with robust nascent RNA cycling but little or no mRNA cycling, genes with robust mRNA cycling with weak nascent RNA oscillations and genes with robust mRNA cycling but even weaker, and perhaps no, nascent RNA cycling [23].

Menet et al. conducted a similar study in mouse liver. Although many genes are rhythmically transcribed in mouse liver (~15 % of all detected genes), only 42 % of these show mRNA oscillation. More importantly, about 70 % of the genes that exhibit rhythmic mRNA expression do not show transcriptional rhythms, suggesting that posttranscriptional regulation plays a major role in defining the rhythmic mRNA landscape. Also the way in which CLOCK:BMAL1 regulates the transcription of its

target genes differs from what would be expected. Although CLOCK:BMAL target genes are significantly enriched for rhythmic transcribed genes, there is a large discrepancy between the phases of rhythmic BMAL1 DNA binding and those of rhythmic transcription. This is because BMAL1 binding is essentially uniform at ZT3-5, whereas the transcription peaks are much more broadly distributed. The dramatic, genome-wide disconnect between the phases of rhythmic CLOCK:BMAL1 DNA binding and rhythmic target gene transcription suggests that other transcription factors and/or mechanisms collaborate with CLOCK:BMAL1 binding and are critical to determine the phase of clock gene [24].

Another way of assessing the presence of posttranscriptional regulation in circadian gene expression is to sequence the transcriptome and consider the intron signal as a representation of pre-mRNA expression or nascent transcription and the exon signal as a representation of mRNA expression, which can reflect not only transcriptional activity but also posttranscriptional processing events. Koike and collegues quantified intron and exon signals for cycling transcripts in mouse liver and found 1371 intron and 2037 exon RNA cycling transcripts. The intron cycling transcripts are clustered, whereas the exon cycling transcripts have three peak phases. Only 458 genes are in common, and this set of common genes is enriched for known circadian clock genes and high-amplitude cycling target genes reported previously. The phases of the common intron and exon cycling transcripts are correlated, suggesting that transcriptional cycles primarily drive these mRNA rhythms. In the intron-cycling/exon non-cycling class, the cycling pre-mRNA transcripts are clustered at the same phase as the overall intron cycling class, but the steady-state mRNAs are likely to have long half-lives, which would dampen oscillation generated at the transcriptional level. By contrast, in the intron not cycling/exon cycling class, the phases are widely distributed as seen in the overall exon cycling class, and these rhythms likely arise from posttranscriptional regulatory processes such as circadian changes in RNA splicing, polyadenylation, or mRNA stability [6].

5 Circadian Regulation of Alternative Splicing

Alternative splicing is a regulated process during gene expression that results in a single gene coding for multiple proteins. In this process, particular exons of a gene may be included within, or excluded from, the final, processed messenger RNA (mRNA). Alternative splicing is of particular importance amongst the posttranscriptional processes that regulate gene expression, as it allows the human genome to direct the synthesis of many more proteins than would be expected from its 20,000 protein-coding genes.

Alternative splicing is widespread in mammalian genes, affecting approximately 95 % and 80 % of multi-exon genes in humans and mice, respectively [25, 26]. Moreover, alternative splicing is highly regulated by the activity, abundance and binding position of various splicing factors and heterogeneous nuclear ribonucleoproteins, and by the kinetics of transcription elongation and chromatin modifications [27–29].

Using an Affymetrix exon array, McGlincy and collegues demonstrated that the circadian clock regulates alternative splicing in the mouse. 55 exon-probesets from 47 genes where identified to have significant circadian variation. The 47 genes were enriched in pathways representing the circadian clock itself, drug detoxification, caffeine and retinol metabolism and the peroxisome proliferator-activated receptor (PPAR) signaling pathway. The circadian regulation of alternative splicing is tissue dependent, in terms of both phase and amplitude. For some of the exons identified the temporal relationship between alternative splicing and transcript level expression was preserved across tissues, suggesting that these two processes may be coupled in these particular cases. Fasting conditions modulate circadian alternative splicing in an exon dependent manner, but they also modulate the temporal relationship between circadian alternative splicing and circadian mRNA abundance in a gene-dependent manner. Moreover, the alternative splicing of the identified exons is under the control of the local liver clock [30].

At least 15 splicing factors where shown to be robustly cycling in the mouse liver. They include well characterized regulators of alternative splicing (*Srsf3*, *Srsf5*, *Tra2b* and *Khdrbs1*(*Sam68*)), a component of the U2 snRNP (*Sf3b1*), two RNA helicases (*Ddx46* (also component of U2 snRNP) and *Dhx9*), three hnRNP proteins better known for their roles regulating RNA stability and translation (*Hnrnpdl*, *Cirbp* (hnRNP-A18) and *Pcbp2* (hnRNP E2)), and six other proteins with less well characterized roles in RNA processing (*Gtl3*, *Rbms1*, *Thoc3*, *Pcbp4* and *Topors*). Some of these circadian splicing factors were under the control of the local liver clock, while others are likely rhythmic in response to systemic rhythmic cues. Some of the known exon targets of these splicing factors where previously identified to be cycling exons. The discovery of robustly circadian splicing factors, and the fact that a number of their previously characterized target exons are circadian, provide candidates for further study into the molecular mechanisms regulating circadian exons and other posttranscriptional processes [30].

Recently, Preußner et al. demonstrated that the rhythmic alternative splicing of the mRNA encoding U2-auxiliary-factor 26 (U2AF26) contributes to the regulation of Period 1 stability. More in detail they found that U2AF26 undergoes circadian alternative splicing of exons 6 and 7 in peripheral clocks (U2AFΔE67) and that the splicing switch generates a shift in the mRNA reading frame. Skipping of U2AF26 exons 6 and 7 generates a domain with homology to *Drosophila* TIM and enables cytoplasmic, circadian expression of the U2AF26ΔE67 isoform. Furthermore, U2AF26ΔE67 interacts with PER1 and induces its proteasomal degradation; this limits the light induced increase of PER1 and it's proposed as buffering mechanism against sudden light changes [31].

6 Circadian Polyadenylation

The addition of a poly(A) tail to a primary transcript RNA is known as RNA polyadenylation. In nuclear polyadenylation, a poly(A) tail is added to an RNA at the end of transcription. The poly(A) tail consists of multiple adenosine monophosphates; in other words, it is a stretch of RNA that has only adenine bases. In eukaryotes, polyadenylation

is part of the process that produces mature messenger RNA (mRNA) for translation. The poly(A) tail protects the mRNA molecule from enzymatic degradation in the cytoplasm and aids in transcription termination, export of the mRNA from the nucleus, and translation [32]. Almost all eukaryotic mRNAs are polyadenylated [33]. The tail is shortened over time, and, when it is short enough, the mRNA is enzymatically degraded [32]. Regulation of poly(A) tail length is traditionally considered to be unidirectional, going from long to short. However more recent evidence has demonstrated that the ultimate poly(A) tail length is determined by a balance between concomitant deadenylation and polyadenylation, and this balance is controlled in a highly regulated and mRNA-specific manner. In some cases mRNAs with short poly(A) tails can be stored for later activation by re-polyadenylation in the cytosol [34].

Some evidences suggest that poly(A) tail length regulation may take part in controlling circadian-regulated rhythmic gene expression. The deadenylase nocturnin (NOC) removes poly(A) tails from its target RNAs and this process is thought to control target RNA expression by either enhancing RNA degradation or silencing translation. NOC shows rhythmic expression in many tissues such as spleen, kidney and heart in mice with peak levels at the time of light offset. This rhythmicity has been shown to be particularly robust in liver. The mouse NOC gene (*mNoc*) is expressed in a broad range of tissues and in multiple brain regions including suprachiasmatic nucleus and pineal gland. The widespread expression and rhythmicity of *mNoc* mRNA parallels the widespread expression of other circadian clock genes in mammalian tissues, and suggests that NOC plays an important role in clock function or as a circadian clock effector [35]. *mNoc* is also an immediate early gene, and its expression is acutely induced by stimuli such as serum and 12-O-tetradecanoyl-phorbol-13-acetate (TPA) in cultured cells. Remarkably, *mNoc* is the unique deadenylase induced by serum shock. Thus NOC may act in turning off the expression of genes that are required to be silenced as a response to extracellular signals [36].

More recently, it has been shown that 2.3 % of all expressed mRNA exhibit statistically significant rhythmicity in the poly(A) tail length (i.e. the ratio between the "long tail" and the "short tail" fraction of an RNA). The "poly(A) rhythmic" (PAR) mRNAs include mRNAs with peak tail lengths at all phases of the daily cycle but with significantly higher numbers of mRNAs with peak long/short ratios during the night. Based on the pre-mRNA and steady-state mRNA profiles, the PAR mRNAs can be categorized into three classes: Class I PAR mRNAs (49.2 %) are rhythmic in their poly(A) tail length and pre-mRNA and steady-state mRNA levels, class II PAR mRNAs (32.3 %) are rhythmic in their poly(A) tail length and pre-mRNA expression but not in steady-state mRNA levels, and class III PAR mRNAs (18.5 %) are rhythmic in their poly(A) tail length rhythms but not in pre-RNA or steady-state mRNA levels. There are significant differences in mRNA half-lives among the different PAR classes; class III mRNAs are the most stable, followed by class II mRNAs, with class I mRNAs being the least stable [37].

The rhythmic poly(A) lengths of both class I and II mRNAs reflect nuclear polyadenylation (likely by the canonical poly(A) polymerase α), coordinated with rhythmic transcription during classical 3′ end processing. The defining characteristics of these two classes are the differences in the steady-state mRNA rhythmicity and mRNA

stability, suggesting that the lack of rhythmicity in the class II PARs reflects the longer half-lives of these mRNAs. The mechanism of poly(A) rhythmicity in both class I and II mRNAs results from the addition of long tails following rhythmic synthesis and subsequent deadenylation that does not cause immediate decay. This delay in decay is more pronounced in the class II mRNAs and results in the arrhythmic steady-state levels. It appears that class I/II PAR mRNAs can exist in short-tailed states and that rhythmic control of poly(A) tail length is somehow correlated with delayed accumulation of steady-state mRNA and may be part of a regulatory mechanism to regulate the timing of mRNA/protein rhythmicity [37].

Class III mRNAs exhibit robust rhythmicity in their poly(A) tail length, yet are not rhythmically transcribed and have longer half-lives. Thus, class III PARs must employ transcription-independent mechanisms to control their rhythmic poly(A) tail lengths. Peak distribution analysis of class III PAR mRNAs revealed that >80 % had their longest poly(A) tails during the day, which is distinct from the nighttime poly(A) rhythmic profile of class I and many of the class II mRNAs. The poly(A) rhythms of class III mRNAs are likely to be controlled by rhythmic cytoplasmic polyadenylation. Indeed, the steady-state mRNA level of several putative cytoplasmic polyadenylation machinery components in the liver, including *Cpeb2*, *Cpeb4*, *Parn*, and *Gld2*, are rhythmically expressed with phases similar to the majority of the class III PAR mRNAs, peaking in the early day [37].

In mouse liver rhythmic poly(A) tail lengths correlate strongly with the ultimate circadian protein expression profiles, with the protein peaking ~4–8 h after the time of the longest poly(A) tail. Therefore poly(A) tail rhythms can generate rhythmic protein levels even when there is no rhythm in the steady-state mRNA levels [37].

7 Regulation at Translation Initiation and Ribosome Biogenesis

Many oscillating proteins in the mouse liver are encoded by constantly expressed mRNAs and among the rhythmically expressed genes in the liver, there are several genes encoding proteins involved in mRNA translation, including components of the translation pre-initiation complex [38]. The circadian clock controls the transcription of translation initiation factors as well as the rhythmic activation of signaling pathways involved in their regulation. Initiation in eukaryotes requires at least ten proteins, which are designated eIFs (eukaryotic initiation factors). The mRNAs of most of the factors involved in translation initiation are rhythmically expressed with a period of 24 h. There isn't a significant variation in protein abundance, but these factors undergo strong rhythmic phosphorylation [38]. The initiation factors eIF4E and eIF4G, in association with eIF-4A and eIF-4B, are involved in binding the mRNA and bringing it to the 40S ribosomal subunit. eIF4E, which recognizes the 5′ cap of the mRNA, is mostly phosphorylated during the day, with a peak at the

end of the light period (ZT6-12). eIF4G, eIF4B and 4E-BP, and ribosomal protein (RP) S6 (RPS6) are mainly phosphorylated during the night, which is, in the case of nocturnal animals like rodents, the period when the animals are active and consume food. Phosphorylation of these factors is well characterized and involves different signaling pathways whose reported activity perfectly correlates with the observed phosphorylation rhythm [38]. eIF4E is phosphorylated by the extracellular signal-regulated protein kinase (ERK)/mitogen activated protein kinase (MAPK)-interacting kinase (MNK) pathway, which is most active during the day, at the time when eIF4E reaches its maximum phosphorylation. On the other hand, eIF4G, eIF4B, 4E-BP1, and RPS6 are mainly phosphorylated by the target of rapamycin (TOR) complex 1 (TORC1), which is activated during the night at the time when the phosphorylation of these proteins reaches its maximum level. It has been shown that mTOR, its partner Raptor, as well as its regulating kinase Map3k4, are also rhythmically expressed, thus potentially further contributing to the rhythmic activation of TORC1. The rhythmic phosphorylation of 4E-BP1 results in the release eIF4F, allowing its binding to the mRNA and the initiation of translation [38].

The polysomal RNA fraction (RNA sub-fraction composed mainly of actively translated RNAs) in mouse liver also follows a diurnal cycle, showing that a rhythmic translation does occur in this tissue. Approximately 2 % of the expressed genes are translated with a rhythm that is not explained by rhythmic mRNA abundance as in most cases the total mRNA levels are constant. Among translationally regulated genes, 70 % were found in the polysomal fraction during the same time interval, starting at ZT8 before the onset of the mouse feeding period and finishing at the end of the dark period [38].

The circadian clock was shown to regulate also ribosome biogenesis by influencing the transcription of ribosomal protein (RP) mRNAs and ribosomal RNAs (rRNAs). RPs show a rhythmic abundance with highest expression during the night. Pre-mRNA accumulation of several RPs exhibits a rhythmic pattern too, with a peak at ZT8, just before the activation of their translation. As for rRNA transcription, the synthesis of the ribosome constituent precursor 45S rRNA (containing 28S, 5.8S and 18S rRNAs) is rhythmic and synchronized with RP mRNAs transcription, indicating that all elements involved in ribosome biogenesis are transcribed in concert and coordinated with the feeding period. In mammals rRNA transcription is highly regulated by the upstream binding factor (UBF). Not surprisingly UBF1 is rhythmically expressed in mouse liver too, at both mRNA and protein levels, in phase with RP mRNAs and rRNA transcription. Mice devoid of a functional circadian clock lose the rhythmic activation of TORC1 and ERK signaling pathways, and the rhythmic expression of UBF1. In addition these animals show lack of synchrony and coordination of 45S rRNA and RP pre-mRNA transcription, highlighting the crucial role of the circadian clock in this mechanism. Ribosomal protein synthesis in eukaryotes is a major metabolic activity that involves hundreds of individual reactions; this energy-consuming process has to be confined to a time when energy and nutrients are available in sufficient amounts, which, in the case of rodents, is during the night [38].

8 RNA-binding Proteins Regulating mRNA Stability and Translational Efficiency Are Important for Oscillation of Core Clock Components

The number of RNA-binding proteins and those with RNA-binding motifs encoded by the human genome is remarkable. As an example a single type of RNA-binding domain, the RNA recognition motif (RRM), is represented in nearly 500 different human genes. RNA-binding proteins (RBPs) couple transcription and subsequent post-transcriptional steps by interacting with their target transcripts. Even though some RBPs bind to common elements present in almost every mRNA in a sequence-independent and nonspecific manner, the majority of RNA-binding factors target particular structures or sequences present in some RNAs but not others [39]. The posttranscriptional events involving multiple mRNAs must be highly coordinated and RBPs, including export proteins, provide coordinating functions at all steps along the posttranscriptional regulatory chains. RBPs allow the mRNA molecules to interface with other intracellular machineries mediating their splicing, transport, stabilization or degradation, localization, or translation into protein, as well as the response to stimuli. Indeed individual mRNAs contain binding sites for different RBPs and can respond to a wide range on inputs, so that their expression can be adjusted to changing environmental conditions. RBPs are thus the leading actors of an intricate regulatory network, which is equally complex as that controlling initial RNA synthesis. Because RBPs can bind to more than one RNA with sequence specificity, the existence of a "posttranscriptional operon" has been postulated whose function is to expand the regulatory plasticity of our relatively "small" genome. In fact the expression of proteins with common functional themes or subcellular distributions is coordinated by large-scale regulatory networks operating at the mRNP level. The final outcome of protein synthesis is thus an mRNP-driven process that responds dynamically to the environment and cellular growth conditions [5, 39].

In particular the posttranscriptional regulation of mRNA stability and translational efficiency are often mediated by cis elements in mRNAs that interact with RNA-binding proteins and/or microRNAs. In most cases, these cis elements reside in the 3′ untranslated region (UTR), and several 3′ UTR motifs have been identified that are critical for mRNA splicing, transport, stability, localization, and translation.

The 3′UTR-dependent mRNA decay is involved in the regulation of circadian oscillation of Period 2 (*per2*) mRNA. In particular the polypyrimidine tract-binding protein (PTB), also known as heterogeneous nuclear ribonucleoprotein I (hnRNP), binds to *per2* 3′UTR and has an mRNA destabilizing activity. Indeed the cytoplasmic PTB expression pattern is reciprocal with *per2* mRNA oscillation and depletion of PTB with RNAi results in *per2* mRNA stabilization [40]. A similar study reported that the 3′UTR is also important for the mRNA stability of another core clock component, mouse cryptochrome 1 (*cry1*). The 3′UTR of *cry1* contains a destabilizing cis-acting element that contributes to the stability of *cry1* mRNA. The binding of hnRNP D to *cry1* 3′UTR is responsible for the rapid decay of *cry1* mRNA during its declining phase and modulates *cry1* circadian rhythm [41].

Also, the stability of mouse Period3 (*per3*) is dramatically changed in a circadian phase-dependent manner. In the case of (*per3*), the control of its circadian mRNA stability requires the cooperative function of both the 5′ and 3′ UTRs. Several studies reported that mRNA stability can be regulated by the 5′UTR, a mechanism called translational regulation-coupled mRNA decay. In such cases translational inhibition causes mRNA stabilization. Similarly hnRNP Q binds to both 5′ and 3′UTR in the *per3* mRNA and not only reduces the translation efficiency but also increases the mRNA stability. *per3* mRNA decay is connected to its translation kinetics and the central region of *per3* 5′UTR is responsible for coupling of translation and mRNA decay. The binding of hnRNP Q of *per3* 5′UTR is phase dependent and maintains robust mRNA oscillation [42].

Mouse LARK, another RBP, has been shown to activate the posttranscriptional expression of the mouse period1 (*per1*) mRNA. A strong circadian cycling of the LARK protein is observed in the suprachiasmatic nuclei with a phase similar to that of PER1, although the level of the *lark* transcripts are not rhythmic. LARK protein binds directly to a cis-element in the 3′ UTR of the *per1* mRNA and causes increased PER1 protein levels, by activating *per1* mRNA translation. Alterations of *lark* expression in cycling cells causes significant changes in circadian period, with *lark* knockdown by siRNA resulting in a shorter circadian period, and *lark* overexpression resulting in a lengthened period [43].

Many studies have shown that mammalian cells utilize internal ribosome entry site (IRES)-mediated translation for rapid adaptation to certain environments, such as chemotoxic stress [44], mitosis [45] and apoptosis [46], and generally under conditions when cap-dependent translation is compromised. For IRES-mediated translation, proteins known as IRES *trans*-acting factors (ITAFs) must recognize IRES elements in a structure or sequence-dependent manner. Recent evidences suggest that IRES-mediated translation might be one of the mechanisms regulating the protein oscillation of key clock components like Rev-erb α. Also known as Nr1d1, Rev-erb α was identified as a regulator of lipid metabolism [47]. It also plays an important role in the maintenance of circadian timing in brain and liver tissue [48, 49] and it is a well-known transcriptional repressor in the positive limb of circadian transcription [3, 50]. Kim and colleagues have demonstrated that hnRNP Q and PTB modulate mRev-erb α IRES-mediated translation. Knockdown of hnRNP Q and PTB leads to the alteration of the mRNA levels of several clock genes, thus posttranscriptional regulation by hnRNP Q and PTB is necessary to maintain the circadian feedback loop [7, 8].

9 Conclusion

There is increasing evidence that the RBPs play an important role in homeostatic control of the periodicity of circadian oscillator and its output regulation. RBP mediated regulation of various steps in the transcription, RNA processing and RNA half-life helps maintain the precision of the clock under diverse cellular and environmental conditions. Circadian regulation of cellular physiology and metabolism is mediated by

daily oscillations in the steadystate levels of nascent RNA, mRNA, and protein levels. However, large fraction of oscillating proteins or mRNA does not exhibit a correlated rhythm in nascent RNAs, which suggests that post-transcriptional regulation involving RBPs is most likely involved. Since many RBPs bind and regulate the location, transport, translation of a large number of target RNAs, a rhythmic level of a given RBP likely helps temporally coordinate the function of the target RNAs. Another challenge in circadian regulation is the newly recognized role of eating pattern and nutrition quality in the daily oscillations of RNA and proteins. In rodent liver, the circadian transcriptome in peripheral organs appears to be heavily determined by the nutrition quality and time of eating. This implies that the nutrition information encoded in several metabolites might affect the circadian transcriptome by both transcriptional and post-transcriptional mechanisms and RBPs will likely play an important role in integrating nutrition status with the endogenous circadian oscillator function.

Much of the evidence for the roles of RBPs in circadian regulation is indirect. Although genome-wide transcriptome studies have shown circadian rhythms in the mRNA levels of several RBPs, whether the RBP proteins and their cellular localization are also circadian is yet to be determined. Similarly, as the target RNAs for many of the RBPs are discovered, informatics approaches to integrate these findings with circadian transcriptome datasets will begin to explain post-transcriptional mechanisms of circadian regulation. Overall, the area of investigation on how RBPs are involved in the circadian regulation is a nascent field with plenty of opportunities for discoveries and mechanistic insight.

References

1. Bell-Pedersen D, Cassone VM, Earnest DJ, Golden SS, Hardin PE, Thomas TL, Zoran MJ (2005) Circadian rhythms from multiple oscillators: lessons from diverse organisms. Nat Rev Genet 6:544–556
2. Lee C, Etchegaray JP, Cagampang FR, Loudon AS, Reppert SM (2001) Posttranslational mechanisms regulate the mammalian circadian clock. Cell 107(7):855–867
3. Preitner N, Damiola F, Lopez-Molina L, Zakany J, Duboule D, Albrecht U, Schibler U (2002) The orphan nuclear receptor REV-ERBalpha controls circadian transcription within the positive limb of the mammalian circadian oscillator. Cell 110(2):251–260
4. Sato TK, Panda S, Miraglia LJ, Reyes TM, Rudic RD, McNamara P, Naik KA, FitzGerald GA, Kay SA, Hogenesch JB (2004) A functional genomics strategy reveals Rora as a component of the mammalian circadian clock. Neuron 43(4):527–537
5. Moore MJ (2005) From birth to death: the complex lives of eukaryotic mRNAs. Science 309(5740):1514–1518
6. Koike N, Yoo SH, Huang HC, Kumar V, Lee C, Kim TK, Takahashi JS (2012) Transcriptional architecture and chromatin landscape of the core circadian clock in mammals. Science 338(6105):349–354
7. Kim DY, Woo KC, Lee KH, Kim TD, Kim KT (2010) hnRNP Q and PTB modulate the circadian oscillation of mouse Rev-erb alpha via IRES-mediated translation. Nucleic Acids Res 38(20):7068–7078
8. Kim TK, Hemberg M, Gray JM, Costa AM, Bear DM, Wu J, Harmin DA, Laptewicz M, Barbara-Haley K, Kuersten S, Markenscoff-Papadimitriou E, Kuhl D, Bito H, Worley PF,

Kreiman G, Greenberg ME (2010) Widespread transcription at neuronal activity-regulated enhancers. Nature 465(7295):182–187
9. Fang B, Everett LJ, Jager J, Briggs E, Armour SM, Feng D, Roy A, Gerhart-Hines Z, Sun Z, Lazar MA (2014) Circadian enhancers coordinate multiple phases of rhythmic gene transcription in vivo. Cell 159(5):1140–1152
10. Brown SA, Ripperger J, Kadener S, Fleury-Olela F, Vilbois F, Rosbash M, Schibler U (2005) PERIOD1-associated proteins modulate the negative limb of the mammalian circadian oscillator. Science 308(5722):693–696
11. Duong HA, Robles MS, Knutti D, Weitz CJ (2011) A molecular mechanism for circadian clock negative feedback. Science 332(6036):1436–1439
12. Fuller-Pace FV (2006) DExD/H box RNA helicases: multifunctional proteins with important roles in transcriptional regulation. Nucleic Acids Res 34(15):4206–4215
13. Das R, Yu J, Zhang Z, Gygi MP, Krainer AR, Gygi SP, Reed R (2007) SR proteins function in coupling RNAP II transcription to pre-mRNA splicing. Mol Cell 26(6):867–881
14. Shi Y, Di Giammartino DC, Taylor D, Sarkeshik A, Rice WJ, Yates JR 3rd, Frank J, Manley JL (2009) Molecular architecture of the human pre-mRNA 3′ processing complex. Mol Cell 33(3):365–376. doi:10.1016/j.molcel.2008.12.028
15. Skourti-Stathaki K, Proudfoot NJ, Gromak N (2011) Human senataxin resolves RNA/DNA hybrids formed at transcriptional pause sites to promote Xrn2-dependent termination. Mol Cell 42(6):794–805. doi:10.1016/j.molcel.2011.04.026
16. Padmanabhan K, Robles MS, Westerling T, Weitz CJ (2012) Feedback regulation of transcriptional termination by the mammalian circadian clock PERIOD complex. Science 337(6094):599–602
17. Schmidt EE, Schibler U (1995) Cell size regulation, a mechanism that controls cellular RNA accumulation: consequences on regulation of the ubiquitous transcription factors Oct1 and NF-Y and the liver-enriched transcription factor DBP. J Cell Biol 128(4):467–483
18. Dibner C, Sage D, Unser M, Bauer C, d'Eysmond T, Naef F, Schibler U (2009) Circadian gene expression is resilient to large fluctuations in overall transcription rates. EMBO J 28(2):123–134
19. So WV, Rosbash M (1997) Post-transcriptional regulation contributes to Drosophila clock gene mRNA cycling. EMBO J 16(23):7146–7155
20. Reddy AB, Karp NA, Maywood ES, Sage EA, Deery M, O'Neill JS, Wong GK, Chesham J, Odell M, Lilley KS, Kyriacou CP, Hastings MH (2006) Circadian orchestration of the hepatic proteome. Curr Biol 16(11):1107–1115
21. Robles MS, Cox J, Mann M (2014) In-Vivo quantitative proteomics reveals a key contribution of post-transcriptional mechanisms to the circadian regulation of liver metabolism. PLoS Genet 10(1), e1004047
22. O'Neill JS, Reddy AB (2011) Circadian clocks in human red blood cells. Nature 469(7331): 498–503
23. Rodriguez J, Tang CH, Khodor YL, Vodala S, Menet JS, Rosbash M (2013) Nascent-Seq analysis of Drosophila cycling gene expression. Proc Natl Acad Sci U S A 110(4):E275–E284
24. Menet JS, Rodriguez J, Abruzzi KC, Rosbash M (2012) Nascent-Seq reveals novel features of mouse circadian transcriptional regulation. Elife 1, e00011
25. Mollet IG, Ben-Dov C, Felício-Silva D, Grosso AR, Eleutério P, Alves R, Staller R, Silva TS, Carmo-Fonseca M (2010) Unconstrained mining of transcript data reveals increased alternative splicing complexity in the human transcriptome. Nucleic Acids Res 38:4740–4754
26. Wang ET, Sandberg R, Luo S, Khrebtukova I, Zhang L, Mayr C, Kingsmore SF, Schroth GP, Burge CB (2008) Alternative isoform regulation in human tissue transcriptomes. Nature 456:470–476
27. Luco RF, Allo M, Schor IE, Kornblihtt AR, Misteli T (2011) Epigenetics in alternative pre-mRNA splicing. Cell 144:16–26
28. Nilsen TW, Graveley BR (2010) Expansion of the eukaryotic proteome by alternative splicing. Nature 463:457–463
29. Witten JT, Ule J (2011) Understanding splicing regulation through RNA splicing maps. Trends Genet 27:89–97
30. McGlincy NJ, Valomon A, Chesham JE, Maywood ES, Hastings MH, Ule J (2012) Regulation of alternative splicing by the circadian clock and food related cues. Genome Biol 13(6):R54

31. Preußner M, Wilhelmi I, Schultz AS, Finkernagel F, Michel M, Möröy T, Heyd F (2014) Rhythmic U2af26 alternative splicing controls PERIOD1 stability and the circadian clock in mice. Mol Cell 54(4):651–662
32. Guhaniyogi J, Brewer G (2001) Regulation of mRNA stability in mammalian cells. Gene 265(1–2):11–23
33. Hunt AG, Xu R, Addepalli B, Rao S, Forbes KP, Meeks LR, Xing D, Mo M, Zhao H, Bandyopadhyay A, Dampanaboina L, Marion A, Von Lanken C, Li QQ (2008) Arabidopsis mRNA polyadenylation machinery: comprehensive analysis of protein-protein interactions and gene expression profiling. BMC Genomics 9:220
34. Richter JD (1999) Cytoplasmic polyadenylation in development and beyond. Microbiol Mol Biol Rev 63(2):446–456
35. Wang Y, Osterbur DL, Megaw PL, Tosini G, Fukuhara C, Green CB, Besharse JC (2001) Rhythmic expression of Nocturnin mRNA in multiple tissues of the mouse. BMC Dev Biol 1:9
36. Garbarino-Pico E, Niu S, Rollag MD, Strayer CA, Besharse JC, Green CB (2007) Immediate early response of the circadian polyA ribonuclease nocturnin to two extracellular stimuli. RNA 13(5):745–755
37. Kojima S, Sher-Chen EL, Green CB (2012) Circadian control of mRNA polyadenylation dynamics regulates rhythmic protein expression. Genes Dev 26(24):2724–2736
38. Jouffe C, Cretenet G, Symul L, Martin E, Atger F, Naef F, Gachon F (2013) The circadian clock coordinates ribosome biogenesis. PLoS Biol 11(1), e1001455
39. Keene JD (2010) Minireview: global regulation and dynamics of ribonucleic acid. Endocrinology 151(4):1391–1397
40. Woo KC, Kim TD, Lee KH, Kim DY, Kim W, Lee KY, Kim KT (2009) Mouse period 2 mRNA circadian oscillation is modulated by PTB-mediated rhythmic mRNA degradation. Nucleic Acids Res 37(1):26–37
41. Woo KC, Ha DC, Lee KH, Kim DY, Kim TD, Kim KT (2010) Circadian amplitude of cryptochrome 1 is modulated by mRNA stability regulation via cytoplasmic hnRNP D oscillation. Mol Cell Biol 30(1):197–205
42. Kim DY, Kwak E, Kim SH, Lee KH, Woo KC, Kim KT (2011) hnRNP Q mediates a phase-dependent translation-coupled mRNA decay of mouse Period3. Nucleic Acids Res 39(20): 8901–8914
43. Kojima S, Matsumoto K, Hirose M, Shimada M, Nagano M, Shigeyoshi Y, Hoshino S, Ui-Tei K, Saigo K, Green CB, Sakaki Y, Tei H (2007) LARK activates posttranscriptional expression of an essential mammalian clock protein, PERIOD1. Proc Natl Acad Sci U S A 104(6):1859–1864
44. Dobbyn HC, Hill K, Hamilton TL, Spriggs KA, Pickering BM, Coldwell MJ, de Moor CH, Bushell M, Willis AE (2008) Regulation of BAG-1 IRES-mediated translation following chemotoxic stress. Oncogene 27(8):1167–1174
45. Schepens B, Tinton SA, Bruynooghe Y, Parthoens E, Haegman M, Beyaert R, Cornelis S (2007) A role for hnRNP C1/C2 and Unr in internal initiation of translation during mitosis. EMBO J 26(1):158–169
46. Bushell M, Stoneley M, Kong YW, Hamilton TL, Spriggs KA, Dobbyn HC, Qin X, Sarnow P, Willis AE (2006) Polypyrimidine tract binding protein regulates IRES-mediated gene expression during apoptosis. Mol Cell 23(3):401–412
47. Coste H, Rodríguez JC (2002) Orphan nuclear hormone receptor Rev-erbalpha regulates the human apolipoprotein CIII promoter. J Biol Chem 277(30):27120–27129
48. Balsalobre A, Damiola F, Schibler U (1998) A serum shock induces circadian gene expression in mammalian tissue culture cells. Cell 93(6):929–937
49. Teboul M, Guillaumond F, Gréchez-Cassiau A, Delaunay F (2008) The nuclear hormone receptor family round the clock. Mol Endocrinol 22(12):2573–2582
50. Ramakrishnan SN, Muscat GE (2006) The orphan Rev-erb nuclear receptors: a link between metabolism, circadian rhythm and inflammation? Nucl Recept Signal 4, e009